AN INVESTIGATION INTO SOME OF THE EFFECTS OF CROSS COUPLING BETWEEN THE LONGITUDINAL AND LATERAL EQUATIONS OF MOTION OF A FIGHTER TYPE AIRCRAFT AT SUBSONIC SPEED

A Thesis Submitted to the
Faculty of the Graduate School of the
University of Minnesota

by

John Joseph Emanski, Jr.
Commander, United States Navy

In Partial Fulfillment of the Requirements
for the Degree of Master of Science
in Aeronautical Engineering

August, 1955

ACKNOWLEDGMENTS

I wish to express my thanks to Professor A. E. Cronk for his advice, assistance, and direction; to P. N. Hess, Instructor in Electrical Engineering, for his instruction and assistance in the use of the analogue computer and for his assistance in setting up the problem for solution on the analogue computer; to Engineering Assistant H. G. Tauss for his technical electronic assistance and aid in the use of the analogue computer.

TABLE OF CONTENTS

SUMMARY

Modern aircraft design trends have been toward aircraft with long, dense fuselages, smaller aerodynamic surfaces, swept wings and higher wing loadings. These aircraft are required to fly at high altitudes. Flight data from such aircraft have indicated that the linearized dynamic equations do not always predict the dynamic behavior accurately. In addition, certain cross-coupling effects were developing between the lateral and longitudinal motion of the aircraft.

The effect of the trend toward concentrating the mass in the fuselage was investigated by making an engineering approximation of the change in the moments of inertia caused by this change in mass distribution. Four configurations were considered, each one approaching nearer the limit of a missile or body of revolution. Since the lower lift curve slopes and smaller wing areas of the swept-wing aircraft sometimes require flight at very high angles of attack, the effect of inclination of the principal longitudinal axis to the flight path was investigated. The effect of sweep was approximated by varying the effective dihedral parameter, C_{l_β}. In addition the effect of varying C_{n_β}, the "weather-cock-stability" parameter, was studied since long fuselages affect this parameter adversely.

The investigation was made using a Reeves Electronic Analogue Computer (REAC) by setting up a mathematical model of a representative military-type airplane flying

at a Mach number of 0.6 at sea level and at 40,000 feet. The mathematical model was based on equations of motion which were extended to include products of the perturbation velocity terms. The effect of changing the mass distribution, the inclination of the longitudinal principal axis, and variation of C_{n_β} and C_{l_β} was investigated by changing the mathematical model as required by the parameter change considered and obtaining the REAC response to a fixed or standard step-function control input.

The results indicated that the lateral motion coupled into the longitudinal motion and that this effect was increased as the fuselage became longer and denser. Altitude aggravated this coupling as it did any trend toward instability caused by a change in the other parameters considered. The rudder caused greater coupling than the aileron. A positive inclination of the principal longitudinal axis caused an increase in dynamic stability and a decrease in coupling while a negative inclination had the opposite effect. A decrease in C_{n_β} produced a marked trend toward instability and an increase in coupling while a decrease in C_{l_β} had the opposite effect.

The investigation required by this thesis was carried out in the Computer Center of the University of Minnesota.

INTRODUCTION

Fighter aircraft of recent design show a trend toward long fuselages where most of the mass is concentrated, smaller aerodynamic surfaces, high rates of roll, and increased use of sweepback. Flight data from such aircraft indicate that the linear equations of motion, which result after several simplifying assumptions, do not always predict accurately the dynamic behavior. In addition, these same design trends have required more emphasis to be placed on the consideration of the dynamic stability of an aircraft in the design stage. In earlier practice, dynamic stability usually took care of itself after the static stability requirements were met.

The effect on coupling and dynamic stability caused by the parameters principally affected by these design trends was investigated by means of a mathematical model entered on the Reeves Electronic Analogue Computer (REAC). An attempt was made to use a representative or typical aircraft of the fighter type. The mathematical model was based on equations of motion which were extended to include the products of the velocity change usually assumed to be zero.

The mass distribution change was investigated by considering four configurations each more nearly approaching a missile from the standpoint of its moment of inertia properties. The effect of the inclination of the principal longitudinal axes was considered at

inclination angles of zero, plus ten, and minus ten degrees. The effect of C_{n_β} and C_{l_β} was studied by changing the mathematical model as required by a change in these parameters over a range of values. Altitude effects were considered by calculating the dimensional derivatives for 40,000 feet, changing the mathematical model accordingly, and running the program as it was done for the sea level case.

The effect of a parameter change was observed by obtaining successive REAC responses to a standard step function control input. Only the parameter investigated was changed so that any variation in the time history response was attributed to the parameter change. The data was presented by superimposing these successive time histories. The trend of the effect of the parameter change considered could then be easily observed.

DEVELOPMENT OF THE PROBLEM

The classical approach to airplane dynamics is outlined here in a very brief manner. The airplane was considered to be a rigid body. Six equations were required to define its motion; one force equation and one moment equation for each axis. These equations included the force and moment components due to aerodynamic and mass reactions together with the force of gravity and thrust effects. Second order effects were neglected and the equations simplified to a degree which permitted hand solution.

Appendix I develops the equations of motion used in this investigation. The classical approach has been used in general but certain departures have been made. In Appendix II the equations developed in Appendix I have been simplified by assuming that the airplane initially is in straight and level, steady, gliding flight. The thrust effects were allowed to go to zero since they are not critically essential in a dynamic stability study.

Derivative terms of order higher than one in the series expansion of the expressions for the forces and moments were neglected. The effect of these terms is known to be secondary, data was available only for the first derivative, and inclusion of these terms, even if available, would require more components than the REAC's provided. A second assumption generally made is that

the product of the perturbation velocities is essentially zero. This yields two independent sets of three linear equations. This assumption was not made. The equations simplified in Appendix II are presented below:

$$(II\text{-}7)\quad \dot{u} = X_u u + X_q q + X_w w + X_{\dot{w}} \dot{w} + vr - wq - g\theta$$

$$\dot{w} = Z_u u + Z_q q + Z_w w + Z_{\delta_e} \delta_e + qu - pv$$

$$\ddot{\theta} = \dot{q} = M_u u + M_q q + M_w w + M_{\delta_e} \delta_e + M_{\dot{w}} \dot{w} - pr\left(\frac{I_x - I_z}{I_y}\right) + r^2 \frac{I_{yz}}{I_y} - p^2 \frac{I_{xz}}{I_y}$$

$$\dot{v} = Y_r r + Y_v v + Y_p p + Y_{\delta_a} \delta_a + Y_{\delta_r} \delta_r + wp - ru + g\theta$$

$$\ddot{\phi} = \dot{p} = L_r r + L_v v + L_p p + L_{\delta_a} \delta_a + L_{\delta_r} \delta_r + \dot{r} \frac{I_{xz}}{I_x} - qr\left(\frac{I_z - I_y}{I_x}\right) + pq \frac{I_{xz}}{I_x}$$

$$\ddot{\psi} = \dot{r} = N_v v + N_r r + N_p p + N_{\delta_r} \delta_r + N_{\delta_a} \delta_a + \dot{p} \frac{I_{xz}}{I_z} + pq\left(\frac{I_y - I_x}{I_z}\right) - qr \frac{I_{xz}}{I_z}$$

The axes used and the sign convention observed is presented in Table I and illustrated in Fig. 8 which heads Table I.

Ref. 2 points out that motion of the longitudinal symmetric type does not induce motion of the lateral assymmetric type. An examination of the equation set presented above indicates that there are no terms which would couple symmetric motion into the assymmetric motion if the assymmetric motion were initially zero.

Duncan in Ref. 2 also points out that when deviations are so small that their squares and products can be neglected, there will be no coupling of the lateral motion into the symmetric motion. When the deviations

are not small longitudinal motion will persist alone, but a purely lateral motion will, in general, induce longitudinal motion. The motion will couple into the forward velocity through the term vr; the pitching velocity through the terms $pr\left(\frac{I_x - I_z}{I_y}\right)$, $r^2 \frac{I_{xz}}{I_y}$ and $p^2 \frac{I_{xz}}{I_y}$; and into the normal velocity, through the term pv. It can be observed that the coupling terms are modified generally by moments and products of inertia.

The study of the effect of the trend in mass distribution toward a long, dense fuselage was made by considering four cases starting with a hypothetical fighter airplane of conventional type. The characteristics of this basic airplane are presented in Table II. The fuselage was considered to represent 60 per cent of the airplane's mass. It was taken to have a maximum width of five feet and to have an eight-to-one slenderness ratio. The pitching moment of inertia calculated using these assumptions and the approximation that, for purposes of making an engineering estimate, the fuselage can be considered a long, slender cylinder resulted in a calculated value of the pitching moment of inertia which was very near the I_y of the airplane. As the mass became completely concentrated in the fuselage it was assumed that the slenderness ratio would increase to twelve to one, the fuselage width would remain the same, and that the pitching and yawing moments of inertia could be calculated using the long cylinder approximation. In this final form, the aircraft would

be a missile with I_z equal to I_y and I_x very small.

Fig. 10 illustrates the engineering approximation that was made of the variation in moments of inertia as the fuselage became longer and denser. The mass distribution changes were made while the aerodynamic damping terms, control power terms, mass and other effects were considered constant. This would, of course, be unrealistic but it has the advantage of studying the effect of a change in one parameter in the "partial derivative" sense.

The product of inertia term resulted largely from the fact that stability axes were used. When the x -axis is so oriented in an airplane in the steady flight condition that it is parallel to the relative wind, the Eulerian axes are referred to as stability axes. NACA TR 589 indicated that the I_{xz} terms were unimportant for conventional aircraft, however, Ref. 7 showed that the I_{xz} term may have a pronounced effect on the lateral stability of some high speed airplanes. It has already been noted that the I_{xz} term is involved in the coupling of the lateral and longitudinal motion.

If the longitudinal axes are inclined at an angle η to the flight path, the moments of inertia about the flight path axis and the axis normal to the flight path are:

$$I_x = I_{x_o} \cos^2\eta + I_{z_o} \sin^2\eta$$

$$I_z = I_{z_o} \cos^2\eta + I_{x_o} \sin^2\eta$$

$$I_{xz} = -(I_{z_o} - I_{x_o}) \sin\eta \cos\eta$$

The angle η largely results from the wing incidence angle and the angle of attack.

The trend toward swept wings and long fuselages makes C_{ℓ_β} and C_{n_β} increasingly important. Long fuselages adversely affect C_{n_β}, the "weather-cock" parameter. Swept wings have very large values of effective dihedral thus affecting, C_{ℓ_β}, the effective dihedral parameter. The effect of a change in these parameters on coupling and on dynamic stability was investigated. The change in the static derivative characteristics was selected for study since general flying characteristics are influenced primarily by the static stability parameters according to Ref. 6.

The coefficients such as L_v are dimensional stability derivatives. They are direct functions of airframe geometry, mass, mass distribution and flight conditions; in addition to being direct functions of the non-dimensional stability derivatives such as, C_{ℓ_β}. These basic non-dimensional stability derivatives are, in turn, implicit functions of airframe geometry, mass, mass distribution and flight conditions. The values of the non-dimensional stability derivatives for the basic airplane appear as Table II. The dimensional stability derivatives are defined in Tables III and IV. The values of the dimensional derivatives were calculated and appear as Table V. Refs. 1, 2, 3, 4, 7, 8, and 9 discuss these derivatives, their characteristics, and how they are determined. They are assumed to be

constant for a certain range of applicability and flight conditions.

The dimensional stability derivatives can be used directly as numerical coefficients in the dynamic equations of the airframe based on real time. Thus, stability derivatives in this form are used in setting up the mathematical model for the analogue computer. The use of this form of derivative permits the extension of the non-dimensional derivatives to other flight conditions with only secondary error. This was done to obtain the mathematical model of the airplane at 40,000 feet. Certain values of the non-dimensional derivatives which were specifically applicable to flight at this altitude were used while others were extended by the change in the values of ρ and U.

Phillips in Ref. 4 considered the effect of steady rolling on longitudinal and directional stability. The equations which he used can be arrived at from the equations developed in Appendix I by applying the assumptions that he made in order to arrive at an equation set which could be handled analytically. He retained the product terms which couple the longitudinal and lateral motions. He found that rapid rates of roll caused instability if the directional and longitudinal stabilities are different when the rolling frequency exceeds the lower of the pitching and yawing natural frequencies of the non-rolling airplane. The instability existed only while the air-

plane was rolling. In airplanes of short span and high fuselage density flying at high altitudes, this instability may cause dangerous attitude changes. Further, he found that when an airplane rolls about an axis which is not alligned with its longitudinal principal axis, forces were introduced which tended to swing the fuselage out of line with the flight path. These are the inertial forces usually neglected when the linearized equations are used.

In Ref. 4, Phillips made many assumptions in an effort to obtain equations which were capable of hand solution yet would predict the effect on coupling of steady rolling. In the investigation conducted incident to this thesis, the effects of the three motions, roll, pitch, and yaw, on coupling as produced by step-function control inputs were investigated. As many influencing factors were retained as the REAC's components would permit.

Solutions of the equations of motion used in this thesis would require the simultaneous solution of six differential equations, three of second order, made non-linear by product terms such as qr and pr. The labor involved would have been prohibitive. The equations were fitted to two REAC's and four servo-multipliers. The solutions were recorded simultaneously on two four-channel Sanborn recorders.

EQUIPMENT AND PROCEDURE

The equipment used to conduct the investigation consisted of two REAC's, four servo-multiplier units, two four channel Sanborn recorders, and a one-shot multi-vibrator time switch. The entire computing system is illustrated in the photograph presented as Fig. 2. The Sanborn recorder is shown in Fig. 3, the lateral motion and control function computer in Fig. 4, the longitudinal motion computer in Fig. 5, and the time switch in Fig. 6.

Each of the four servo-mechanisms drove three multiplying potentiometers. These multipliers provided $\frac{1}{100}$ of the product of the inputs. This restriction made it necessary to build up the perturbation velocities to ten times their actual value in order to obtain a simple product such as pr. The additional amplification required by the servo-multipliers made computer balance very delicate and this was a source of difficulty.

The Sanborn recorder made time history records of four quantities simultaneously. The imprint was made by a heated pen on sensitized paper. The point did not touch the paper, thus eliminating the drag usually associated with a recording pen.

The time switch was designed to provide an accurately timed step-function as a standard input. Basically, the switch is a one-shot multi-vibrator which fires just once when the operating button is pressed. This allows

current to flow in the coil of a relay in the plate circuit of the "normally-off" tube. The relay contacts send plus or minus 100 volts through the aileron, rudder, or elevator function switch, whichever is closed. The time that the relay remains closed is governed by the RC time constant controlled by the variable potentiometer. A range of from approximately 0.5 to 2.5 seconds was available. The electrical schematic is presented as Fig. 7. A photograph of the "bread-board" model appears as Fig. 6. The contacts of the relay carrying plus or minus 100 volts would appear electrically just ahead of the function switches in the REAC solution schematic which appears as Fig. 9.

The six equations of motion were put in computer form in Appendix II. These equations are II-13 through II-18. A computer schematic for the simultaneous solution of these equation was laid-out and appears as Fig. 9. From the schematic, patchboards were wired for the lateral motion and control computer and the longitudinal motion computer. This division of the problem was based on the wiring scheme which would use the fewest amplifiers. The apparent symmetry was incidental. The numerical values of the quantities entering the problem were translated into potentiometer settings. The values recorded were u, 10θ, w,

and $10\dot{\phi}$ on one recorder; v, 10ϕ, $10\dot{\psi}$, and $\dot{\theta}$ on the other recorder. The plus and minus 100 volts was placed on one side of the timer relay contacts. The other side of the relay contacts was connected to each of the control function switches, plus or minus, whichever was required by the schematic.

The graph representing the estimated mass distribution changes as the fuselage becomes longer and more dense is presented in Fig. 10. Values of the moments of inertia of three configurations were picked off this graph. New stability derivatives were calculated as necessary for these configurations. All of the moment derivatives such as L_v were affected. These calculated values were translated into potentiometer settings and appear as Tables VII and VIII.

The configurations investigated were called Case I, II, III and IV. The lateral computer was referred to as the "blue" computer and the longitudinal computer as the "red" computer. These are occasionally referred to in the tables using the abbreviations B and R.

The computers were balanced and the recorders calibrated. The patchboards were then installed on the computers. A rudder, elevator, or aileron control movement was then selected and the recorder tape set in motion at the desired speed. Pushing the time switch

button sent an accurately timed standard step-function through the control switch selected. The solutions of the equations of motion in response to a step-function input were recorded as time histories of the variables on eight recorder channels simultaneously. The next case was then entered on the potentiometers and the solutions obtained as before. These solutions are presented as Figs. 12A, 12B, 13A, 13B, 14A, and 14B.

The dimensional stability derivatives were recalculated using data for 40,000 feet and the required angle of attack increase obtained from Table II. Where specific non-dimensional derivatives were not available for this altitude, those for low altitude were extended by using the values of ρ and U at 40,000 feet in the formulae of Tables III and IV. These stability derivatives and other factors of the problem which changed at 40,000 feet were translated into potentiometer settings and run off as before. The settings appear in Tables IX and X. The results for Cases I and IV are presented in Figs. 15A, 15B, 16A, 16B, 17A and 17B. It should be pointed out that the airplane which was marginal in dynamic directional stability at sea-level was unstable at 40,000 feet. In order to "fly" even marginally at this altitude the N_v potentiometer was set to 0.0115 and the L_v potentiometer to zero. This had the effect of increasing the "weather-cock" stability parameter about six times and reducing the effective dihedral

parameter to zero. The computer procedure was as before. It should be noted that solutions were obtained only for Cases I and IV modified as described above.

The effect of inclination of the longitudinal principal axis to the flight path was investigated by calculating values of moments and products of inertia for inclination angles η of plus ten, zero, and minus ten degrees. The equations below obtained from Ref. 6 were used:

$$I_x = I_{x_o} \cos^2\eta + I_{z_o} \sin^2\eta$$

$$I_z = I_{z_o} \cos^2\eta + I_{x_o} \sin^2\eta$$

$$I_{xz} = -(I_{z_o} - I_{x_o}) \sin\eta \cos\eta$$

It was found that only the I_{xz} value varied significantly. New values of the coefficients containing I_{xz} were calculated and translated into potentiometer settings. These are presented in Table XI. Several sign changes were required. These were accomplished by using inverters as necessary. The computer was operated as before using Case I at low altitude.

The C_{n_β} and C_{ℓ_β} programs were accomplished by changing these values over the range considered, recalculating the affected stability derivatives, and translating them into potentiometer settings. This was done for Case I at sea level and at 40,000 feet. These values are presented in Tables XII and XIII. The computer operation was similar to the other programs.

RESULTS AND DISCUSSION

Time histories of the variables u, w, θ, v, ϕ, $\dot{\theta}$, $\dot{\phi}$, and $\dot{\psi}$ were recorded as the airplane responded to a step function control input for each change in a parameter being investigated. To study the trend of the effect of the parameter changes, the curves were superimposed, each curve being drawn with a characteristic line. These composite solution curves are presented as Figs. 12A through 23B. The standard step function time plot appears as Fig. 11. It should be noted that the A and B parts of the figures each represent one of the four channels which were simultaneously recorded. Where separate lines for each parameter change can not be observed, it should be assumed that the curve lies behind the previous curve, or curves, and that no significant change was caused by the new value of the parameter.

The mass distribution program is presented in the Figs. 12A, 12B, 13A, 13B, 14A, and 14B. The elevator response curves show no significant changes caused by the changed moments of inertia. The elevator set-up the phugoid motion which remained essentially constant. The short period motion was virtually dead-beat damped. The amplitude of $\dot{\theta}$ in Case IV is reduced since the aircraft was more sluggish to pitch change due to the increased pitching moment of inertia. A slight dutch-roll was induced. This was not anticipated since the equations indicated that there would be no coupling

from the symmetric motion into the lateral motion if there was no initial lateral motion. A possible explanation might be that there was some unbalance in the servo-multipliers or jitter in the lateral motion computer due to small line current variations. The same effect might be observed in flight tests caused by slightly unsymmetrical control application or small trim unbalance. Spiral instability was set-up presumably by the same mechanism which caused the slight dutch-roll to start.

The cross-coupling set-up by the aileron and rudder motion can be observed in the ω plot. The coupling caused by the more assymmetric motion induced by the rudder step is several times that of the aileron cross-coupling. The aileron's cross-coupling decreased as the values of I_4 and I_z were increased. This was unexpected but can possibly be explained by the fact that two opposing effects were taking place. The coupling increased but the airplane became more sluggish since the pitch and yaw moments of inertia were increased. This sluggishness can be observed in the progressive decrease in amplitude and frequency of and v . The large decrease in roll moment of inertia had very little effect on ϕ and $\dot{\phi}$.

The altitude effects on coupling and dynamic stability are presented in Figs. 15A, 15B, 16A, 16B, 17A, and 17B. Many of the observations made in the

sea-level program apply here. The short period oscillation damping decreased increasing the period of this motion. The aileron coupling was larger for Case IV, that is, as the fuselage became long and dense. The same effect was observed in the coupling caused by the rudder. This time there was little amplitude difference between the aileron and rudder coupling. The sluggishness caused by increased I_y and I_z, together with decreased aerodynamic damping, made the swings progressively larger in amplitude and period. The roll angle did not significantly change.

In the program which considered the effect of changing the inclination of the longitudinal principal axis to the flight path, the I_{xz} program essentially, only the rudder and aileron step input response was investigated. As η became more positive, dynamic stability increased; more negative, dynamic stability decreased. At an η of minus ten degrees, dynamic instability developed. From the coupling standpoint, the same effect was observed. There is less coupling when η becomes more positive; more when η becomes more negative. The rudder curves show these effects more clearly than the aileron curves.

The effects caused by varying the "weather-cock" parameter, C_{n_β}, is presented in Figs. 20A, 20B, 21A and 21B. Only the aileron and rudder forcing functions were considered. The curves for two values of C_{n_β}

at high altitude were superimposed on the sea-level curves. At both altitudes similar effects were observed. Coupling increased as C_{n_β} decreased. The dynamic lateral stability decreased as C_{n_β} decreased. This was to be expected, of course, since decreased tail arm, or tail area, lead toward lateral instability. As the angular velocity changes increased with this instability the coupling increased.

The curves for the C_{l_β} program are presented in Figs. 22A, 22B, 23A and 23B. The entire sea-level program was presented but only the curve for a C_{l_β} of 0.20 at 40,000 feet was added. As C_{l_β} was increased dynamic, lateral instability quickly developed along with increasing coupling. The effect was more apparent in the motion caused by the rudder forcing function. The reduced damping at altitude hastened the development of instability and the coupling increased. The curve for a C_{l_β} of 0.20 was marginally stable at sea level but unstable at 40,000 feet.

The parameters C_{n_β} and C_{l_β} had very significant effects on dynamic stability. The effective dihedral parameter, C_{l_β}, was very critical. This would appear to make analysis of the dynamics of the airframe very important in the design stage of swept-wing and delta-wing aircraft. The REAC provides a powerful tool for such an analysis.

The use of a standard step-function input provided a good means for studying the effect of a parameter change. However, this method was inadequate from the standpoint of bringing out any instabilities caused by cross-coupling of the type investigated in Ref. 4.

It should be pointed out that the dynamic behavior observed was that of one airplane, or variation of one airplane. Although effort was made to make the mathematical model investigated "typical" , it would not be reasonable to suggest that all airplanes behave in the manner of the airplane investigated. On the other hand, the procedures used in the analysis were straight-forward and it is felt that the dynamic behavior observed might be considered reasonably typical.

CONCLUSIONS AND RECOMMENDATIONS

1. Mass distribution changes had no significant effect on the motion of the aircraft in the longitudinal plane.
2. The motion of the aircraft in the symmetrical plane coupled into the lateral motion in the form of a slight dutch roll and also triggered the spiral instability mode. However, this is believed to have been due to slight assymmetry in the computing system.
3. The assymmetrical motion of the airplane coupled into the motion in the symmetrical plane and is most significant as a change in w . This would be equivalent to a change in the angle of attack.
4. The coupling effect increased as the fuselage became longer and more dense.
5. The assymmetrical motion caused by the rudder had a greater coupling effect than the motion caused by the aileron.
6. At high altitudes both the coupling and the trend toward instability increased.
7. At a positive inclination of the principal longitudinal axis to the flight path, there was less coupling and increased dynamic stability. A negative inclination angle had the opposite effect.

8. A decrease in the "weather-cock" stability parameter, C_{n_β}, resulted in a decrease in dynamic stability and an increase in coupling.

9. An increase in the effective dihedral parameter, C_{l_β}, resulted in a decrease in dynamic stability and an increase in coupling.

10. The standard step-function input which supplied the forcing function provided a means for studying the effect of a parameter change on the coupling and the dynamic stability of the airplane. However, it does not appear adaptable to the investigation of instabilities which may develop from the coupling caused by rapid rolling or yawing. An investigation might do this by using a programmed input which would reverse before the REAC limits were reached.

The dynamic behavior observed in this investigation was that of the mathematical model of one airplane or variation of one airplane. Effort was made to use a mathematical model which could be considered reasonably "typical". However, it would not be reasonable to suggest that all airplanes would respond similarly.

BIBLIOGRAPHY AND REFERENCES

1. "Dynamics of the Airframe", BuAer Report AE-61-4II, Servomechanisms section and Aerodynamics Section, Northrup Aircraft, Inc., 1953.
2. Duncan, W. J., "The Principles of the Control and Stability of Aircraft," Cambridge at the University Press, 1952.
3. Dommasch, D. O.; Sherby, S. S.; Connolly, T. F.; "Aeroplane Aerodynamics", Pitman Publishing Corporation, 1951.
4. Phillips, W. H.; "Effect of Steady Rolling on Longitudinal and Directional Stability", NACA TN No. 1627, 1948.
5. McKinney, Marion O. Jr. and Drake, H. M., "Correlation of Experimental and Calculated Effects of Product of Inertia on Lateral Stability", NACA TN No. 1370, 1947.
6. Sternfield, L., "Effect of Product of Inertia on Lateral Stability", NACA TN No. 1193, 1947.
7. Bird, J. D. and Jaquet, B. M.; "A Study of the use of Experimental Stability Derivatives in the Calculation of the Lateral Disturbed Motions of a Swept-wing Airplane and Comparison with Flight Results", NACA TN No. 2013, 1950.
8. Diehl, W. S., "Engineering Aerodynamics", The Ronald Press Company, New York, 1936.

9. Perkins, C. D. and Hage, R. E., "Airplane Performance Stability and Control", John Wiley & Sons, Inc., 1949.

10. Jones, R. T. and Cohen, Doris; "An Analysis of the Stability of an Airplane with Free Controls", NACA Rep. No. 709, 1941.

11. Jones, R. T., "A Simplified Application of the Method of Operators to the Calculation of Disturbed Motions of an Airplane", NACA Rep. No. 560, 1936.

12. Jones, R. T. and Weick, F. E.; "The Effect of Lateral Controls in Producing Motion of an Airplane as Computed from Wind Tunnel Data", NACA Rep. No. 570, 1936.

13. Jones, R. T., "The Influence of Lateral Stability on Disturbed Motions of an Airplane with Special Reference to the Motion Produced by Gusts", NACA TR 638, 1938.

14. Korn, G. A. and Korn, T. M.; "Electronic Analogue Computers", McGraw-Hill Book Company, Inc., 1952.

SYMBOLS

U_o initial airspeed, feet per second

ρ mass density of air, slugs per cubic foot

b wing span, feet

S wind area, square feet

W weight of airplane, pounds

m mass, slugs

g acceleration of gravity, feet per second per second

AR aspect ratio

M Mach number

c_t wing chord tip, feet

c_r wing chord root, feet

I_{x_o} moment of inertia about principal longitudinal axis, slug-feet^2

I_{y_o} moment of inertia about principal tranverse axis, slug-feet^2

I_{z_o} moment of inertia about principal normal axis, slug-feet^2

I_{xz} moment of inertia about flight path axis, slug-feet^2

I_Y moment of inertia about the pitching axis, slug-feet^2

I_z moment of inertia about the yawing axis, slug-feet^2

I_{xz} product of inertia with respect to the flight path axis and axis normal to flight path, slug-feet^2

F force, pounds

h moment of momentum, (slug-ft)-ft per second

C_L lift coefficient, $\frac{\text{Lift force}}{qS}$

C_ℓ rolling moment coefficient, $\frac{\text{Rolling moment}}{qSb}$

C_y lateral-force coefficient, $\frac{\text{lateral force}}{qS}$

C_m aerodynamic pitching moment coefficient about the c.g.

C_D drag coefficient, $\frac{\text{Drag force}}{qS}$

ϕ angle of bank, radians

θ angle of pitch, radians

ψ angle of yaw, radians

δ control deflection, radians

β angle of sideslip, radians

γ flight path angle; angle between relative wind and the horizontal, radians

η angle between the longitudinal axis of the fuselage and the relative wind, radians

ξ angle between the thrust line and the longitudinal axis of the fuselage, radians

z_j perpendicular distance from c.g. to the thrust line, feet

ζ fraction of critical damping

ω frequency, radians/sec.

U initial forward velocity in direction of positive axis (feet per second)

V initial side velocity (feet per second)

W initial normal velocity (feet per second)

u forward velocity change after disturbance (feet per second)

v side velocity change after disturbance (feet per second)

w normal velocity change after disturbance (feet per second)

P initial rolling angular velocity (radians per second)

Q initial pitching angular velocity (radians per second)

R initial yawing angular velocity (radians per second)

$p, \dot{\phi}$ rolling angular velocity increment, radians per second

$q, \dot{\theta}$ pitching angular velocity increment, radians per second

$r, \dot{\psi}$ yawing angular velocity increment, radians per second

C_{D_u} the change in drag coefficient with varying forward velocity

C_{D_α} the change in drag coefficient with varying angle of attack, per radian

C_{Y_p} rate of change of lateral-force coefficient with rolling-angular-velocity factor, per radian

C_{Y_r} rate of change of lateral-force coefficient with yawing-angular-velocity factor, per radian

C_{Y_β} lateral force derivative, rate of change of lateral force coefficient with angle of sideslip, per radian

$C_{Y_{\delta_r}}$ the change in side force coefficient with variation in rudder deflection, per radian

$C_{Y_{\delta_a}}$ the change in side force coefficient with aileron deflection, per radian

C_{L_u} change in lift coefficient with variation in forward velocity, angle of attack and attitude remaining constant

C_{L_q} change in lift coefficient with varying pitching velocity, no change of airplane angle of attack as a whole, per radian

C_{L_α} the change in lift coefficient with varying angle of attack, "lift curve slope", per radian

$C_{L_{\delta_e}}$ change in lift coefficient with changes in elevator deflection, per radian

C_{l_r} rate of change of rolling moment coefficient with yawing angular velocity factor, per radian

C_{l_β} effective-dihedral derivative, rate of change of rolling moment coefficient with angle of side-slip, per radian

C_{l_p} damping in roll derivative, rate of change of rolling moment coefficient with rolling-angular-velocity factor, per radian

$C_{l_{\delta_r}}$ change in rolling moment coefficient with variation in rudder deflection, per radian

$C_{l_{\delta_a}}$ aileron effectiveness on aileron power, the change in rolling moment coefficient with change in aileron deflection, per radian

C_{m_α} longitudinal static stability derivative, change in pitching moment coefficient with varying angle of attack, per radian

$C_{m_{\dot{\alpha}}}$ the change in pitching moment coefficient with variation in rate of change of angle of attack, per radian

C_{m_q} pitch damping derivative, change in pitching moment coefficient with varying pitch velocity, per radian

$C_{m_{\delta_e}}$ elevator effectiveness or elevator power, the change in pitching moment coefficient with change in elevator deflection, per radian

C_{n_β} directional stability derivative, weather-cock stability, rate of change of yawing-moment coefficient with angle of sideslip $\left(\frac{\partial C_n}{\partial \beta}\right)$ per radian

C_{n_r} damping in yaw derivative, rate of change of yawing moment with yawing angular velocity factor, per radian $\left(\frac{\partial C_n}{\partial \frac{rb}{2V_o}}\right)$

C_{n_p} rate of change of yawing moment coefficient with rolling angular velocity factor, per radian $\left(\frac{\partial C_n}{\partial \frac{pb}{2V_o}}\right)$

$C_{n_{\delta_r}}$ rudder effectiveness or rudder power, the change in yawing moment coefficient with variation in rudder deflection, per radian

$C_{n_{\delta_a}}$ change in yawing moment coefficient with change in aileron deflection, per radian

X_u change in fore and aft force with change in forward velocity, per second

X_q change in fore and aft force, change in pitching velocity, feet per second-radian

X_w change in fore and aft force with change in normal velocity, per second

$X_{\dot{w}}$ change in fore and aft force with rate of change in normal velocity, per foot

X_r change in side force with change in yawing velocity, per radian

Y_v change in side force with change in side velocity, per second-radian

Y_p change in side force with change in rolling velocity, per radian

Y_{δ_a} change in side force with aileron deflection, per second-radian

Y_{δ_r} change in side force with rudder deflection, per second-radian

Z_u change in normal force with varying forward velocity, per second

Z_q change in normal force with varying pitching velocity, feet per second-radian

Z_w change in normal force with varying vertical velocity, per second

Z_{δ_e} change in normal force with elevator deflection, feet per second^2-radian

L_r change in rolling moment with varying yawing velocity, per second-radian

L_v change in rolling moment with varying side velocity, per second-feet

L_p change in rolling moment with varying rolling velocity, per second-radian

L_{δ_r} change in rolling moment with rudder deflection, per second^2-radian

L_{δ_a} change in rolling moment with aileron deflection, per second^2-radian

M_u change in pitching moment with varying forward velocity, per second-feet

M_w change in pitching moment with varying vertical velocity, per second-feet

$M_{\dot{w}}$ change in pitching moment with rate of change of vertical velocity, per foot

M_q change in pitching moment with varying pitching velocity, per second-radian

M_{δ_e} change in pitching velocity with elevator deflection, per second^2-radian

N_v change in yawing moment with varying side velocity, per second-feet

N_r change in yawing moment with varying yawing velocity, per second-radian

N_p change in yawing moment with varying rolling velocity, per second-radian

N_{δ_r} change in yawing moment with rudder deflection, per second^2-radian

N_{δ_a} change in yawing moment with aileron deflection, per second^2-radian

N_β change in yawing moment with side-slip angle, per second^2-radian

$( )_o$ refers to initial steady flight condition

$( )_x$ pertains to the fore and aft axis

$( )_y$ pertains to the transverse axis

$( )_z$ pertains to the normal axis

$( )_e$ elevator

$( )_a$ aileron

$( )_r$ rudder

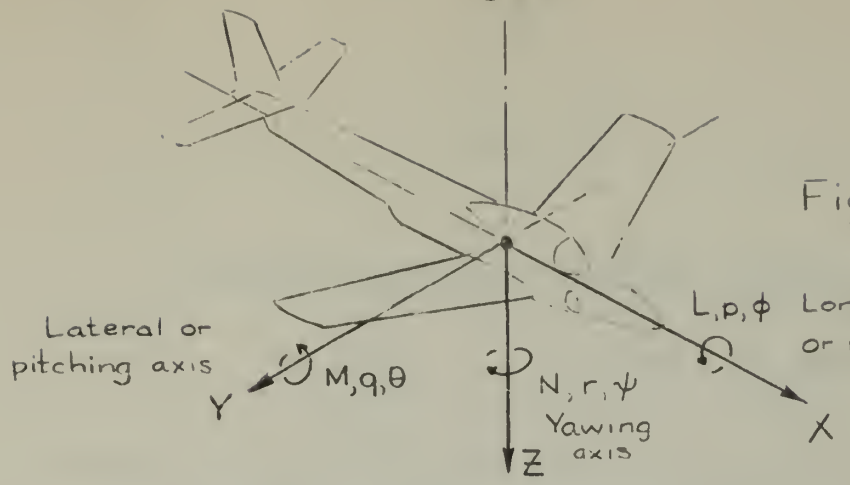

Fig. 8

TABLE I NOTATION FOR AXES SYSTEM

Axis Designation	Longitudinal	Lateral	Yawing
Symbol	X	Y	Z
Force (parallel to axis) symbol	X	Y	Z
Sign convention	Forward +	To right +	Down +
Linear Velocity	U	V	W
Change in linear velocity	u	v	w
Sign Convention	Forward +	To right +	Down +
Moment about axis	Rolling moment	Pitching moment	Yawing moment
Symbol	L	M	N
Coefficient	C_ℓ	C_m	C_n
Formula	$L=\frac{1}{2}\rho V^2 S b C_L$	$M=\frac{1}{2}\rho V^2 S c C_m$	$N=\frac{1}{2}\rho V^2 S b C_n$
Sign convention	Right roll $+(Y\rightarrow Z)$	Nose up $+(Z\rightarrow X)$	Nose right $+(X\rightarrow Y)$
Moment of Inertia	I_x	I_y	I_z
Angular Displacement	Roll angle	Pitch angle	Yaw angle
Symbol	ϕ	θ	ψ
Sign convention	Right roll +	Nose up +	Nose right +
Angular Velocity	Rolling velocity	Pitching velocity	Yawing velocity
Symbol	P	Q	R
Change in angular velocity	$p=\dot{\phi}$	$q=\dot{\theta}$	$r=\dot{\psi}$
Sign convention	Right roll +	Nose up +	Nose right +

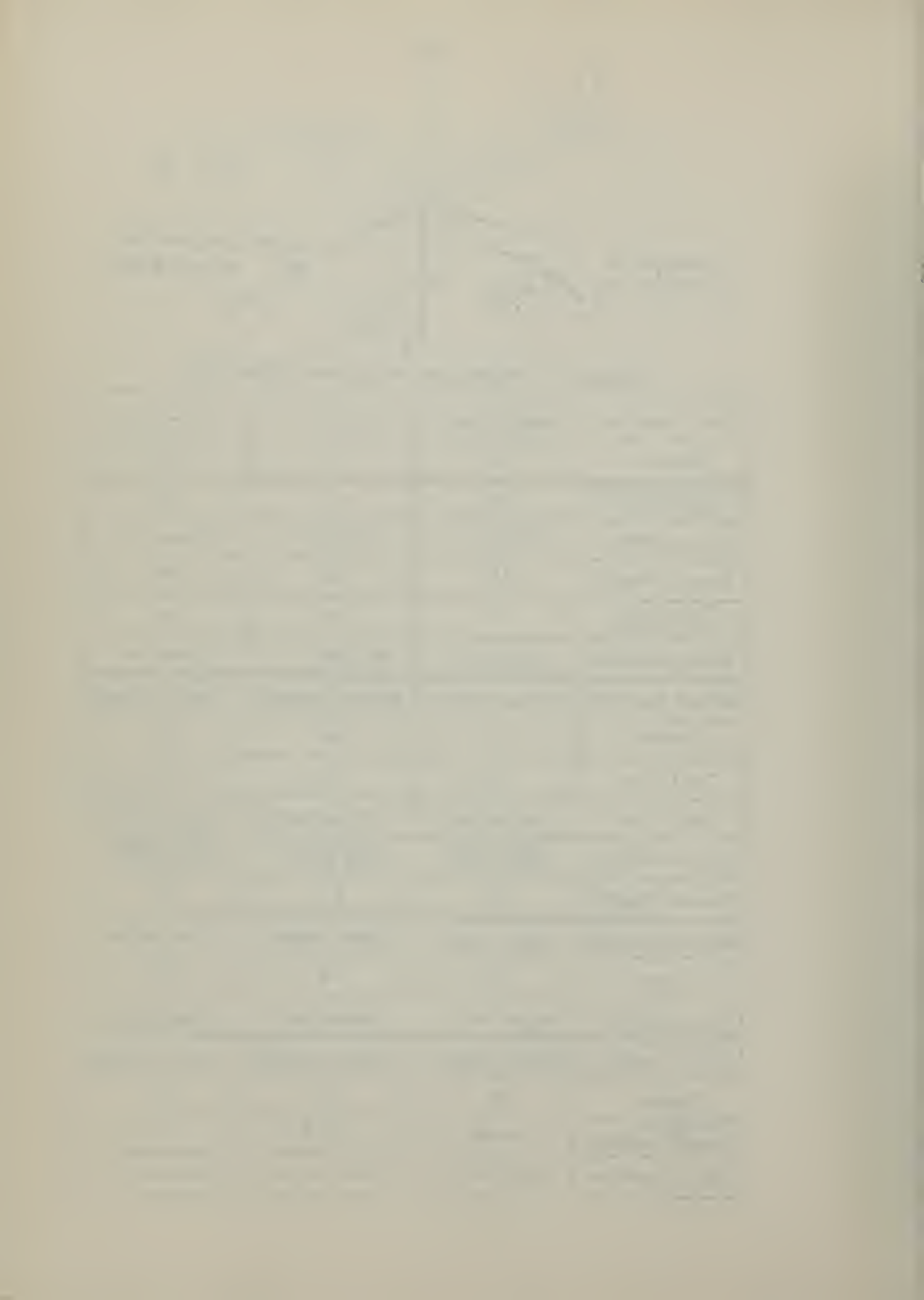

Table II

CHARACTERISTICS OF THE BASIC AIRPLANE

M = 0.6 Altitude = Sea level

W	30,000 lbs.	C_D	.024 at C_L=.4	C_{Y_p}	-.02 at C_L=0
m	932 slugs	C_L	.1 at s.l.	C_{Y_p}	+.04 at C_L=.6
U_o	670 ft/sec	C_L	.56 at 40,000'	$C_{Y_{\delta_r}}$	.062
ρ_{SL}	.00238 $\frac{slugs}{ft^3}$	C_{D_u}	0	C_{n_r}	-.03
S	630 ft^2	C_{D_α}	.05 at C_L=.1	C_{n_p}	.008 at C_L=0
b	56 ft.	$C_{D_{\dot\alpha}}$	.21 at C_L=.4	C_{n_p}	-.024 at C_L=.6
c_t	7.5 ft.	C_{L_u}	.02 at C_L=.1	$C_{n_{\delta_r}}$	-.036
c_r	15 ft	C_{L_α}	+ 5.0	$C_{n_{\delta_a}}$	.008 at C_L=0
AR	5	$C_{L_{\dot\alpha}}$	1.4	$C_{n_{\delta_a}}$	-.012 at C_L=.6
I_x	53000 slug-ft^2	C_{L_q}	3.8	C_{ℓ_β}	-.10 heavy wing loading
I_y	80,000 slug-ft^2	$C_{L_{\delta_e}}$	-.17	C_{ℓ_r}	.012 at C_L=0
I_z	124,000 slug-ft^2	C_{m_u}	-.002 at C_L=.1	C_{ℓ_r}	.11 at C_L=.6
I_{xz}	4000 slug-ft^2	C_{m_α}	-.24 c.g. at 25% MAC	C_{ℓ_p}	-.44 heavy wing loading
I_{x_o}	52,500 slug-ft^2	$C_{m_{\dot\alpha}}$	- 3.1	$C_{\ell_{\delta_r}}$	.008 at C_L=0
I_{y_o}	80,000 slug-ft^2	C_{m_q}	- 10.6	$C_{\ell_{\delta_r}}$	.003 at C_L=.5
I_{z_o}	124,500 slug-ft^2	$C_{m_{\delta_e}}$	.81	$C_{\ell_{\delta_a}}$	.176
η	- 3.25°	C_{Y_β}	-.32 at C_L=0	C_{n_β}	.055
C_D	.014 at C_L=0.1	C_{Y_r}	.12	$C_{m_{c.g.}}$	0

Table III

LONGITUDINAL STABILITY DERIVATIVES			
X_u	$\frac{\rho US}{m}(-C_{D_u}-C_D)$	$X_q \doteq$	0
Z_u	$\frac{\rho US}{m}(-C_{L_u}-C_L)$	Z_q	$-\frac{\rho USc}{4m}C_{L_q}$
M_u	$\frac{\rho USc}{I_x}(C_{m_u}+C_m)$	M_q	$\frac{\rho USc^2}{4I_Y}C_{m_q}$
T_u	$\frac{\rho US}{m}(C_{T_u}+C_T)$	$T_{\delta_{rpm}}$	$\frac{30\rho USc}{m}C_{T_{\delta_{rpm}}}$
X_w	$\frac{\rho US}{2m}(C_L-C_{D_\alpha})$	X_{δ_e}	$-\frac{\rho U^2S}{2m}C_{D_{\delta_e}}$
Z_w	$\frac{\rho US}{2m}(C_{L_\alpha}-C_D)$	Z_{δ_e}	$-\frac{\rho U^2S}{2m}C_{L_{\delta_e}}$
M_w	$\frac{\rho USc}{2I_y}C_{m_\alpha}$	M_{δ_e}	$\frac{\rho U^2Sc}{2I_Y}C_{m_{\delta_e}}$
$X_{\dot{w}} \doteq$	0	X_{δ_F}	$-\frac{\rho U^2S}{2m}C_{D_{\delta_F}}$
$Z_{\dot{w}}$	$-\frac{\rho Sc}{4m}C_{L_{\dot{\alpha}}}$	Z_{δ_F}	$-\frac{\rho U^2Sc}{2m}C_{L_{\delta_F}}$
$M_{\dot{w}}$	$\frac{\rho Sc^2}{4I_y}C_{m_{\dot{\alpha}}}$	M_{δ_F}	$\frac{\rho U^2Sc}{2I_Y}C_{m_{\delta_F}}$

Table IV

LATERAL STABILITY DERIVATIVES			
Y_v	$\frac{\rho US}{2m}C_{Y_\beta}$	Y_r	$\frac{\rho USb}{4m}C_{Y_r}$
L_v	$\frac{\rho USb}{2I_x}C_{l_\beta}$	L_r	$\frac{\rho USb^2}{4I_x}C_{l_r}$
L_β	$U_o L_v$	N_r	$\frac{\rho USb^2}{4I_z}C_{n_r}$
N_v	$\frac{\rho USb}{2I_z}C_{n_\beta}$	Y_{δ_r}	$\frac{\rho U^2S}{2m}C_{y_{\delta_r}}$
N_β	$U_o N_v$	L_{δ_r}	$\frac{\rho U^2Sb}{2I_x}C_{l_{\delta_r}}$
Y_p	$\frac{\rho USb}{4m}C_{Y_p}$	N_{δ_r}	$\frac{\rho U^2Sb}{2I_z}C_{n_{\delta_r}}$
L_p	$\frac{\rho USb^2}{4I_x}C_{l_p}$	Y_{δ_a}	$\frac{\rho U^2S}{2m}C_{Y_{\delta_a}}$
N_p	$\frac{\rho USb^2}{4I_z}C_{n_p}$	L_{δ_a}	$\frac{\rho U^2Sb}{2I_x}C_{l_{\delta_a}}$
		N_{δ_a}	$\frac{\rho U^2Sb}{2I_z}C_{n_{\delta_a}}$

Table V

DIMENSIONAL DERIVATIVES OF THE BASIC AIRPLANE M = 0.6 ALTITUDE, SEA LEVEL			
X_u, $\frac{1}{sec}$	-.0151	L_v, $\frac{1}{sec\text{-}ft}$	-.054
X_q, $\frac{ft}{sec\text{-}rad}$	0	L_p, $\frac{1}{sec\text{-}rad}$	-6.53
X_w, $\frac{1}{sec}$	+.0269	L_{δ_r}, $\frac{1}{sec^2\text{-}rad}$	+2.84
$X_{\dot{w}}$ $\frac{1}{ft}$	0	L_{δ_a}, $\frac{1}{sec^2\text{-}rad}$	+62.5
Y_r, $\frac{1}{rad}$	+1.81	M_u, $\frac{1}{sec\text{-}ft}$	-.000282
Y_v, $\frac{1}{sec\text{-}rad}$	-.173	M_w, $\frac{1}{sec\text{-}ft}$	-.034
Y_p, $\frac{1}{rad}$	-.302	M_q, $\frac{1}{sec\text{-}rad}$	-16.86
Y_{δ_a}, $\frac{1}{sec\text{-}rad}$	0	M_{δ_e}, $\frac{1}{sec^2\text{-}rad}$	+76.3
Y_{δ_r}, $\frac{1}{sec\text{-}rad}$	+22.4	$M_{\dot{w}}$, $\frac{1}{ft}$	-.00184
Z_u, $\frac{1}{sec}$	-.130	N_v, $\frac{1}{sec\text{-}ft}$	+.0125
Z_q, $\frac{ft}{sec\text{-}rad}$	+11.55	N_r, $\frac{1}{sec\text{-}rad}$	-.190
Z_w, $\frac{1}{sec}$	-2.70	N_p, $\frac{1}{sec\text{-}rad}$	+.0508
Z_{δ_e}, $\frac{ft}{sec^2\text{-}rad}$	+61.3	N_{δ_a}, $\frac{1}{sec^2\text{-}rad}$	+1.21
L_r, $\frac{1}{sec\text{-}rad}$	+1785	N_{δ_r}, $\frac{1}{sec^2\text{-}rad}$	-5.46

Table VI

POTENTIOMETER SETTINGS FOR LATERAL AND CONTROL COMPUTER · MASS DISTRIBUTION PROGRAM (Sea Level)

POTENTIOMETER	PARAMETER AFFECTED	CASE I	CASE II	CASE III	CASE IV
1	$\frac{1}{4}\ \frac{I_{xz}}{I_y}$	0.3	.0058	.0028	.001
2	$\frac{I_x - I_z}{I_y}$	.890	.943	.970	.982
3	$\frac{1}{40}\ M_q$	.435	.260	.185	.143
4	$\frac{1}{4}\ g$	.819	.819	.819	.819
5	X_u	.015	.015	.015	.015
6	Z_u	.130	.130	.130	.130
7	$\frac{1}{1000}\ U_o$	.674	.674	.674	.674
8	$\frac{1}{40}\ Z_q$	.297	.297	.297	297
9	$\frac{1}{4}\ Z_w$	.692	.692	.692	.692
10	X_w	.027	.027	.027	.027
11	M_w	.034	.0203	.0145	.0112
12	Z_{δ_e} (2.5°)	.027	.027	.027	.027
13	$\frac{1}{100}\ M_{\delta_e}$ (2.5°)	.034	.0203	.0145	.0112
14	$\frac{1}{100}\ N_{\delta_a}$ (5°)	.0011	.0008	.0006	.0005
15	$\frac{1}{100}\ N_{\delta_r}$ (5°)	.0047	.0035	.0028	.0023
16	$\frac{1}{10}(N_{\delta_a}\delta_a + N_{\delta_r}\delta_r)$	.103	.103	.103	.103
17	Y_{δ_r} (5°)	.020	.020	.020	.020
18	$\frac{1}{100}\ L_{\delta_r}$ (5°)	.0025	.0032	.0045	.0077
19	$\frac{1}{100}\ L_{\delta_a}$ (5°)	.055	.071	.100	.172
20	$\frac{1}{4}(Y_{\delta_r}\delta_r + w\dot{\theta})$	.256	.256	.256	.256
21	$\frac{1}{4}(L_{\delta_a}\delta_a + L_{\delta_r}\delta_r)$	.256	.256	.256	.256

Table VII

POTENTIOMETER SETTINGS FOR LONGITUDINAL COMPUTER MASS DISTRIBUTION PROGRAM - SEA LEVEL

POTENTIOMETER SETTING	PARAMETER AFFECTED	CASE I	CASE II	CASE III	CASE IV
1	N_r	.013	.010	.008	.006
2	$\frac{N_n}{10}$	.019	.0141	.0011	.0092
3	$\frac{1}{4}\left(\frac{I_y - I_x}{I_z}\right)$	.055	.1405	.190	.224
4	$\frac{I_{xz}}{I_z}$	.033	.0184	.0097	.004
5	$\frac{N_p}{10}$	.005	.0037	.0029	.0024
6	$\frac{1}{4}\frac{I_{xz}}{I_z}$	.008	.0045	.0024	.001
7	$\frac{I_z - I_y}{I_x}$	.859	.833	.821	.733
8	$\frac{1}{4}\frac{I_{xz}}{I_x}$	.019	.0184	.0174	.0148
9	$\frac{I_{xz}}{I_x}$	.076	.0737	.0695	.0593
10	$\frac{L_p}{100}$	.067	.087	.122	.209
11	$\frac{1}{10} L_r$	.018	.0232	.033	.0562
12	$\frac{1}{1000} U_o$	.711	.711	.711	.711
13	$\frac{1}{40} g$	.819	.819	.819	.819
14	$\frac{1}{10} Y_r$	.182	.182	.182	.182
15	$\frac{1}{10} Y_p$	.030	.030	.030	.030
16	Y_v	.174	.174	.174	.174
17	L_v	.054	.0696	.0987	.168

Table VIII

Moments and Products of Inertia

for Cases I, II, III and IV

Case	I	II	III	IV
I_x (slug - ft²)	53,000	41,000	29,000	17,000
I_y (slug - ft²)	80,000	134,000	188,000	243,000
I_z (slug - ft²)	124,000	167,000	211,000	255,000
I_{xz} (slug - ft²)	4,000	3,000	2,000	1,000

Table IX

POTENTIOMETER SETTINGS
FOR LATERAL AND CONTROL COMPUTER
MASS DISTRIBUTION PROGRAM (40,000 FEET)

POTENTIOMETER	CASE I	CASE II	CASE III	CASE IV
1	.013	.0058	.0028	.0011
2	.890	.943	.970	.982
3	.0925	.0553	.0384	.0308
4	.819	.819	.819	.819
5	.0070	.0070	.0070	.0070
6	.134	.134	.134	.134
7	.583	.583	.583	.583
8	.0632	.0632	.0632	.0632
9	.1474	.1474	.1474	.1474
10	.0299	.0299	.0299	.0299
11	.0073	.0043	.0031	.0024
12	.0099	.0099	.0099	.0099
13	.0128	.0074	.0053	.00408
14	.0005	.0004	.0003	.0003
15	.0025	.0018	.0014	.0012
16	.103	.103	.103	.103
17	.0018	.0018	.0018	.0018
18	.0001	.0002	.0003	.0006
19	.005	.007	.0092	.0143
20	.256	.256	.256	.256
21	.256	.256	.256	.256

Note: $\delta_e = 5°$
$\delta_r = \delta_a = 2.5°$

Table X

POTENTIOMETER SETTINGS

FOR LONGITUDINAL COMPUTER

MASS DISTRIBUTION PROGRAM 10,000 FEET

POTENTIOMETER	CASE I	CASE II	CASE III	CASE IV
1	.0115	(.0019)	(.0016)	.0056
2	.0041	.003	.0024	.0020
3	.055	.1405	.190	.224
4	.033	.0184	.0097	.004
5	.00325	.0024	.0019	.0016
6	.008	.0045	.0024	.001
7	.859	.833	.821	.733
8	.019	.0184	.0174	.0148
9	.076	.0737	.0695	.0593
10	.0139	.0181	.0253	.0433
11	.0348	.0448	.0638	.1087
12	.583	.583	.583	.583
13	.819	.819	.819	.819
14	.0386	.0386	.0386	.0386
15	.0013	.0013	.0013	.0013
16	.037	.037	.037	.037
17	0	(.0148)	(.0210)	0

Note: Cross-hatching indicate a sign change.

Table XI

POTENTIOMETER SETTINGS

FOR I_{xz} PROGRAM

η	$\frac{I_{xz}/I_z}{4R}$	$\frac{1}{4}\frac{I_{xz}}{I_z}$ 6R	$\frac{1}{4}\frac{I_{xz}}{I_x}$ 8R	$\frac{I_{xz}}{I_x}$ 9R	$\frac{1}{4}\frac{I_{xz}}{I_y}$ 1B	$\frac{1}{4}\frac{I_y - I_x}{I_z}$ 3R	$\frac{I_z - I_y}{I_x}$ 7R	$\frac{I_x - I_z}{I_y}$ 2B
−10°	.105	.0255	.074	.227	.050	.067	.813	.850
0°	0	0	0	0	0	.0553	.859	.902
+10°	.105	.0255	.074	.227	.050	.067	.813	.850

Cross hatch = sign change

Table XII

C_{n_β} PROGRAM

C_{n_β}	N_r (1R) SEA LEVEL	N_r (1R) 40,000 FT
+ .0	0	0
+.055	.013	
+.10	.0236	.0073
+.15	.0354	
+.30	.0708	.0155

Table XIII

C_{l_β} PROGRAM

C_{l_β}	L_r (17R)	L_r (17R)
0	0	0
.10	.054	.0115
.20	.108	.0230
.30	.162	
.40	.216	

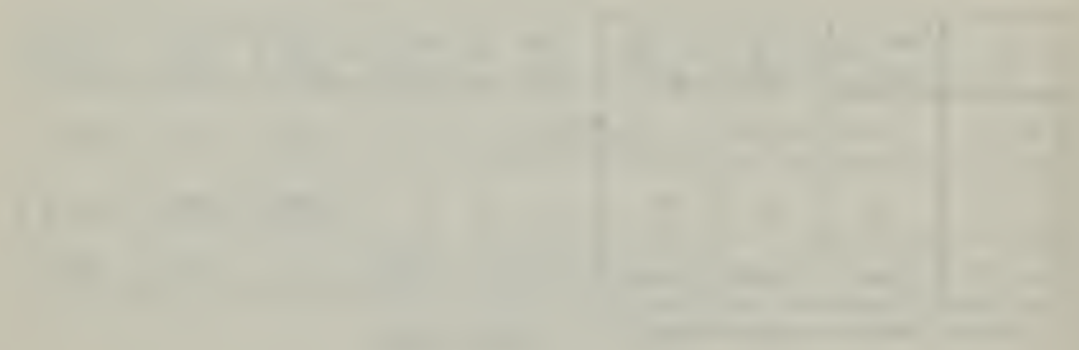

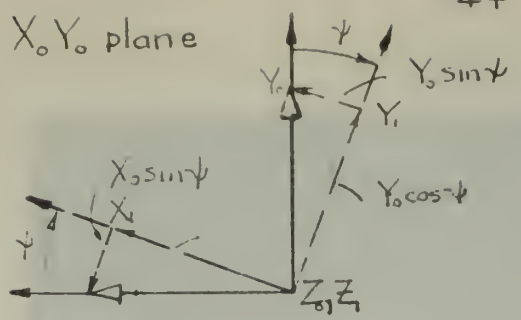

$$X_1 = X_o \cos\psi + Y_o \sin\psi$$
$$Y_1 = Y_o \cos\psi - X_o \sin\psi$$
$$Z_1 = Z_o$$

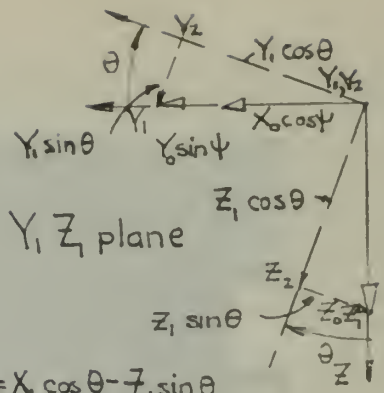

$$X_2 = X_1 \cos\theta - Z_1 \sin\theta$$
$$Y_2 = Y_1$$
$$Z_2 = Z_1 \cos\theta + X_1 \sin\theta$$

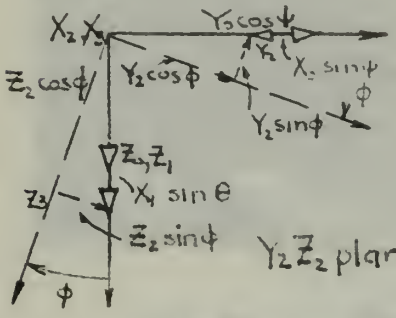

$$X_3 = X_2$$
$$Y_3 = Y_2 \cos\phi + Z_2 \sin\phi$$
$$Z_3 = Z_2 \cos\phi - Y_2 \sin\phi$$

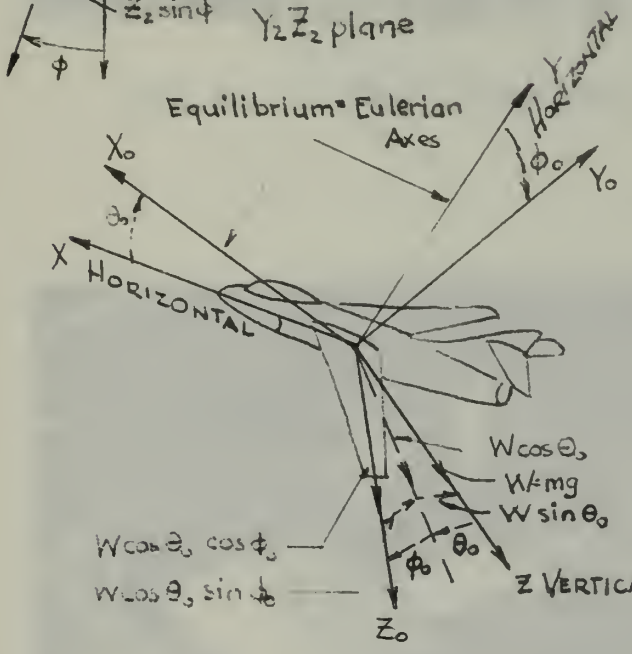

$$X_o = -W\sin\theta_o$$
$$Y_o = W\cos\theta_o \sin\phi_o$$
$$Z_o = W\cos\theta_o \cos\phi_o$$

Components of gravity acting on an aircraft in steady flight with initial angles θ_o and ϕ_o

$$X_3 = (-W\sin\theta_o)\cos\theta\cos\psi + (W\cos\theta_o \sin\phi_o)\cos\theta\sin\psi - (W\cos\theta_o \cos\phi_o)\sin\theta,$$

$$Y_3 = (-W\sin\theta_o)(\cos\psi \sin\theta\sin\phi - \sin\psi\cos\phi) + (W\cos\theta_o \sin\phi_o)(\cos\psi\cos\theta + \sin\psi\sin\theta\sin\phi) + (W\cos\theta_o \cos\phi_o)(\cos\theta\sin\phi),$$

$$Z_3 = (-W\sin\theta_o)(\cos\psi\sin\theta\cos\phi + \sin\psi\sin\phi) + (W\cos\theta_o \sin\phi_o)(\sin\psi\sin\theta\cos\phi - \cos\psi\sin\phi) + (W\cos\theta_o \cos\phi_o)(\cos\theta\cos\phi)$$

Fig. 1 DETERMINATION OF THE COMPONENTS OF GRAVITY ACTING ALONG DISTURBED EULERIAN AXES

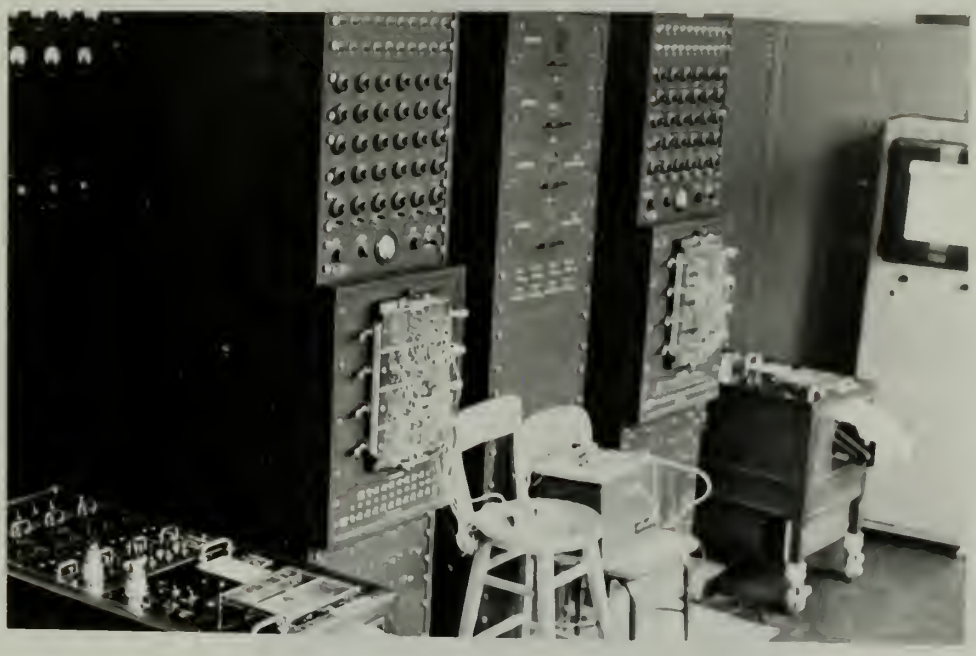

Fig. 2 THE COMPUTING SYSTEM

Fig. 3 THE SANBORN FOUR-CHANNEL RECORDER

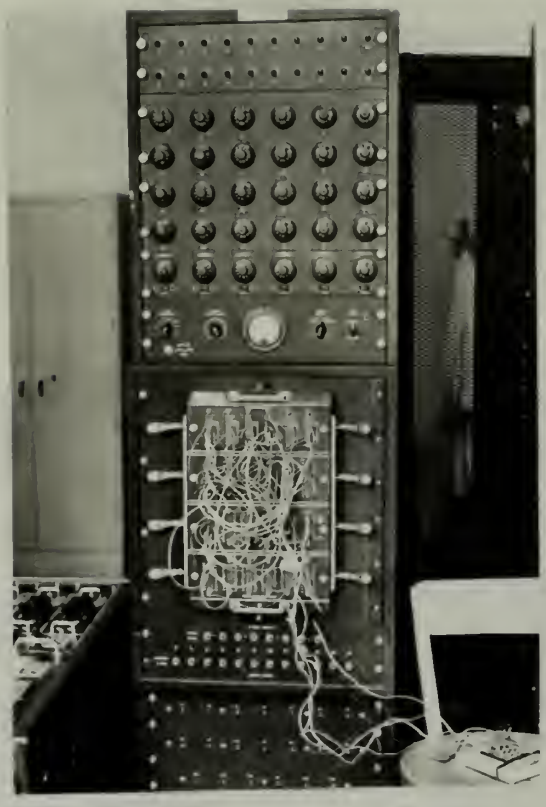

Fig. 4 THE LATERAL MOTION AND CONTROL FUNCTION COMPUTER

Fig. 5 THE LONGITUDINAL MOTION COMPUTER

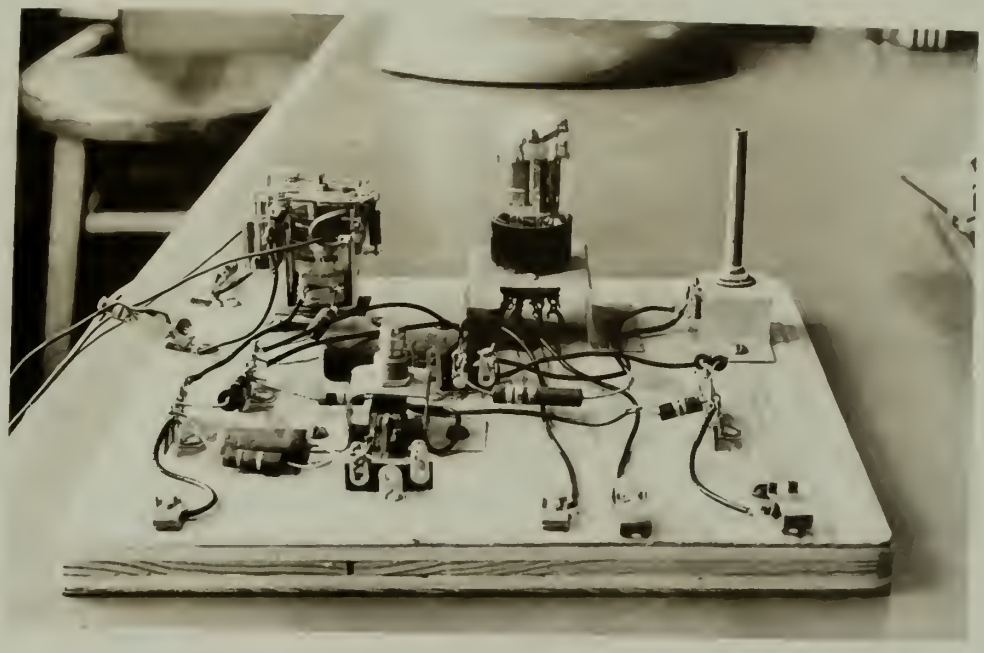

Fig. 6 THE ONE-SHOT MULTIVIBRATOR TIME SWITCH

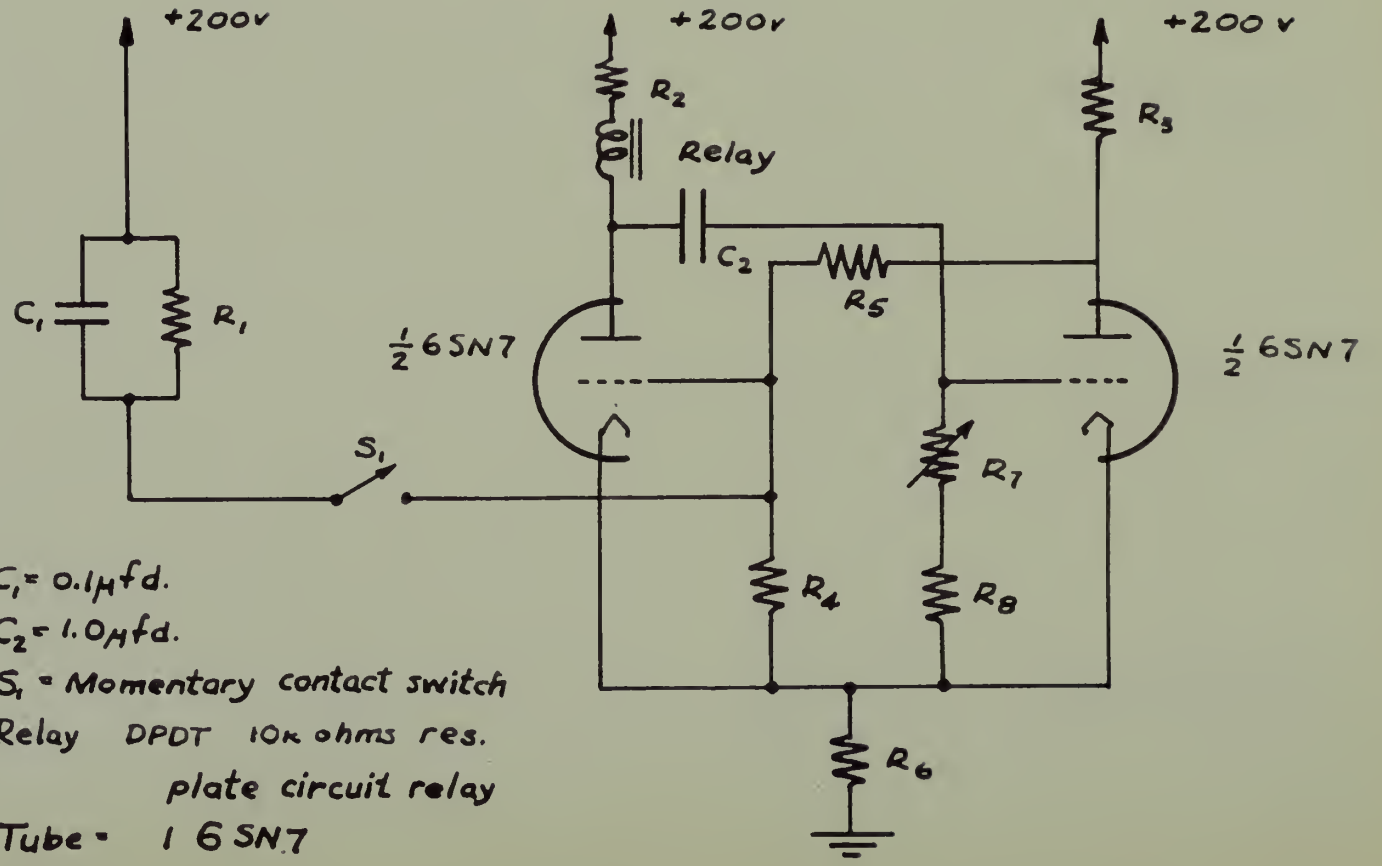

$R_1 = 10^6$ ohms $C_1 = 0.1 \mu fd.$
$R_2 = 10K$ " $C_2 = 1.0 \mu fd.$
$R_3 = 20K$ " S_1 = Momentary contact switch
$R_4 = 150K$ " Relay DPDT 10K ohms res.
$R_5 = 300K$ " plate circuit relay
$R_6 = 11K$ " Tube = 1 6SN7
$R_7 = 750K$ " linear pot.
$R_8 = 250K$ "

Fig. 7 One Shot Multivibrator Time Switch

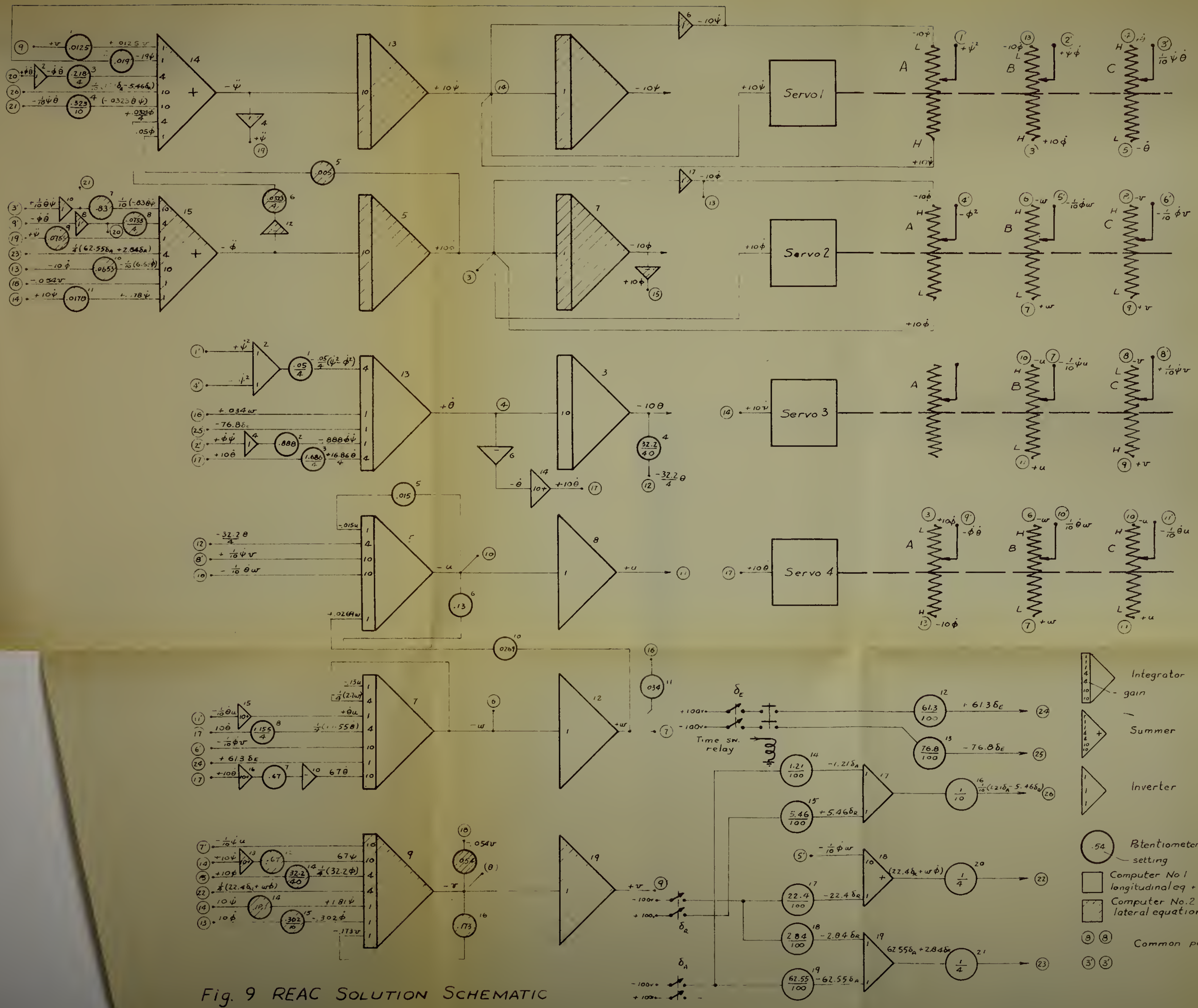

Fig. 9 REAC Solution Schematic

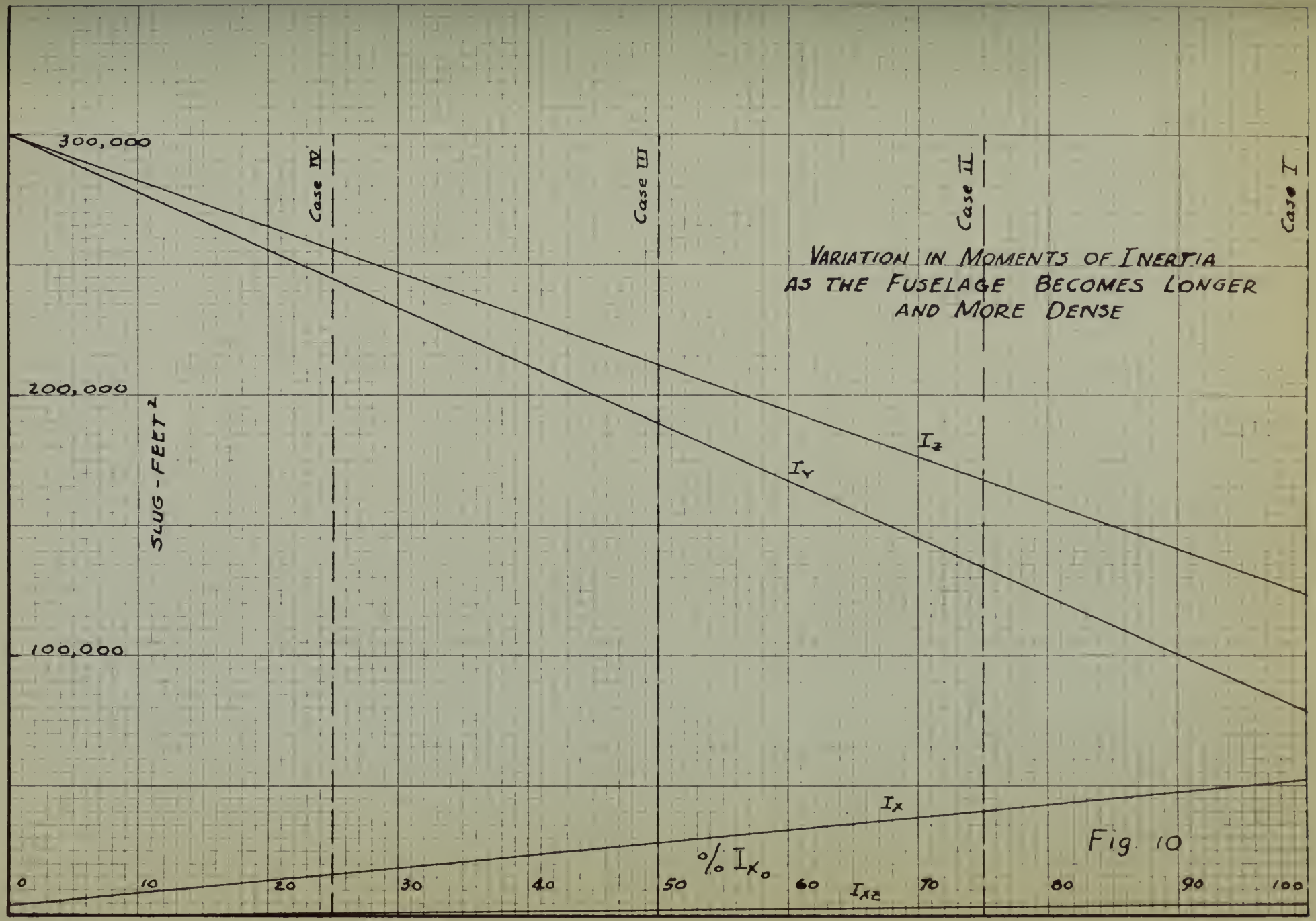
VARIATION IN MOMENTS OF INERTIA
AS THE FUSELAGE BECOMES LONGER
AND MORE DENSE
Case IV
Case III
Case II
Case I
300,000
200,000
100,000
SLUG-FEET²
I_Z
I_Y
I_X
0
10
20
30
40
50
60
70
80
90
100
% I_{X_0}
I_{XZ}

Fig. 10

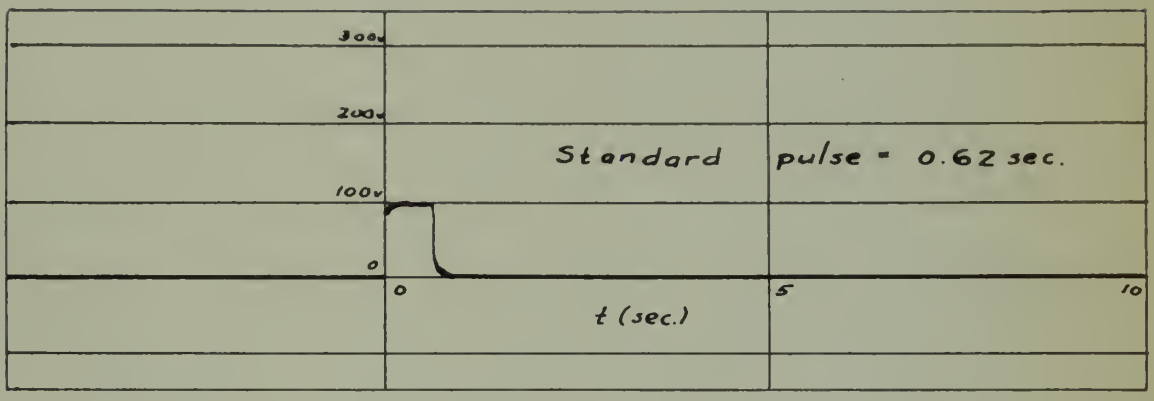

Fig. 11 Standard [illegible] Function Input.

[illegible]

The input was supplied to the rudder, elevator, or aileron position at the origin.

Eight channels were recorded simultaneously. In the measurement figures the 1 and 2 parts of the figure refer to the right channel response to the indicated function.

The [illegible] curves [illegible] the [illegible] area [illegible]. The [illegible] for each change in the variable parameter. [illegible] the [illegible] the change from the [illegible] curves was not sufficient and the curves [illegible].

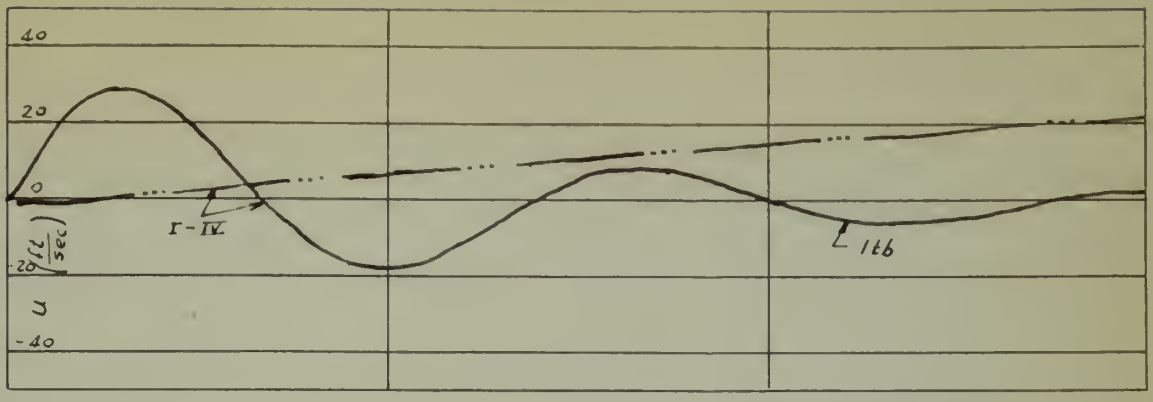

ltb = long time base

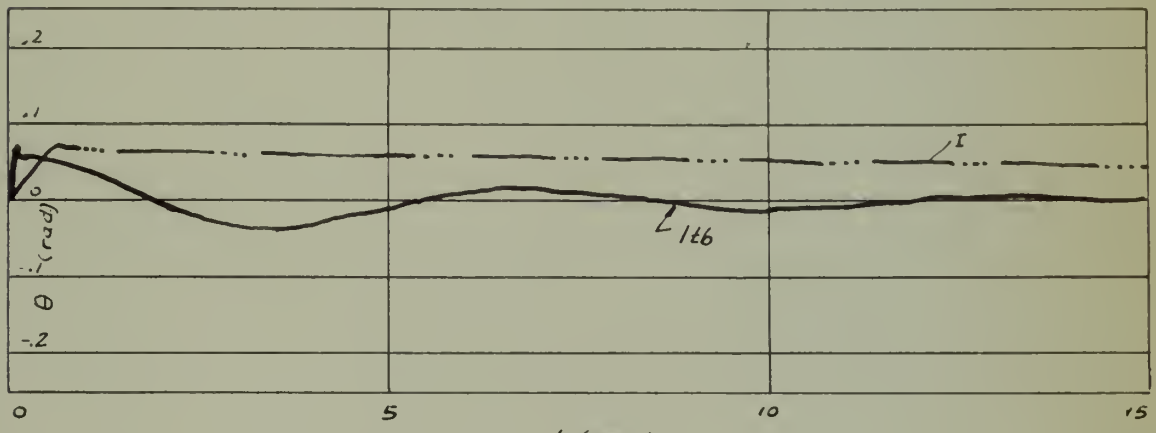

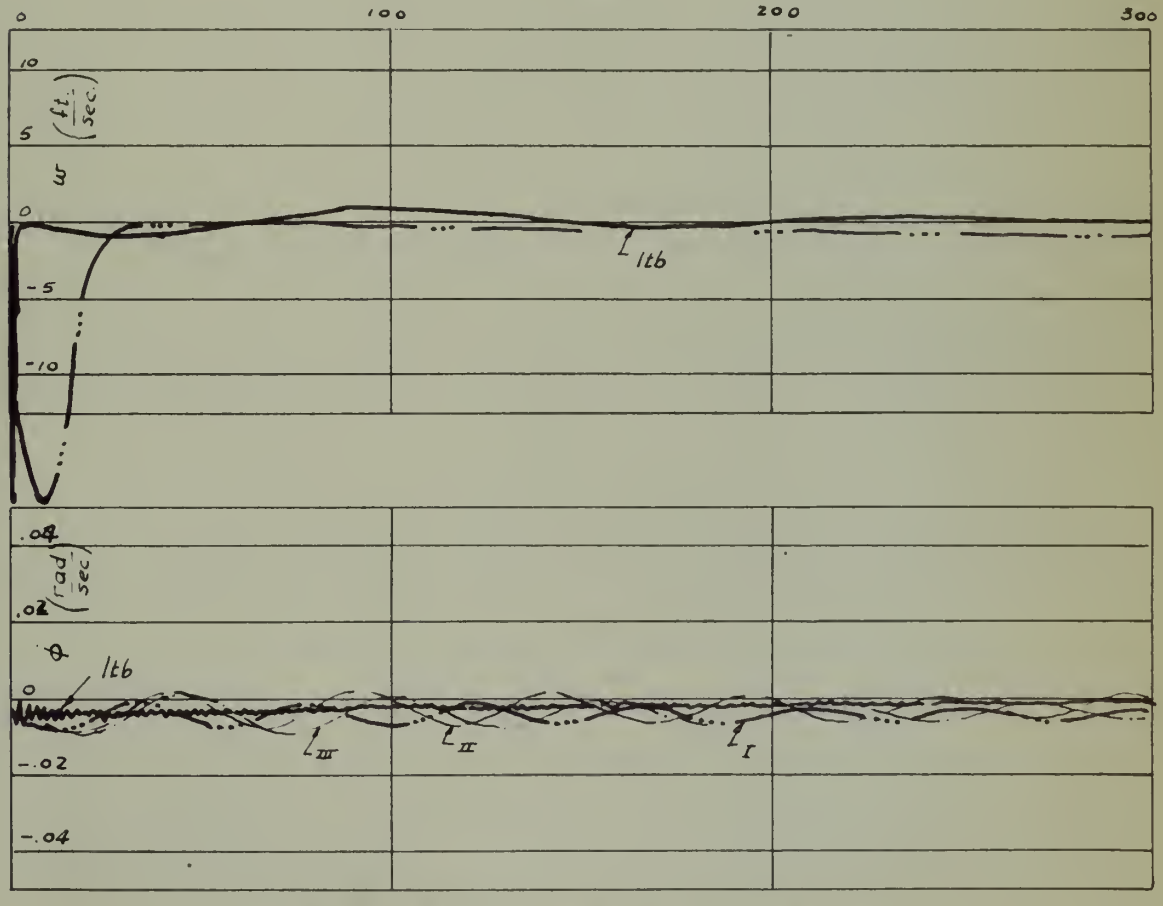

Fig. 13b Response to elevator pulse.
Cases I, II, III and IV (see text).

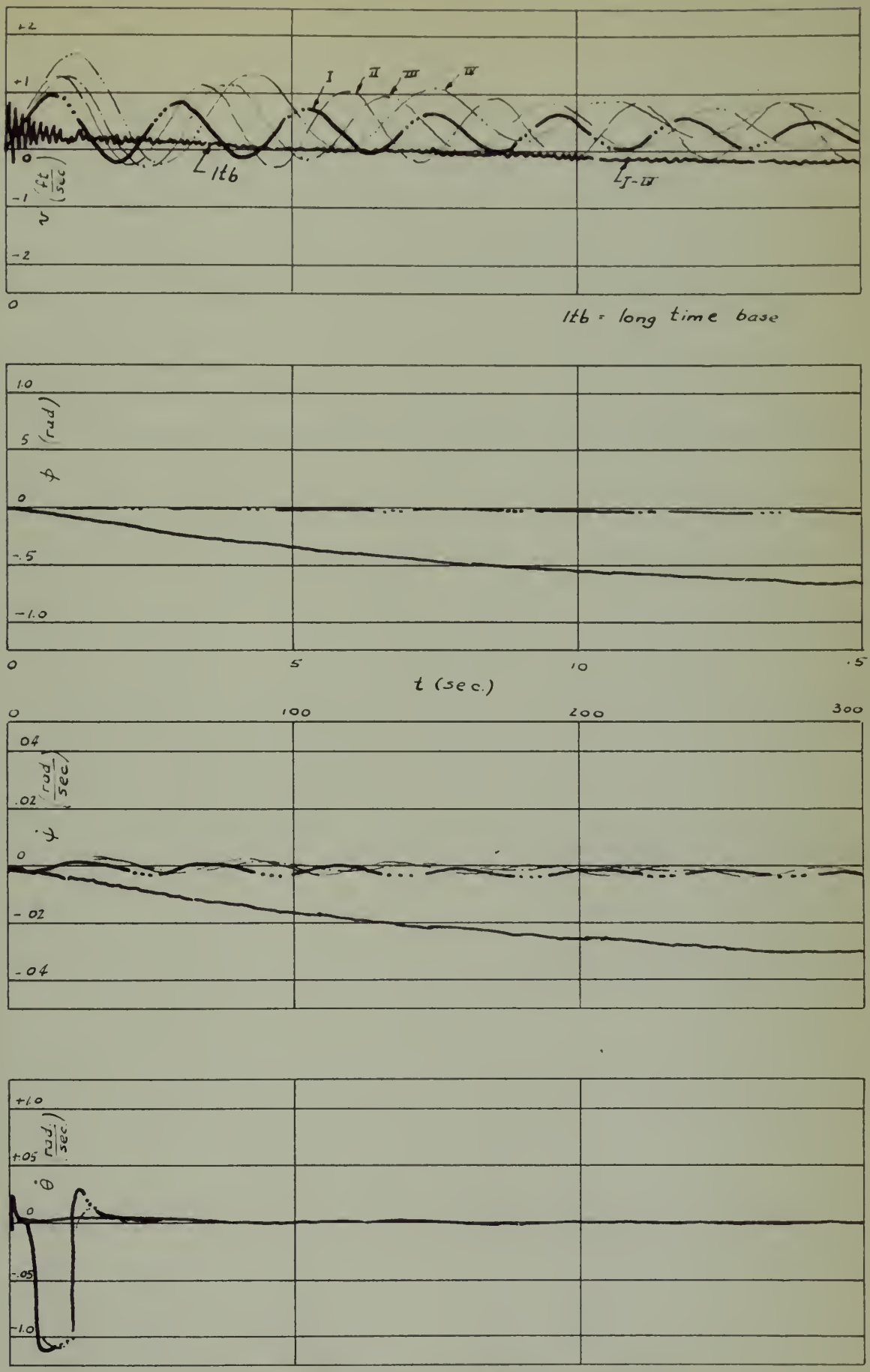

FIG. [illegible] RESPONSE TO AN ELEVATOR PULSE, CASES I, II, III, AND IV (SEA LEVEL).

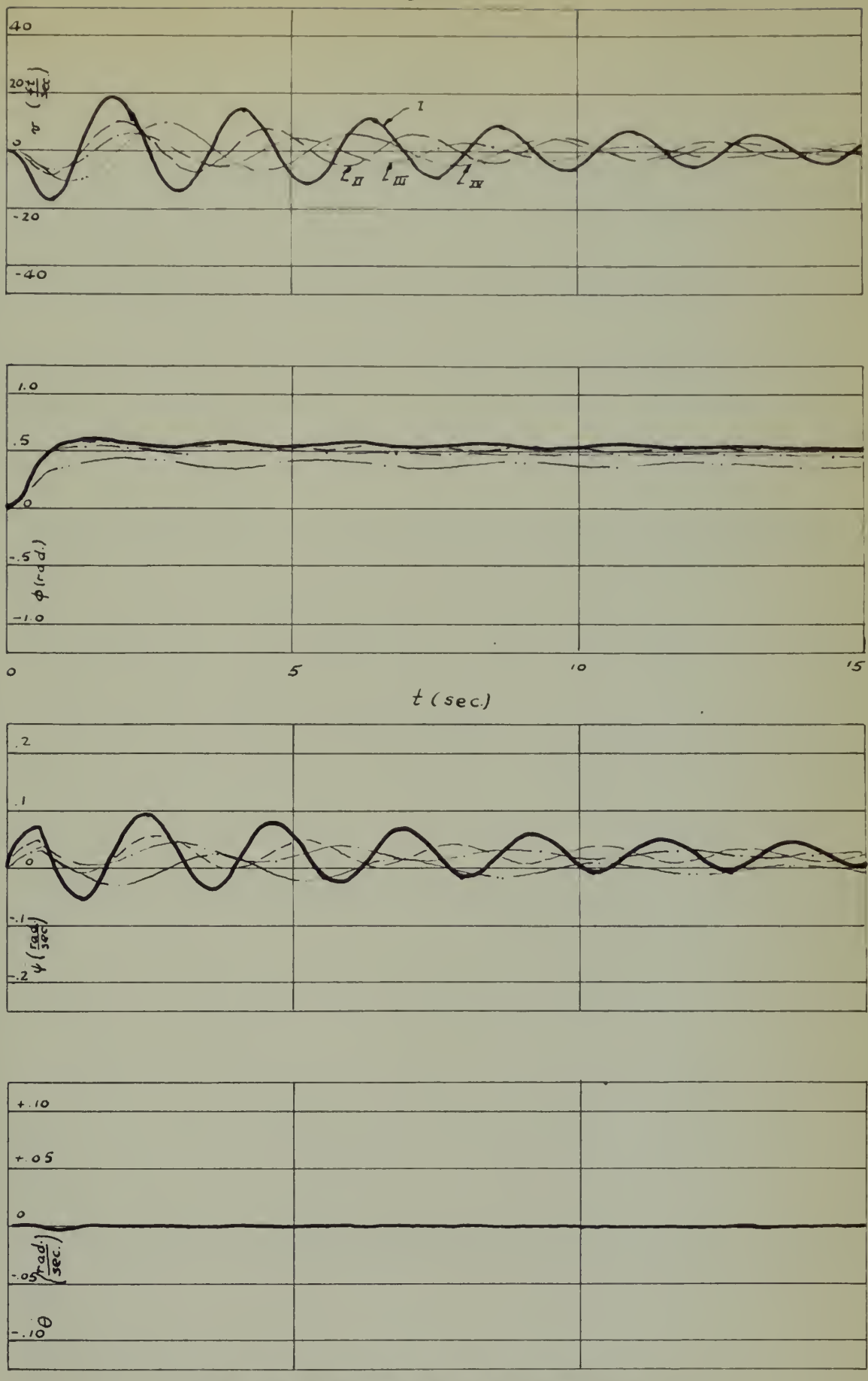

FIG. 17A [illegible] TO AN [illegible] PULSE,
[illegible] I, II, III [illegible] (SEE [illegible].

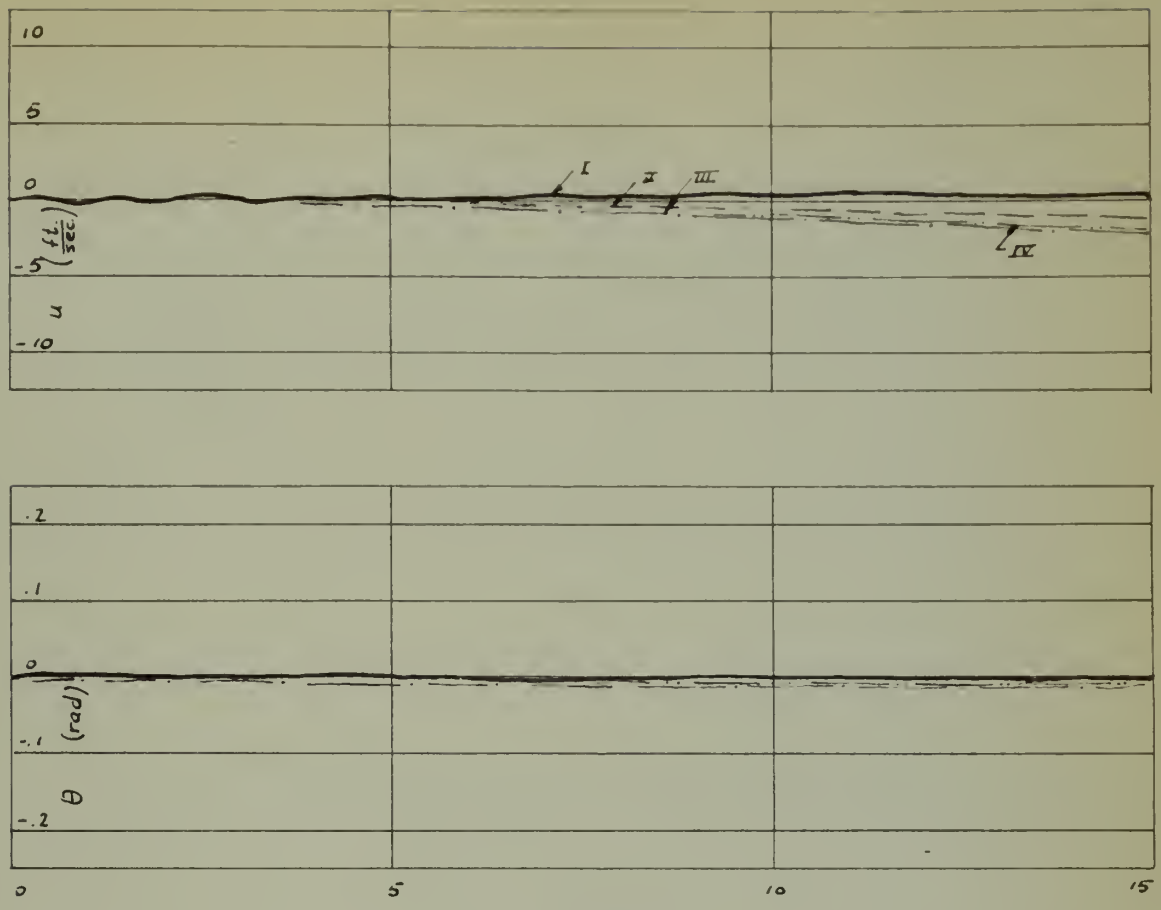

Fig. 13 [illegible] for Cases I, II, III, and IV (see p. [illegible]).

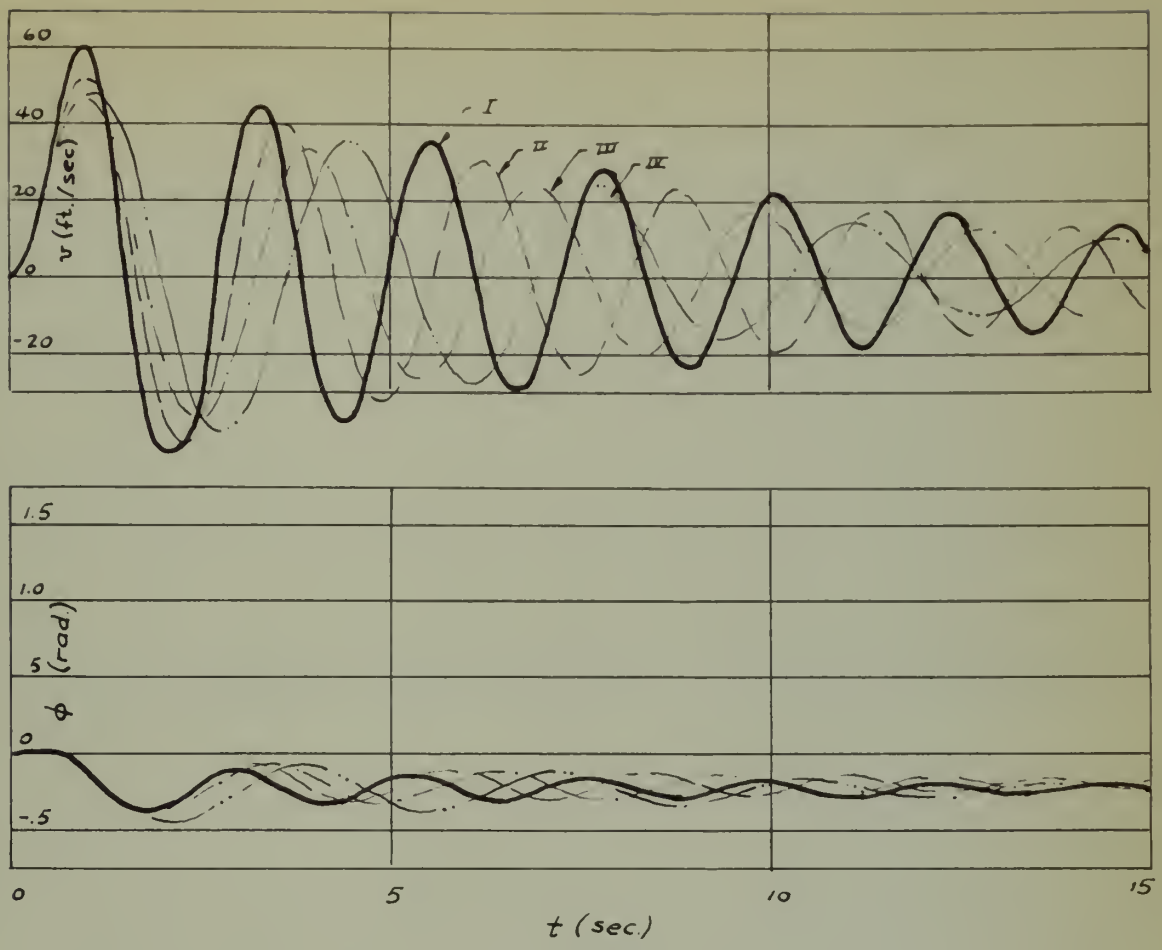

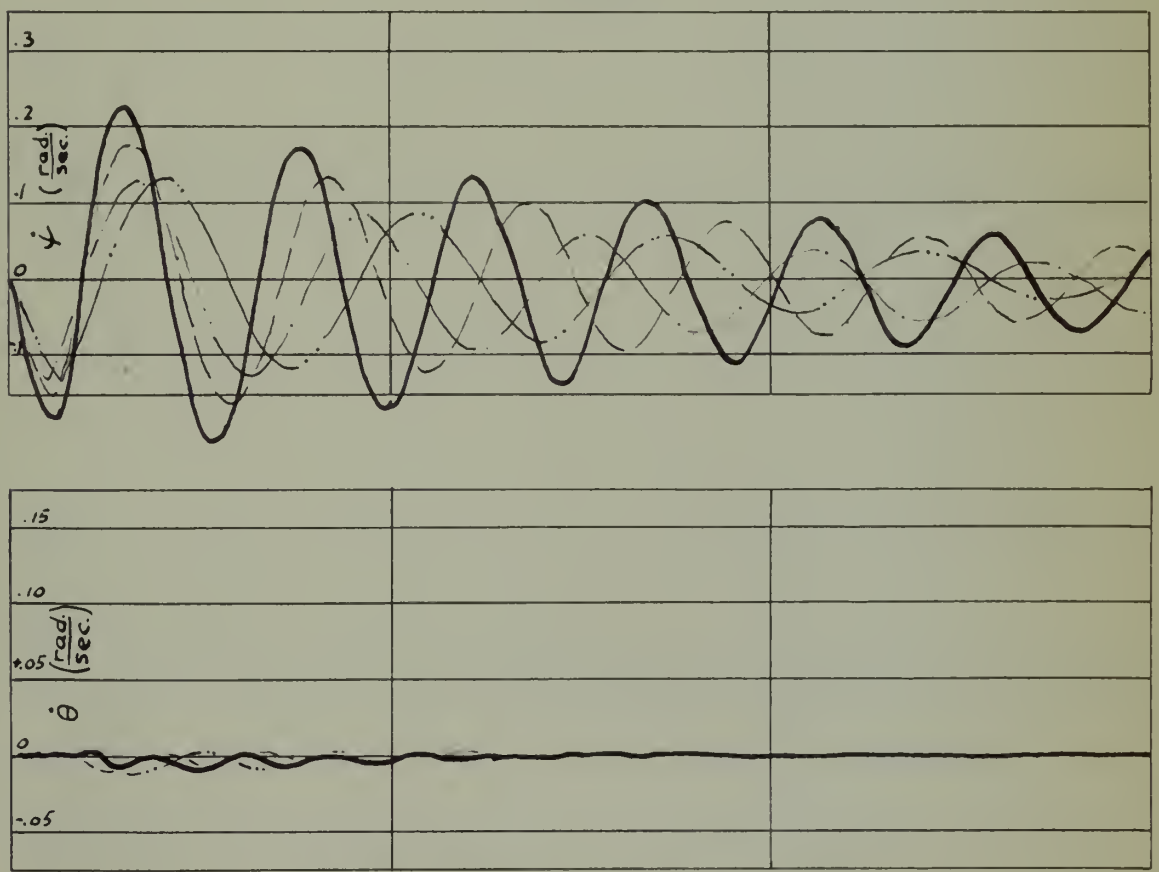

Fig. 14. Response of a rocket plane, Cases I, II, III, and IV (Ref. 4).

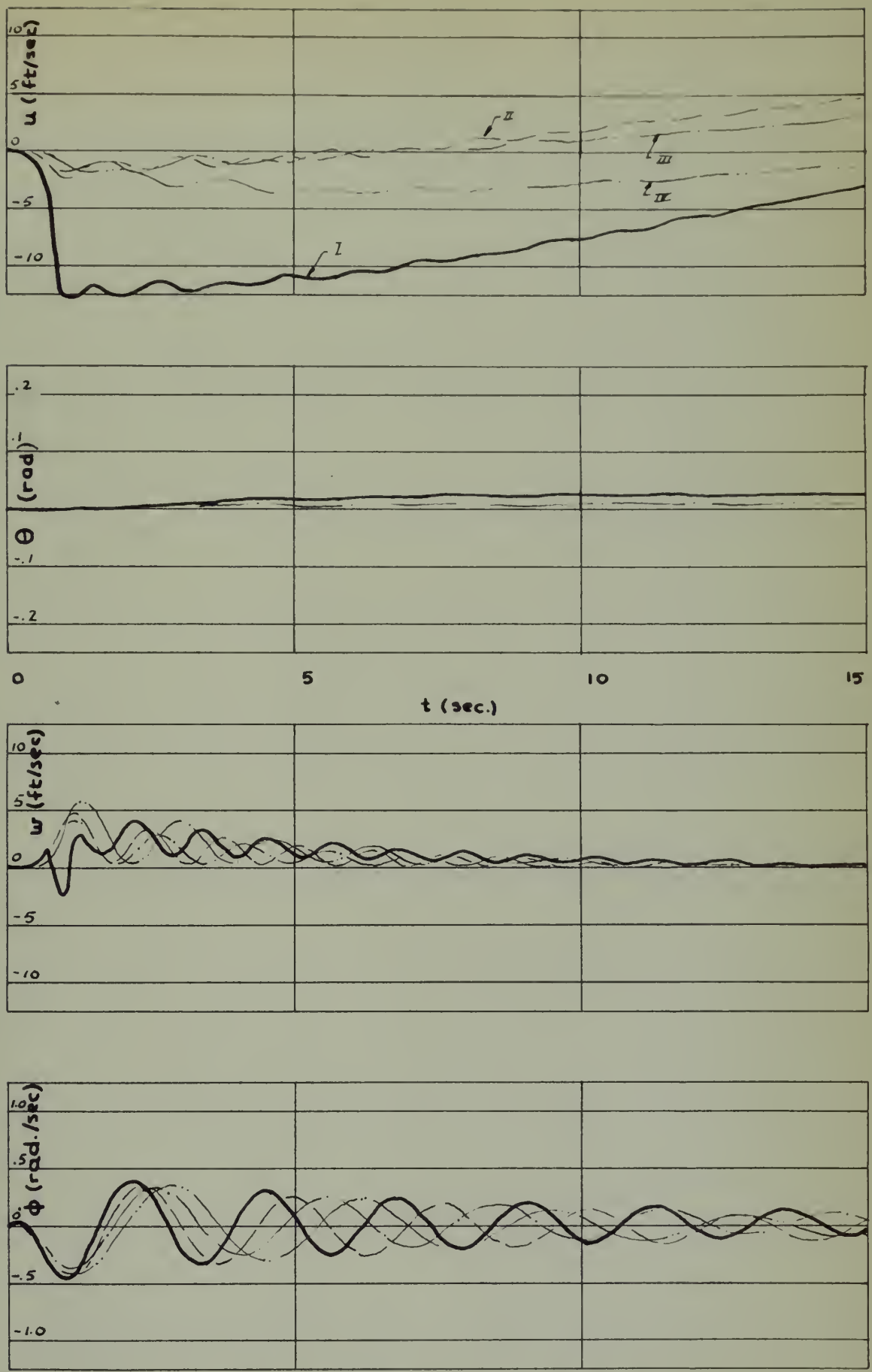

FIG. 14: RESPONSE TO A RUDDER PULSE, CASES I, II, III, AND IV (SEA LEVEL).

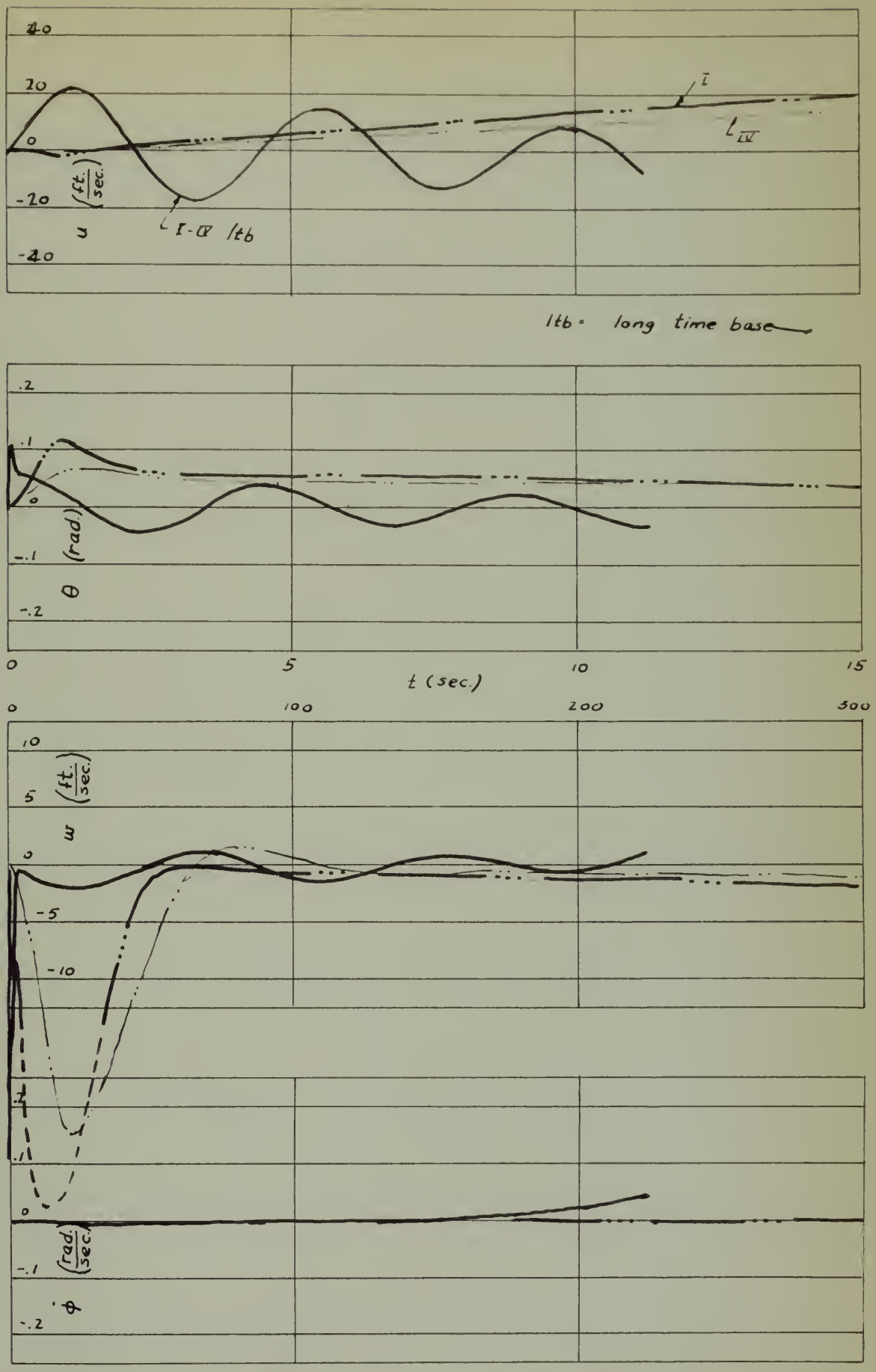

FIG. 17A [illegible] VATOR RU[illegible],
[illegible] ,000 ft.

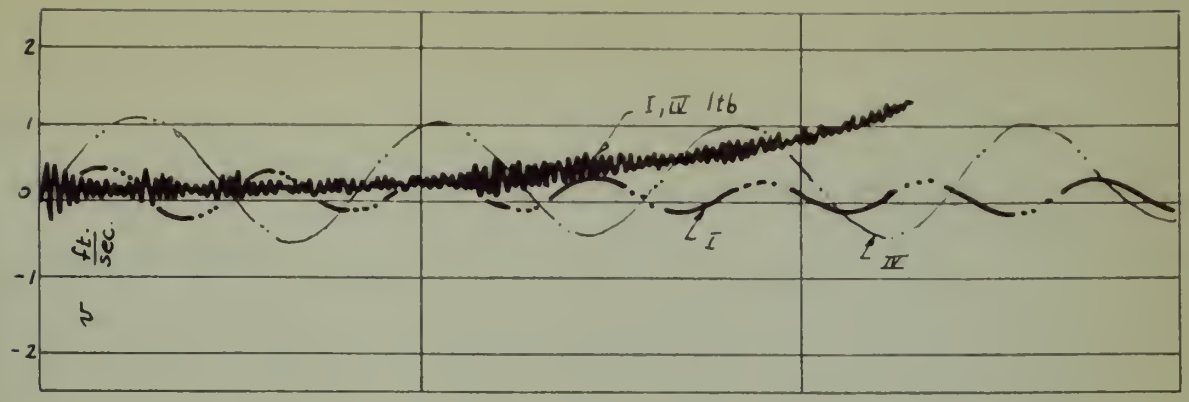

ltb = long time base

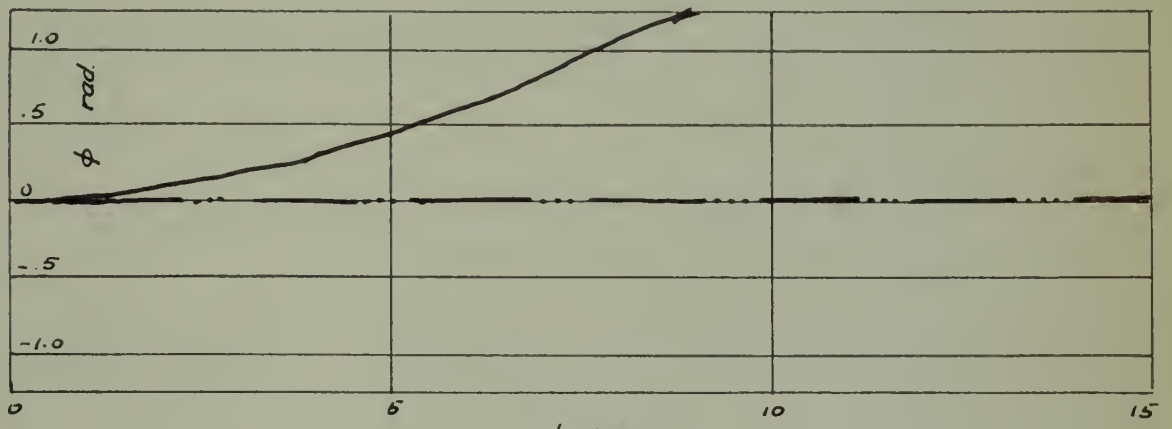

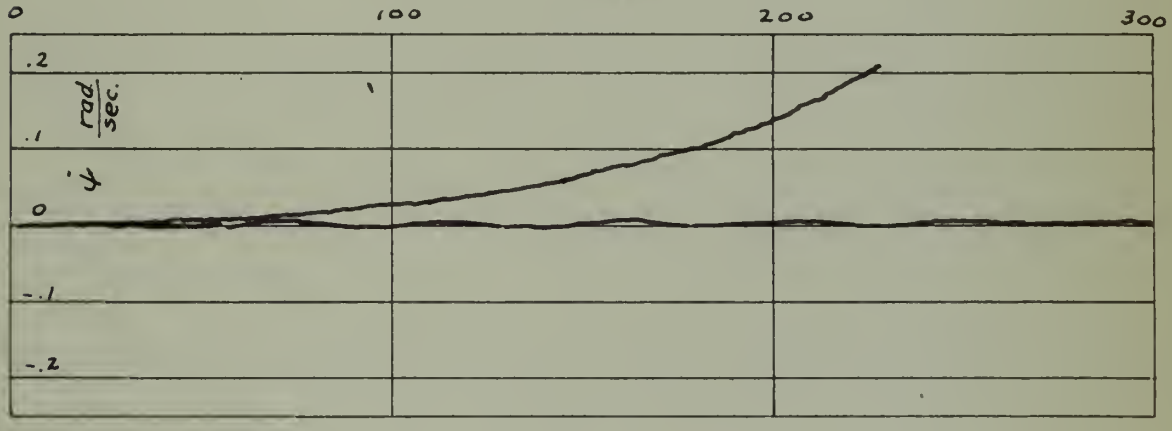

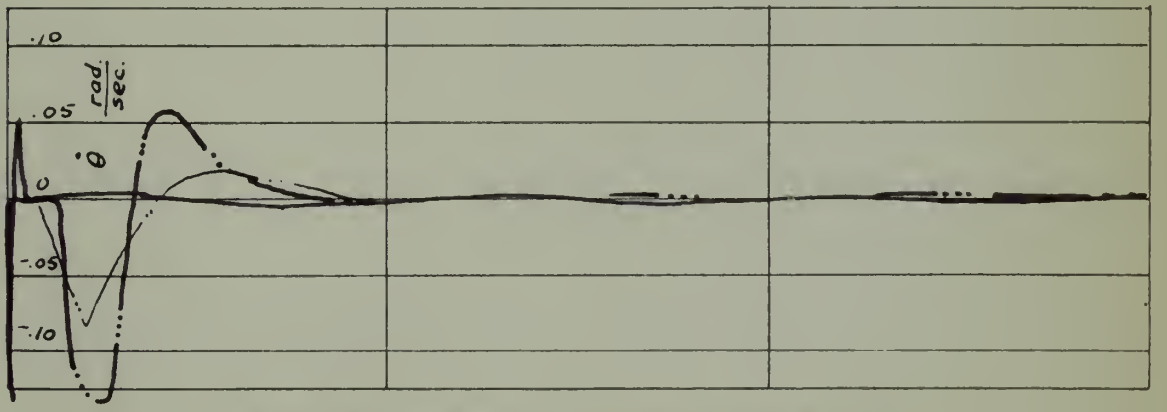

Fig. 17 [illegible]
[illegible] MODIFIED [illegible] T.

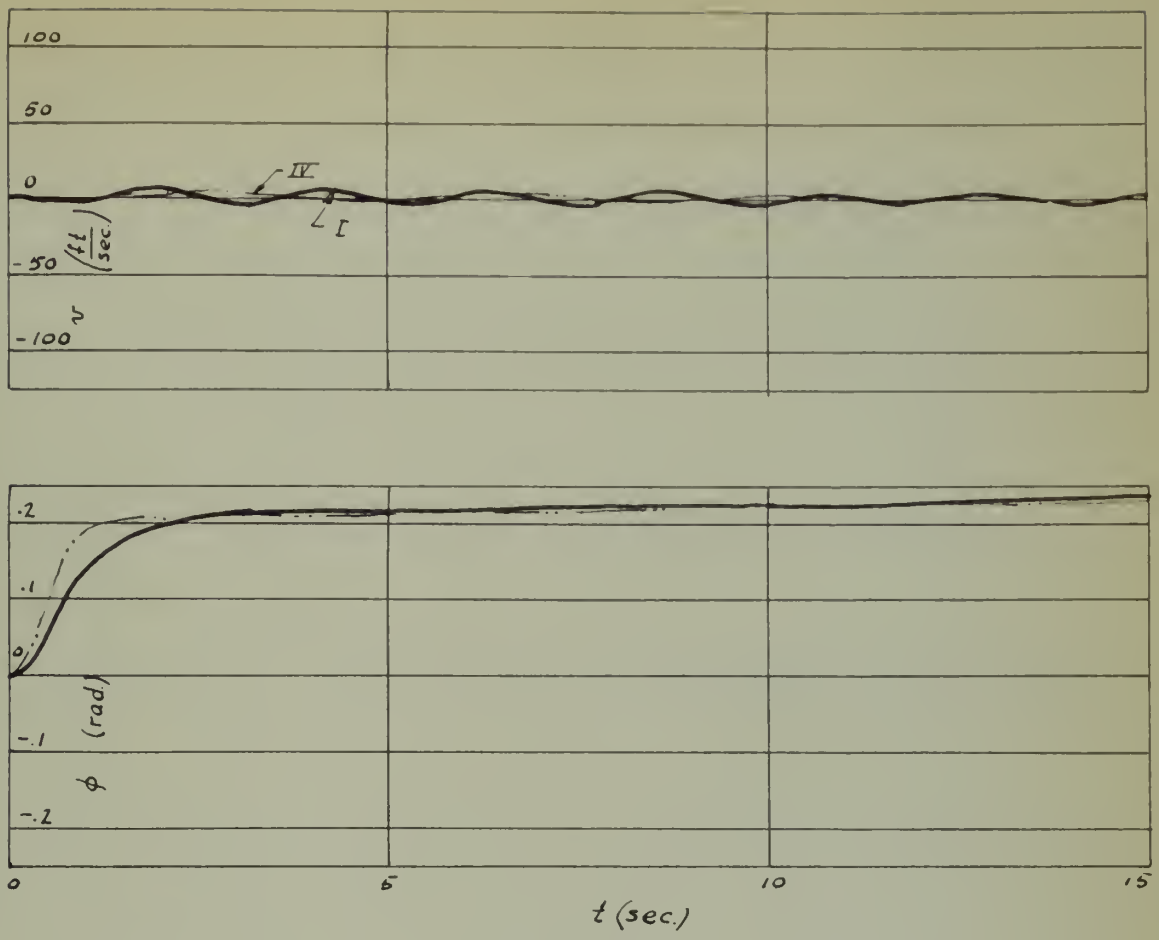
100
50
0
-50
-100
v (ft/sec)
IV
I
.2
.1
0
-.1
-.2
φ (rad)
0
5
10
15
t (sec.)
1.0
.5
0
-.5
-1.0
ψ̇ (rad/sec)
.10
05
0
-.05
-.10
θ̇ (rad/sec)

Fig. [illegible]
[illegible] (.300 [illegible]).

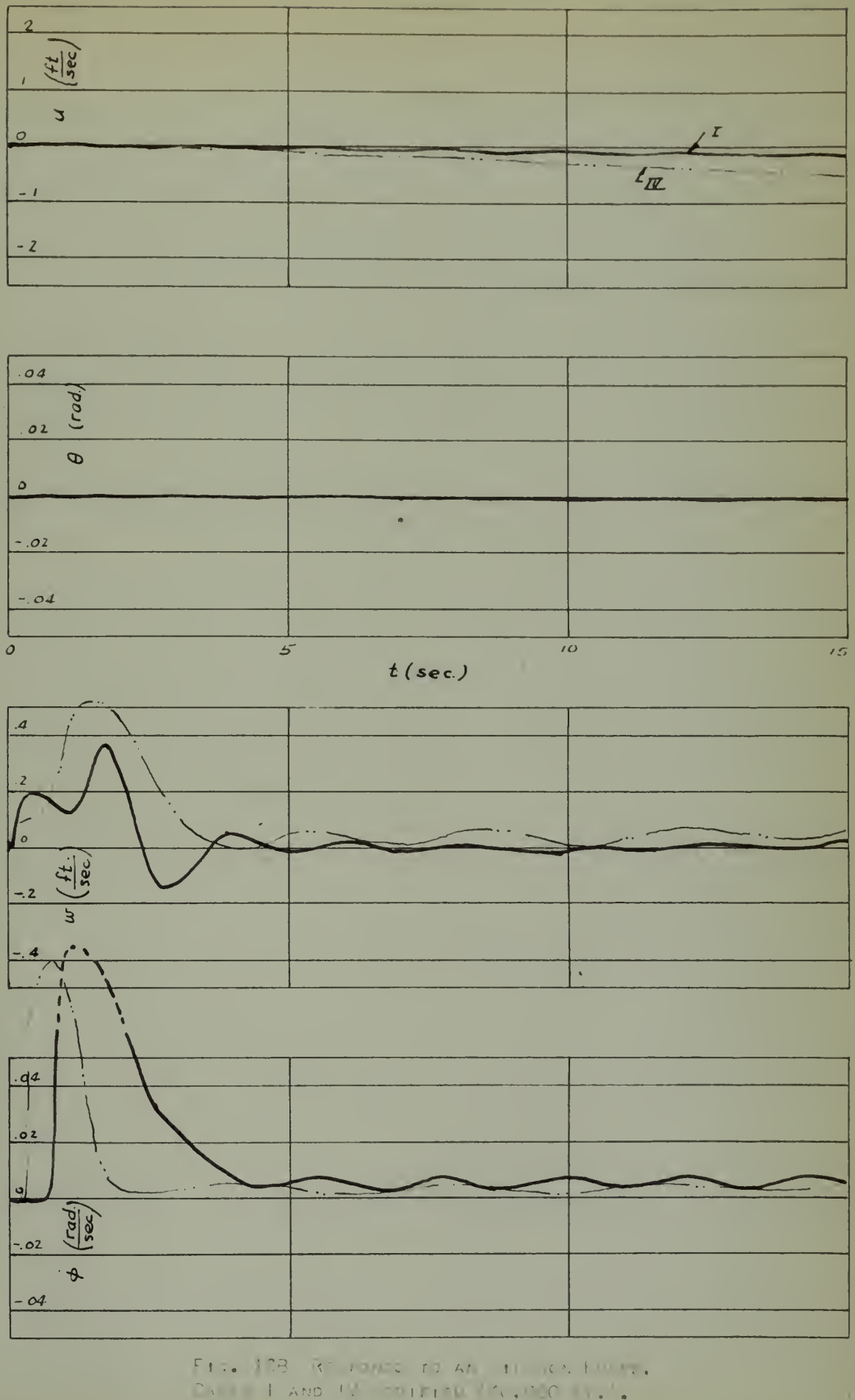

FIG. 10B RESPONSE TO AN ELEVATOR PULSE.
CASES I AND IV, SUPERSONIC, SEA LEVEL.

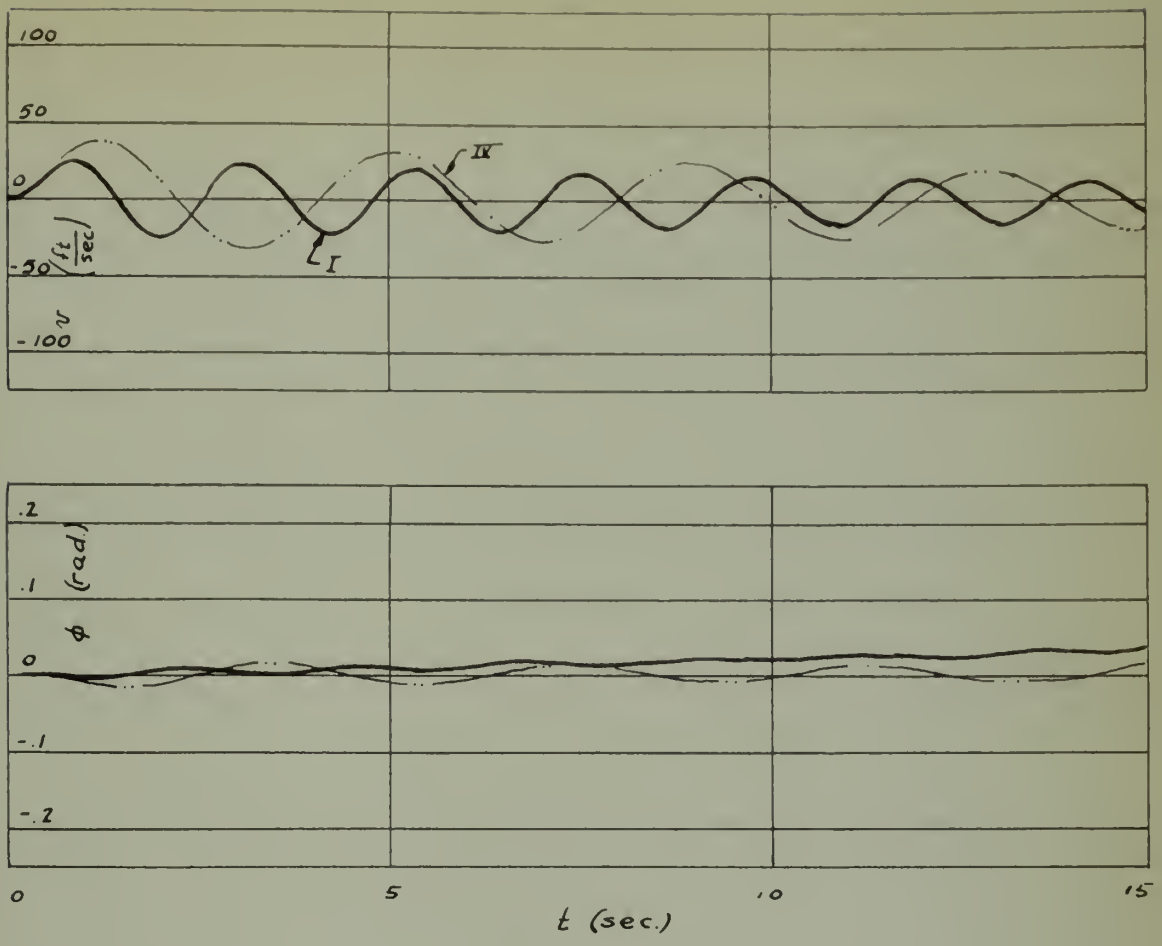

FIG. 17A RESPONSE TO A ROLLING MOMENT.
CASES I AND II [illegible] (AC,700 (F.).

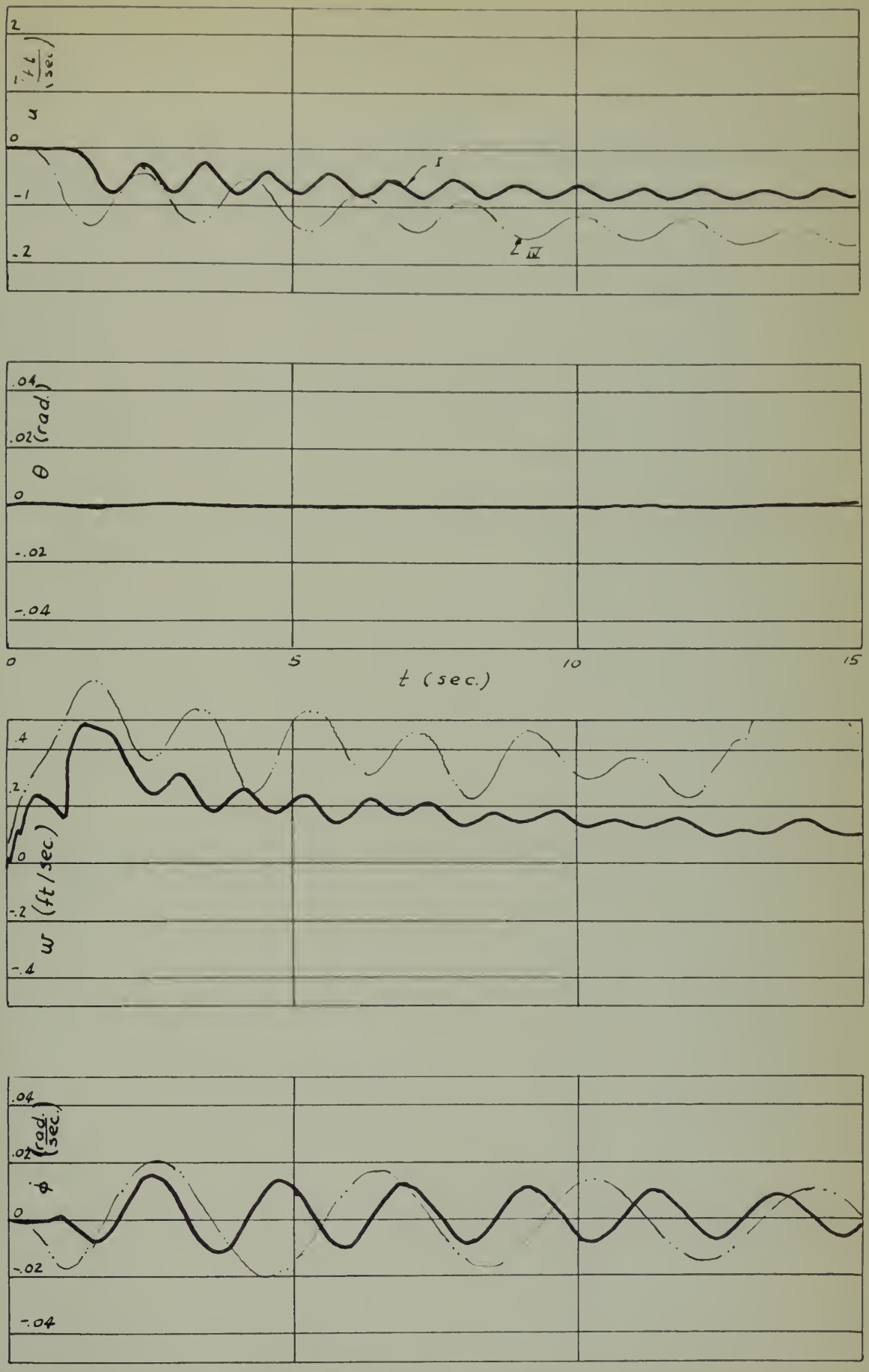

FIG. [illegible] FOR A [illegible],
CASE I, [illegible], [illegible] SEC.

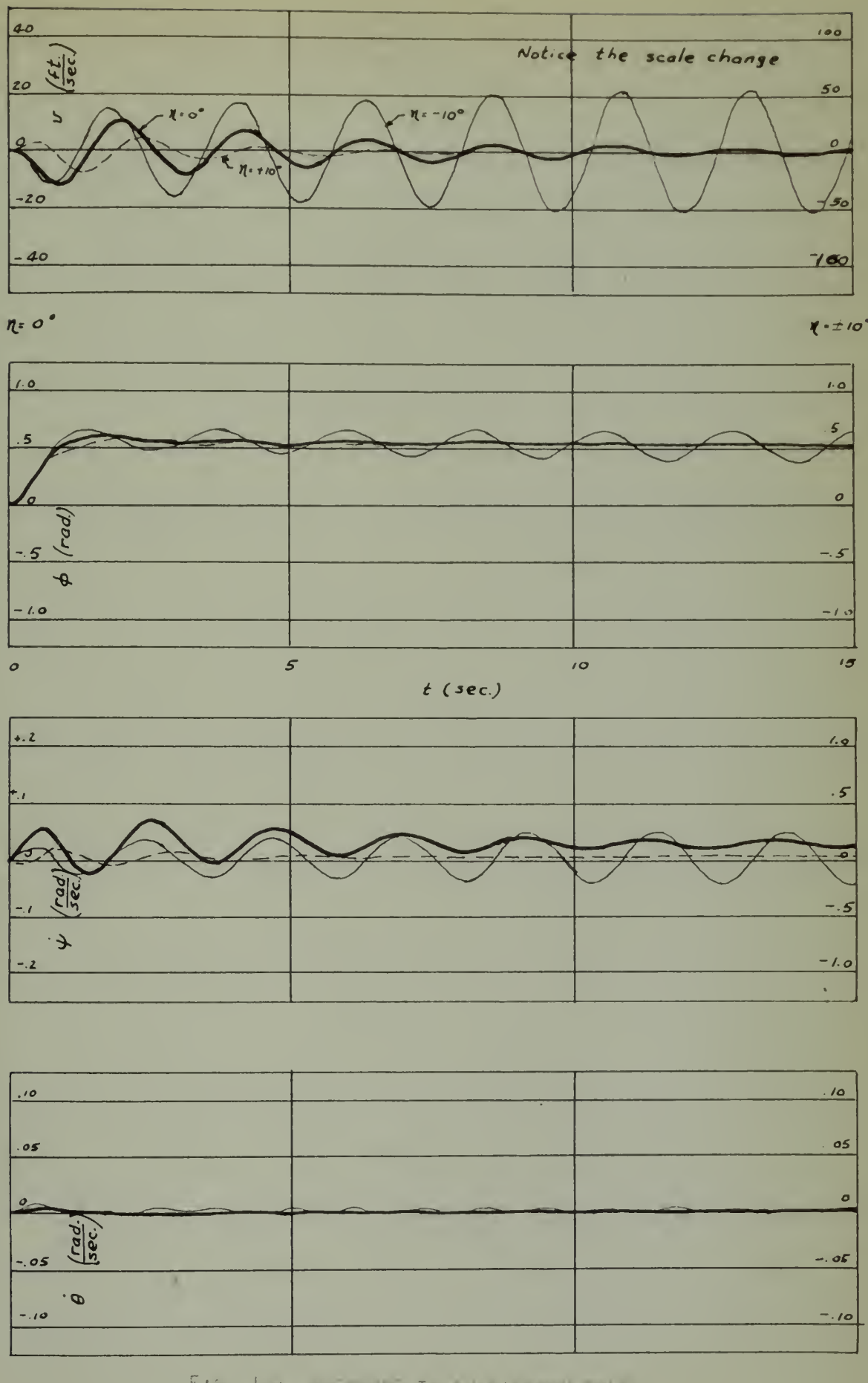

FIG. [illegible] RESPONSE TO [illegible] CONTROL.
η = [illegible], η = [illegible], η = [illegible] (SCALE LEVEL).

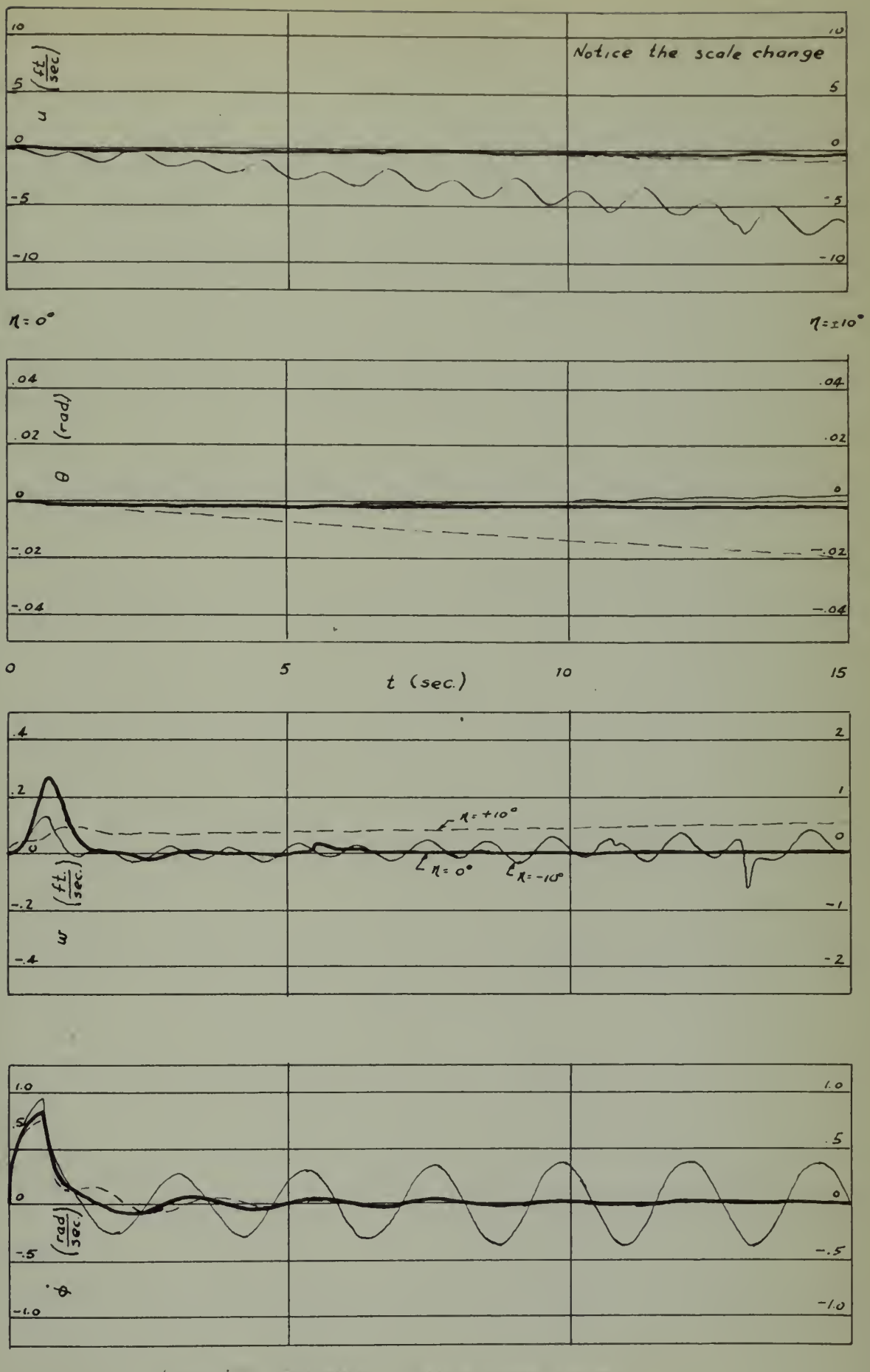

Fig. [illegible] Response to elevator pulses, $\eta = 0°, \eta = \pm 10°, \eta = -10°$ (see text).

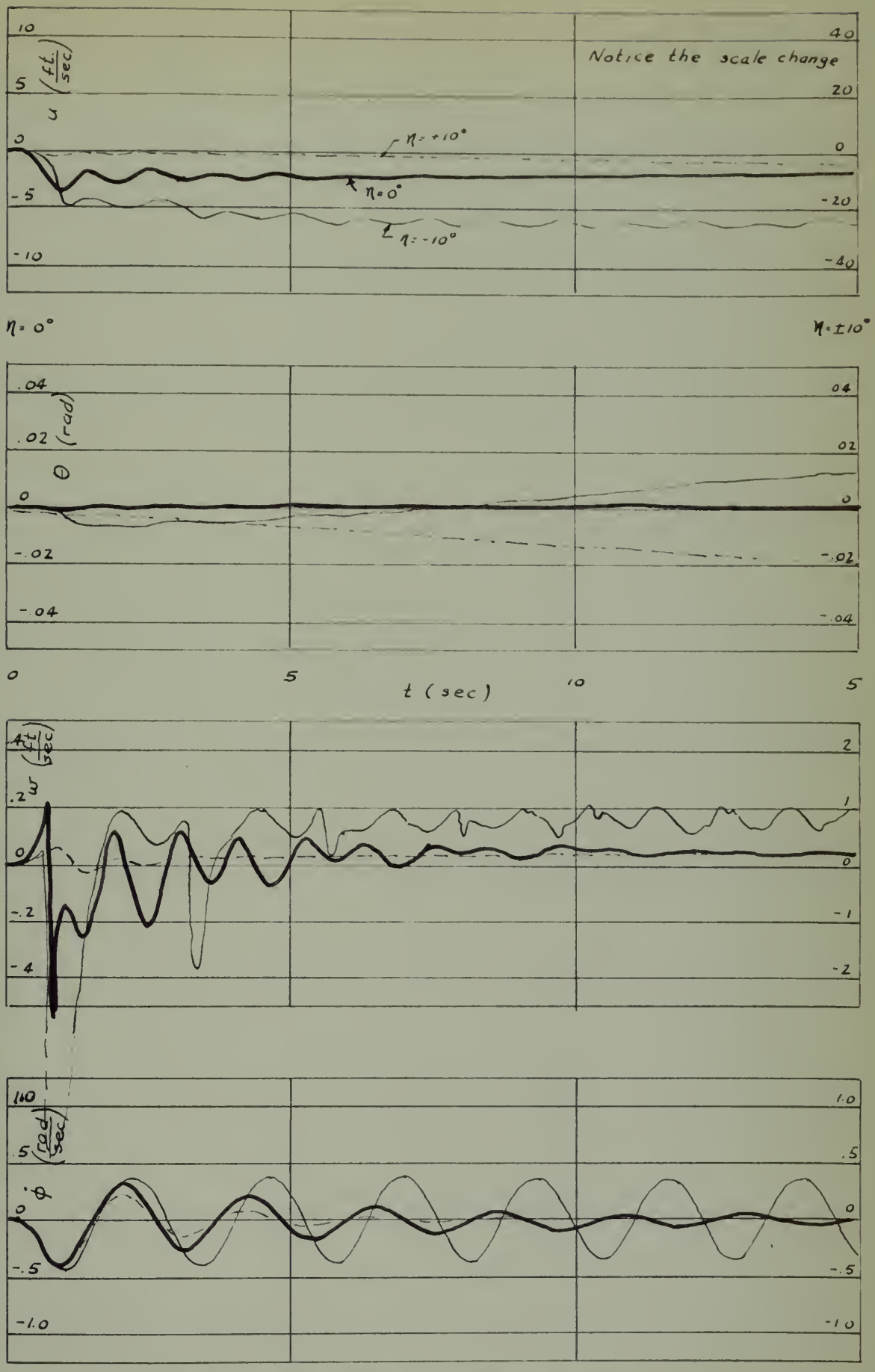

η = 0°, η = [illegible], η = -10° (SEA LEVEL).

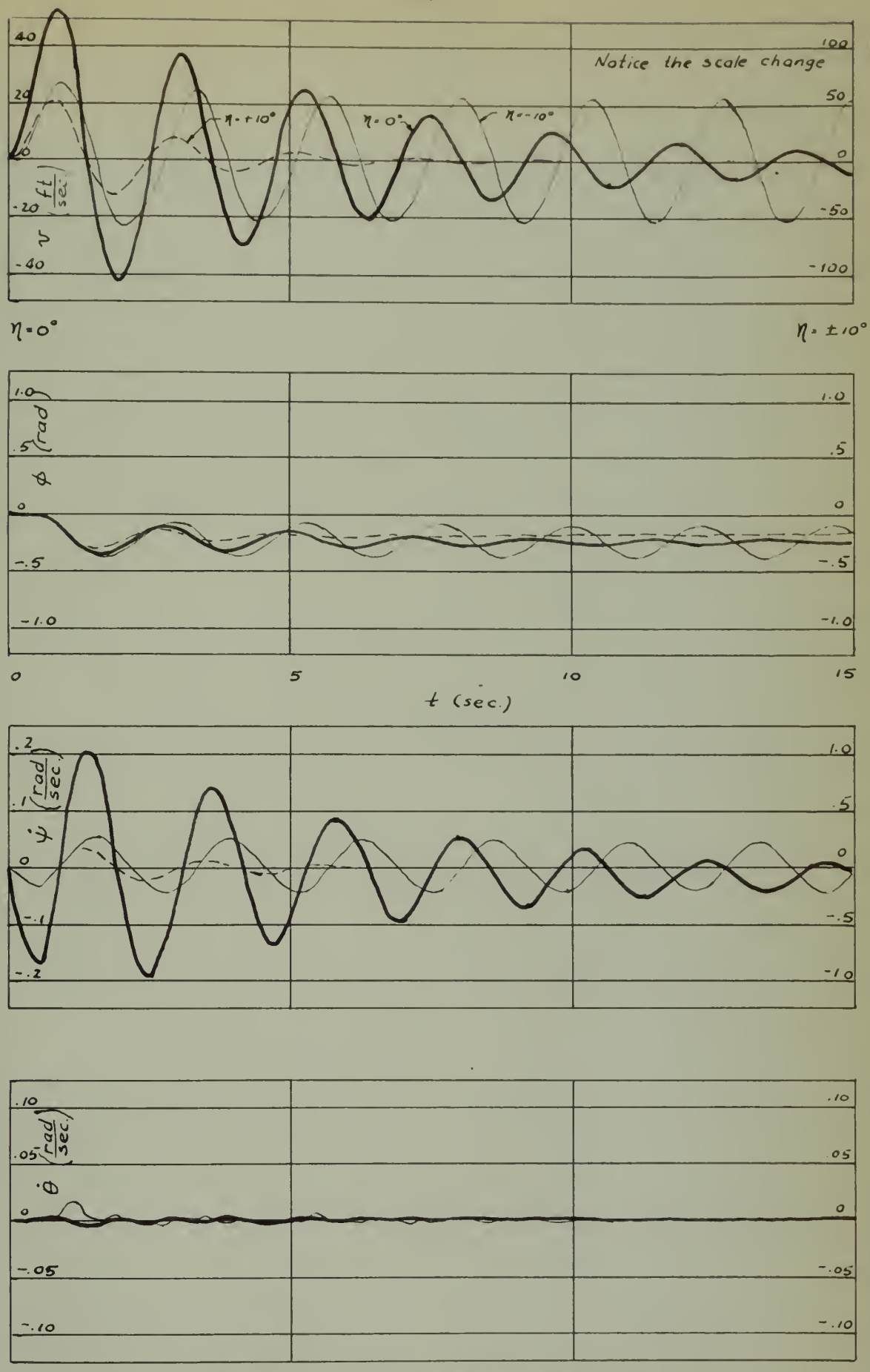
Notice the scale change
η = +10°
η = 0°
η = -10°
v (ft/sec)
φ (rad)
ψ̇ (rad/sec)
θ̇ (rad/sec)
t (sec.)
η = 0°
η = ±10°

Fig. [illegible]
η = , η = , η = [illegible].

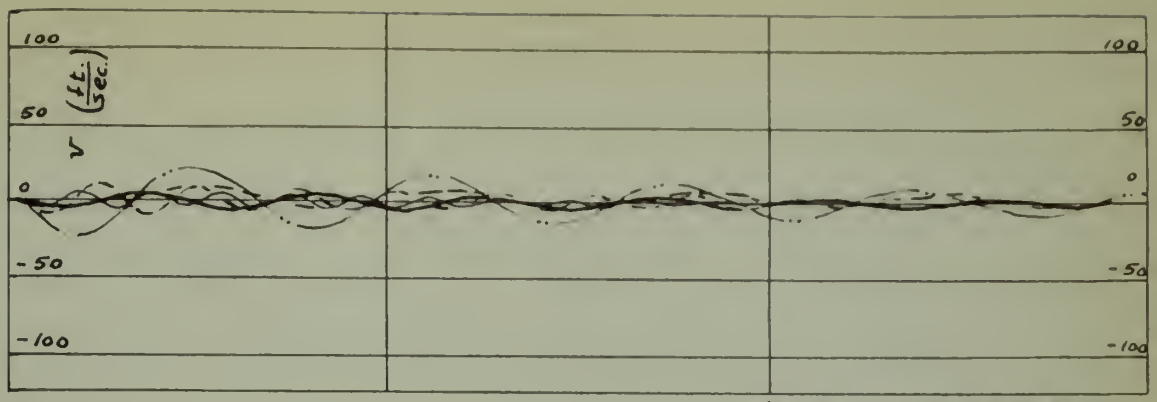

Notice the scale change

S.L. H.A.

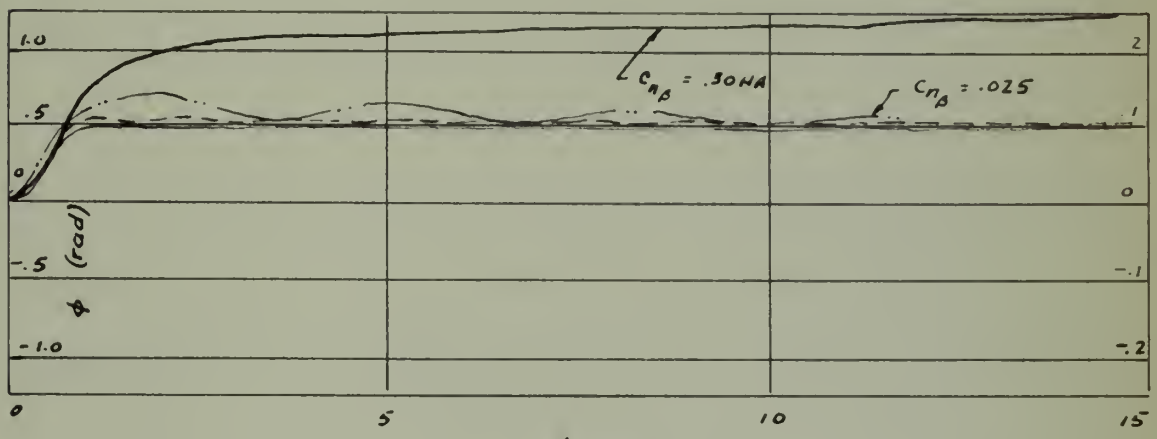

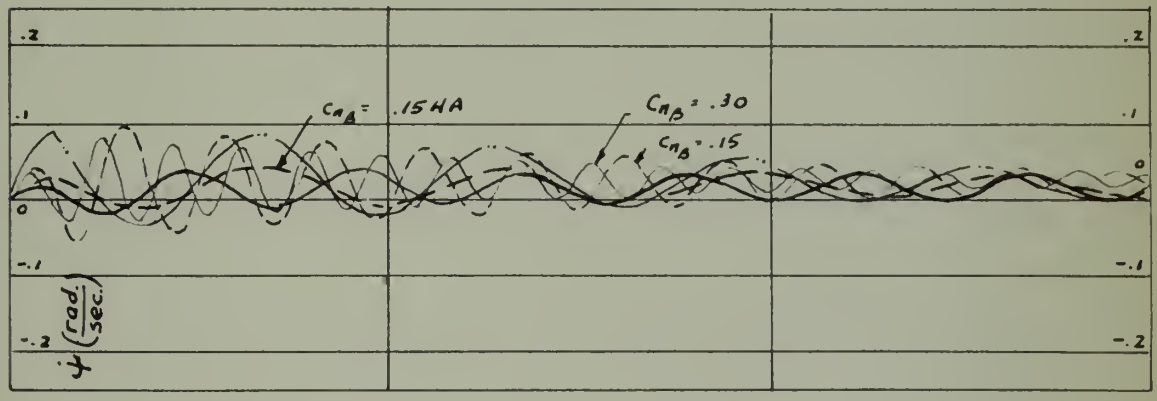

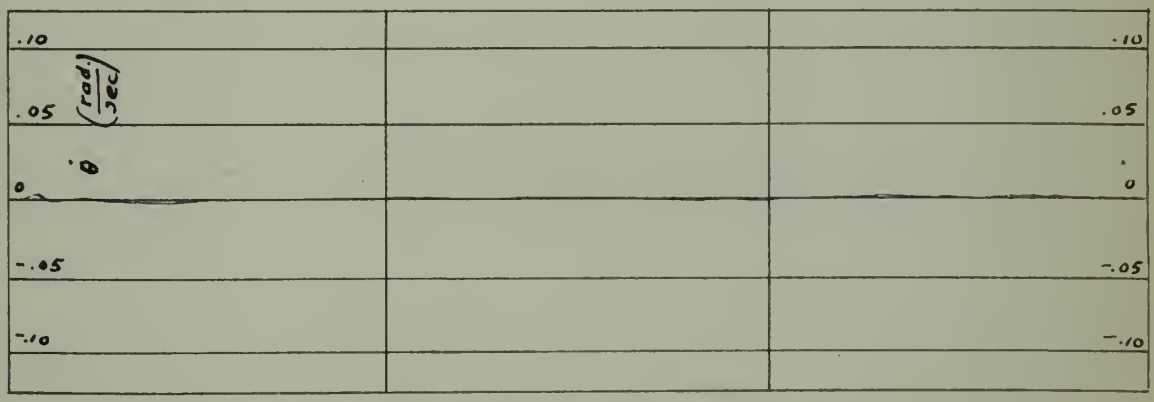

F[illegible]. 10A [illegible] TO A [illegible]
C_{n_β} [illegible] (SEA LEVEL AND 40,000 FT.).

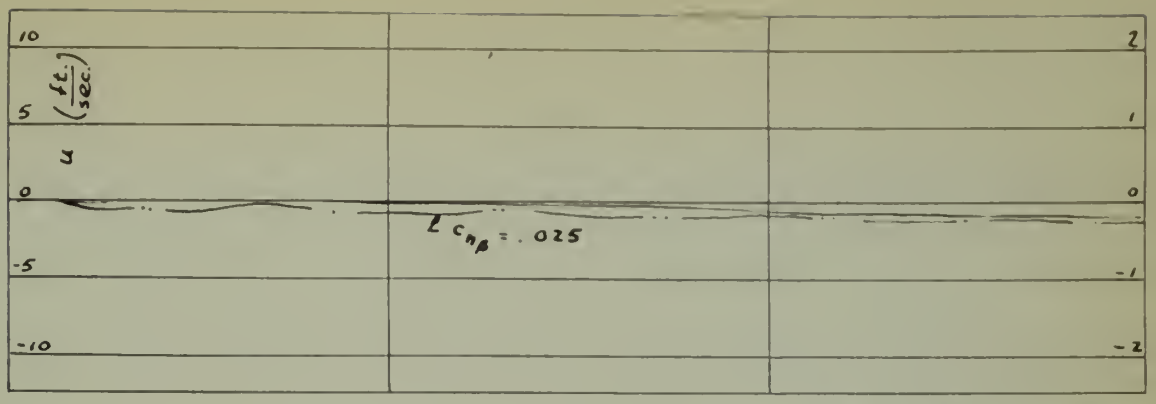

S.L.

Notice the scale change H.A.

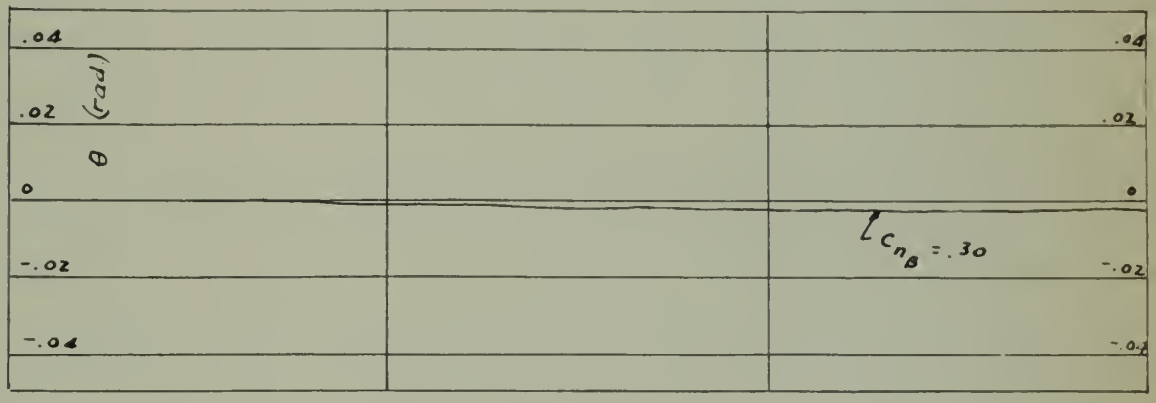

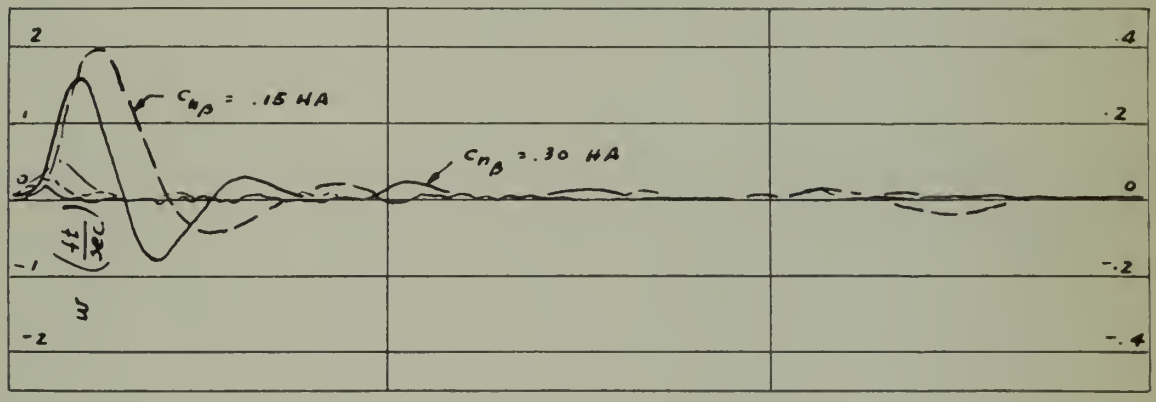

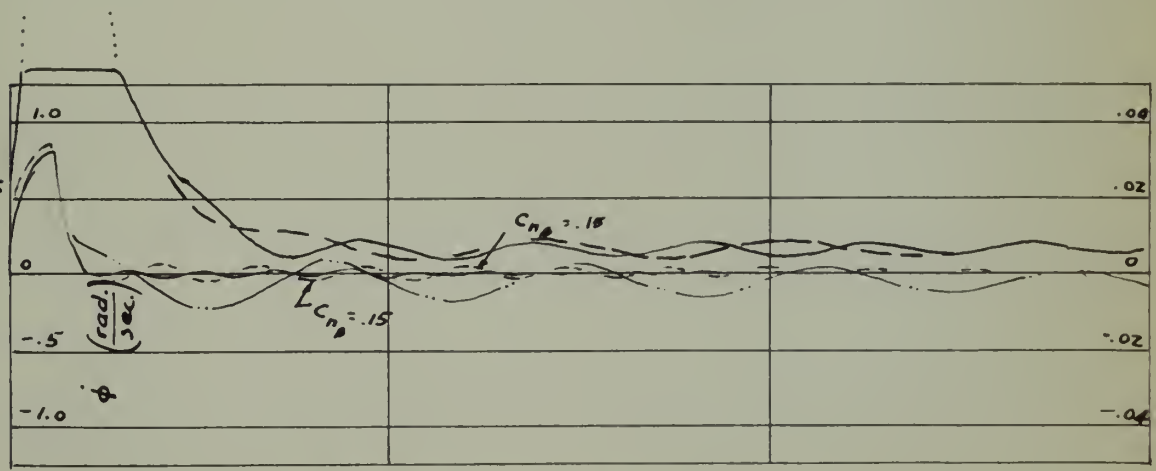

Fig. [illegible] Response to Unit Impulse in C_{n_β}

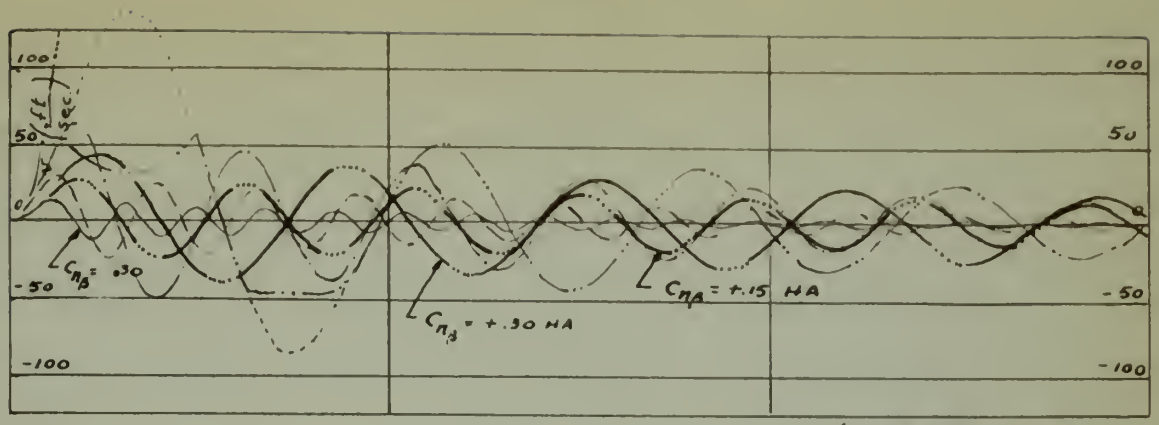

S.L.

Notice the scale change

High Altitude

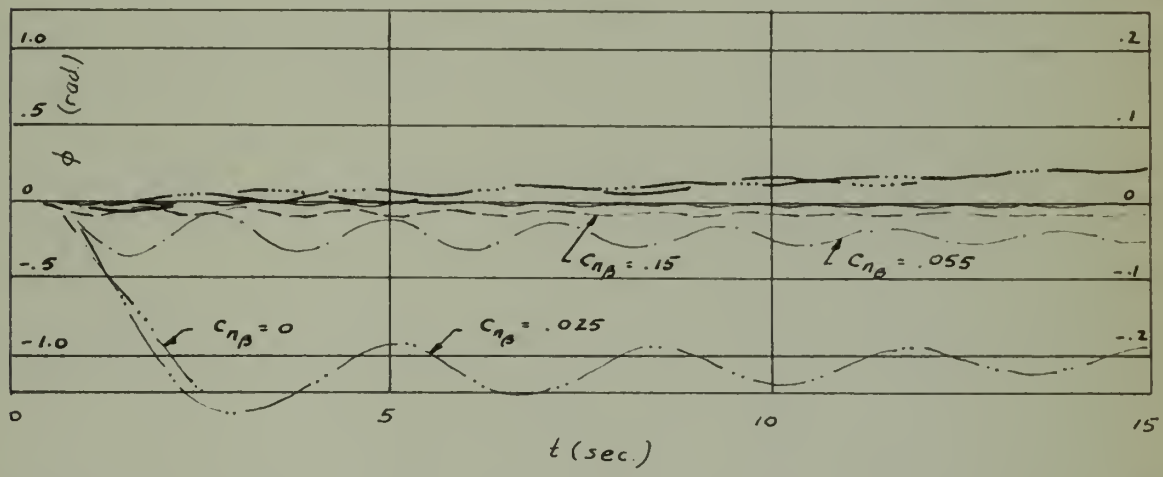

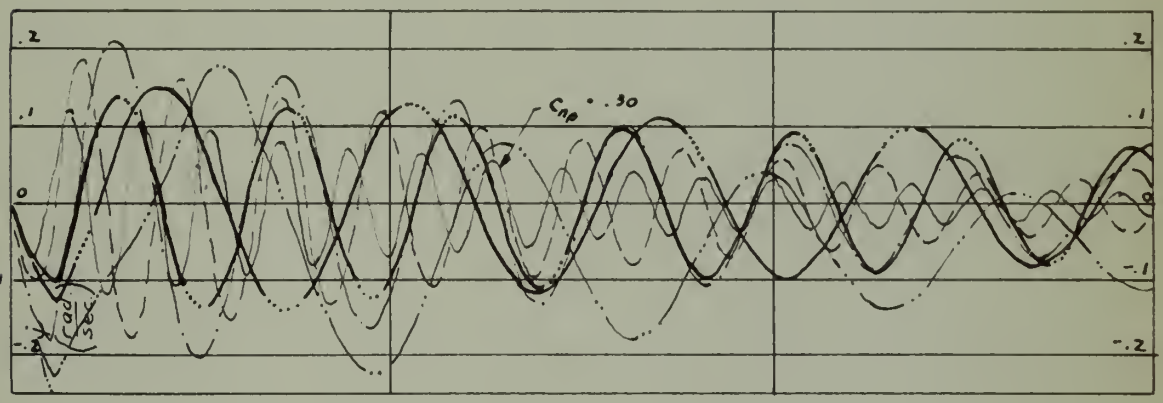

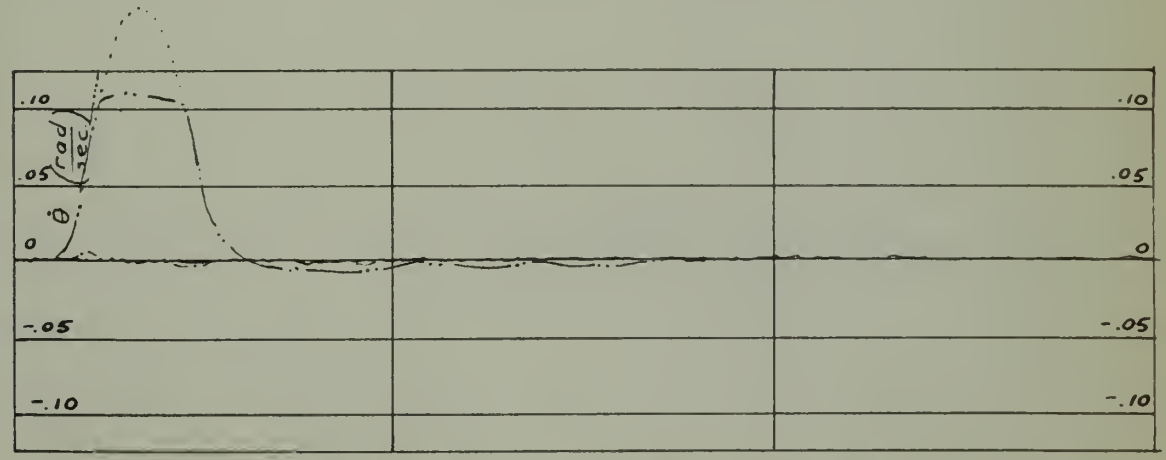

FIG. [illegible]

C_{n_β} [illegible]

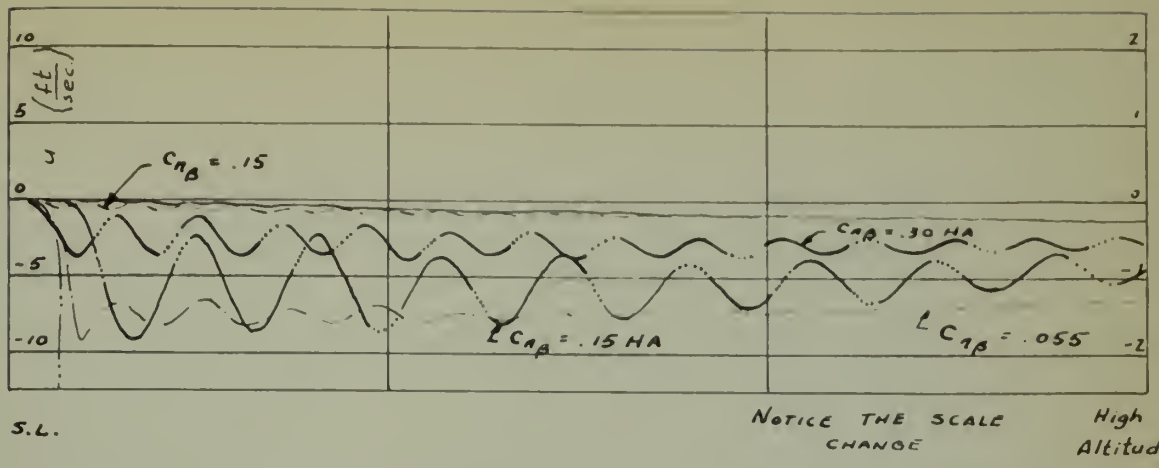
10
5
(ft/sec)
J
0
-5
-10
$C_{n_\beta} = .15$
$C_{n_\beta} = .30$ HA
$C_{n_\beta} = .15$ HA
$C_{n_\beta} = .055$
2
1
0
-1
-2
S.L.
NOTICE THE SCALE CHANGE
High Altitude

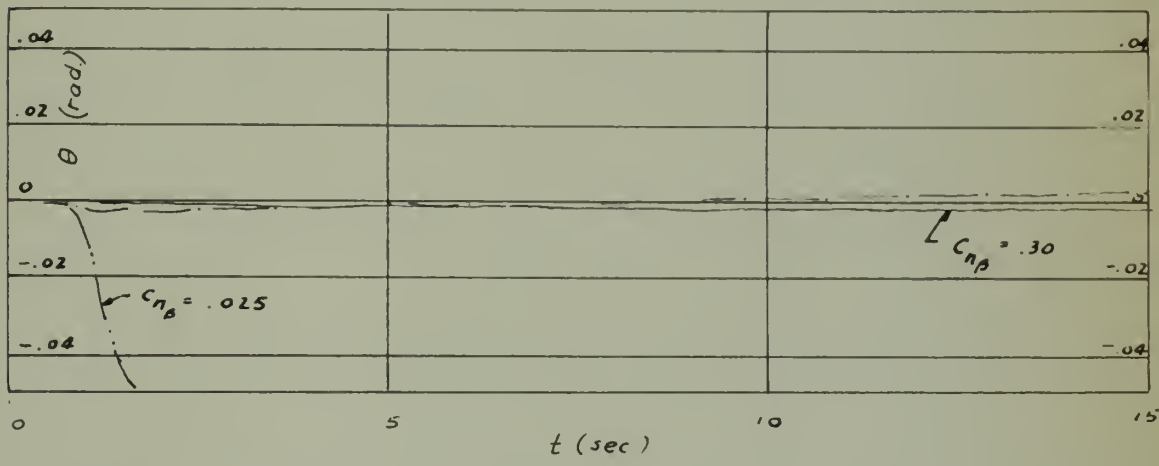
.04
.02
(rad)
θ
0
-.02
-.04
$C_{n_\beta} = .025$
$C_{n_\beta} = .30$
0
5
10
15
t (sec)

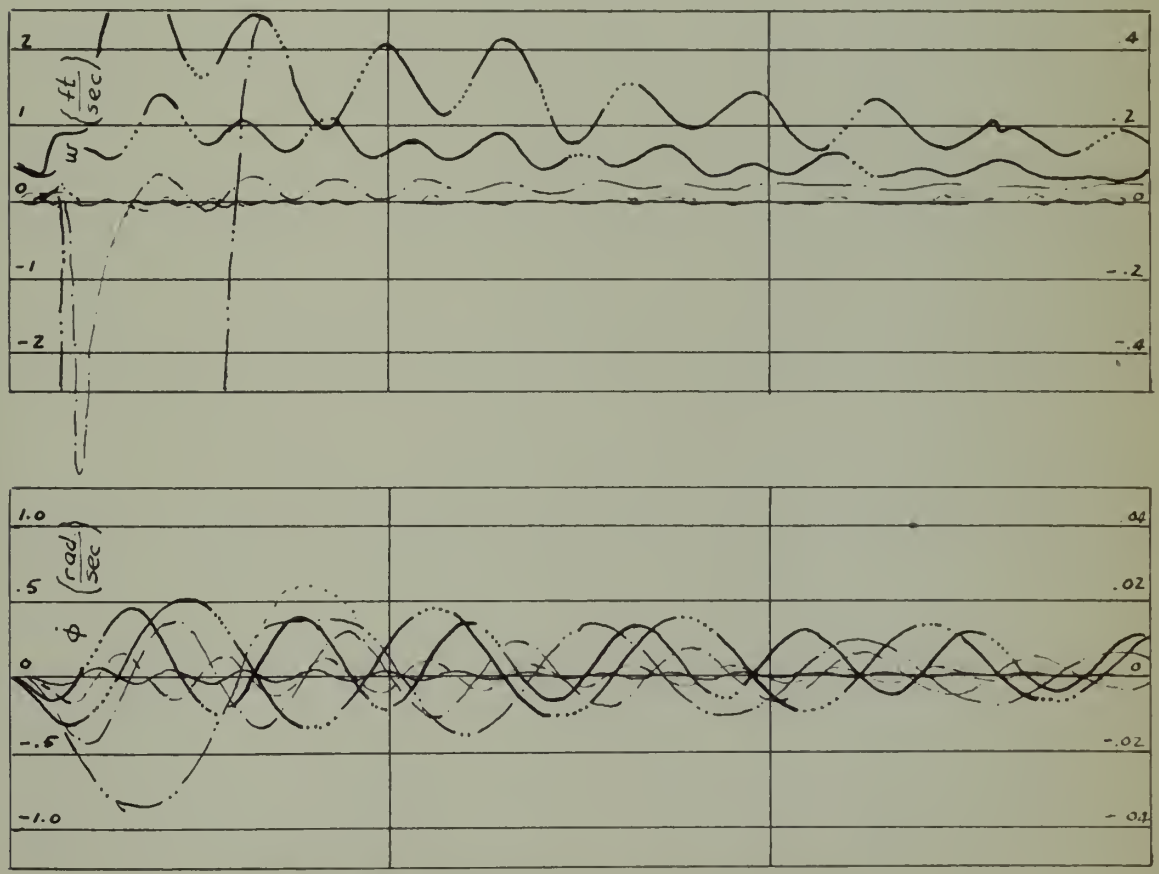
2
1
0
-1
-2
(ft/sec)
w
.4
.2
-.2
-.4
1.0
.5
(rad/sec)
φ
-.5
-1.0
.04
.02
-.02
-.04

Fig. [illegible]

C_{n_β}

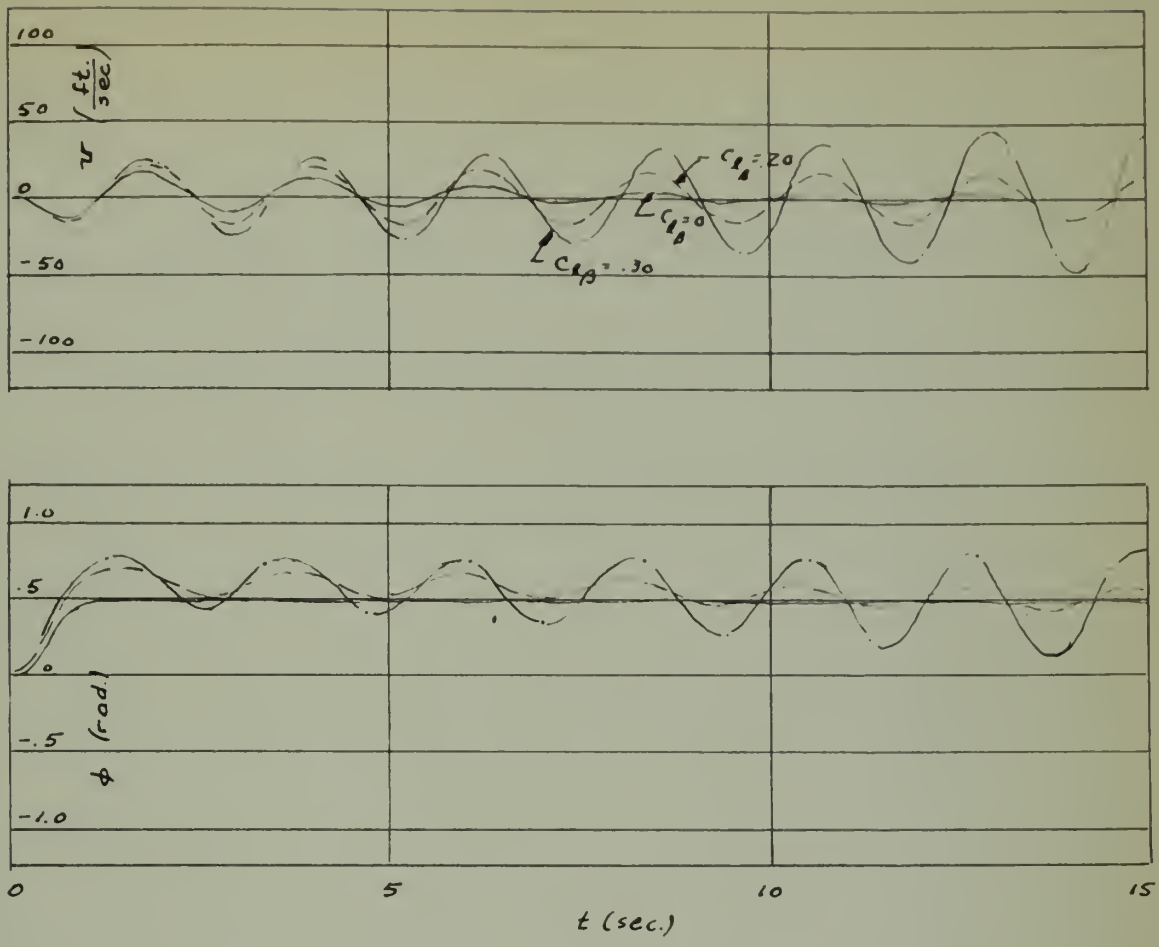

FIG. 23 TO ...
C_{l_β} ...

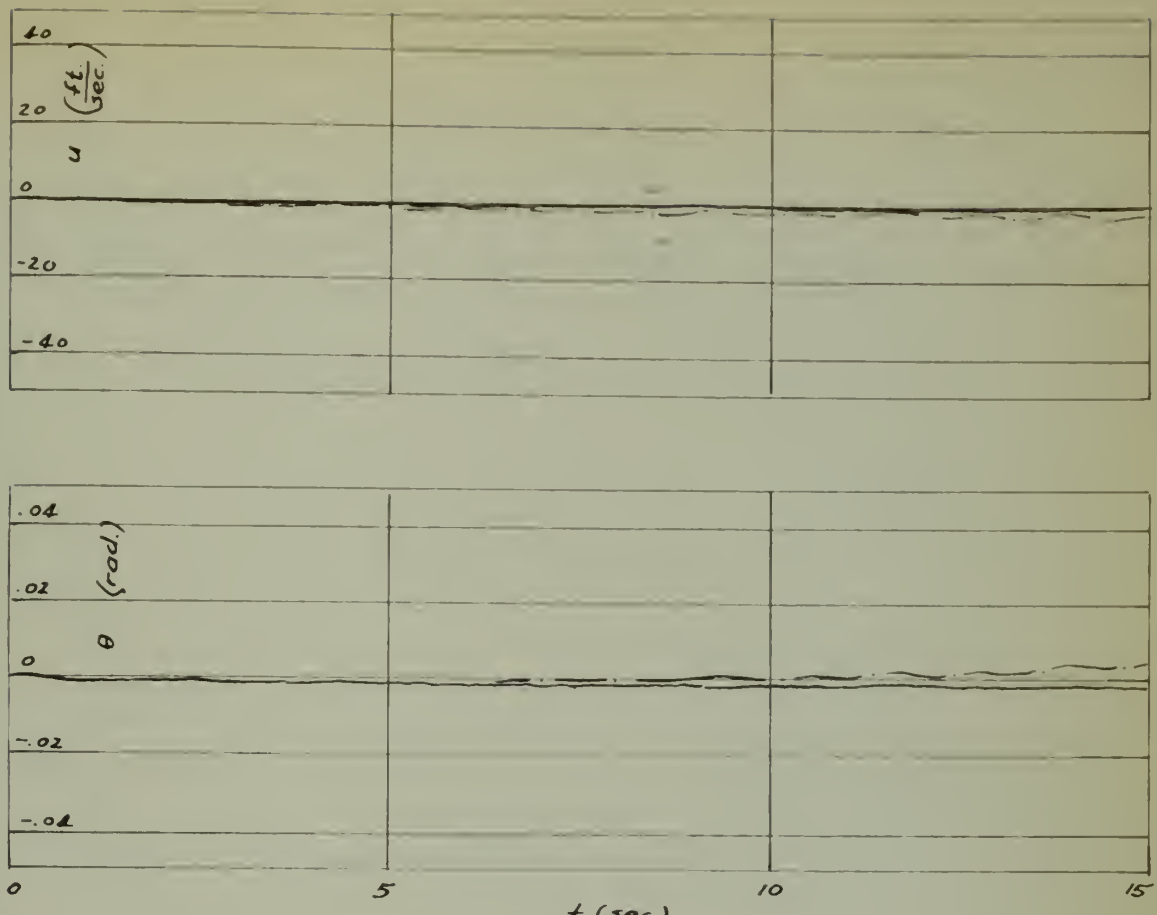
40
20
u (ft./sec.)
0
-20
-40
.04
.02
θ (rad.)
0
-.02
-.04
0
5
10
15
t (sec.)
2
1
0
-1
-2
w (ft./sec.)
4
2
0
-2
-4
φ (rad./sec.)
$C_{\ell_\beta} = 0$
$C_{\ell_\beta} = .20$
$C_{\ell_\beta} = .30$

C_{ℓ_β}

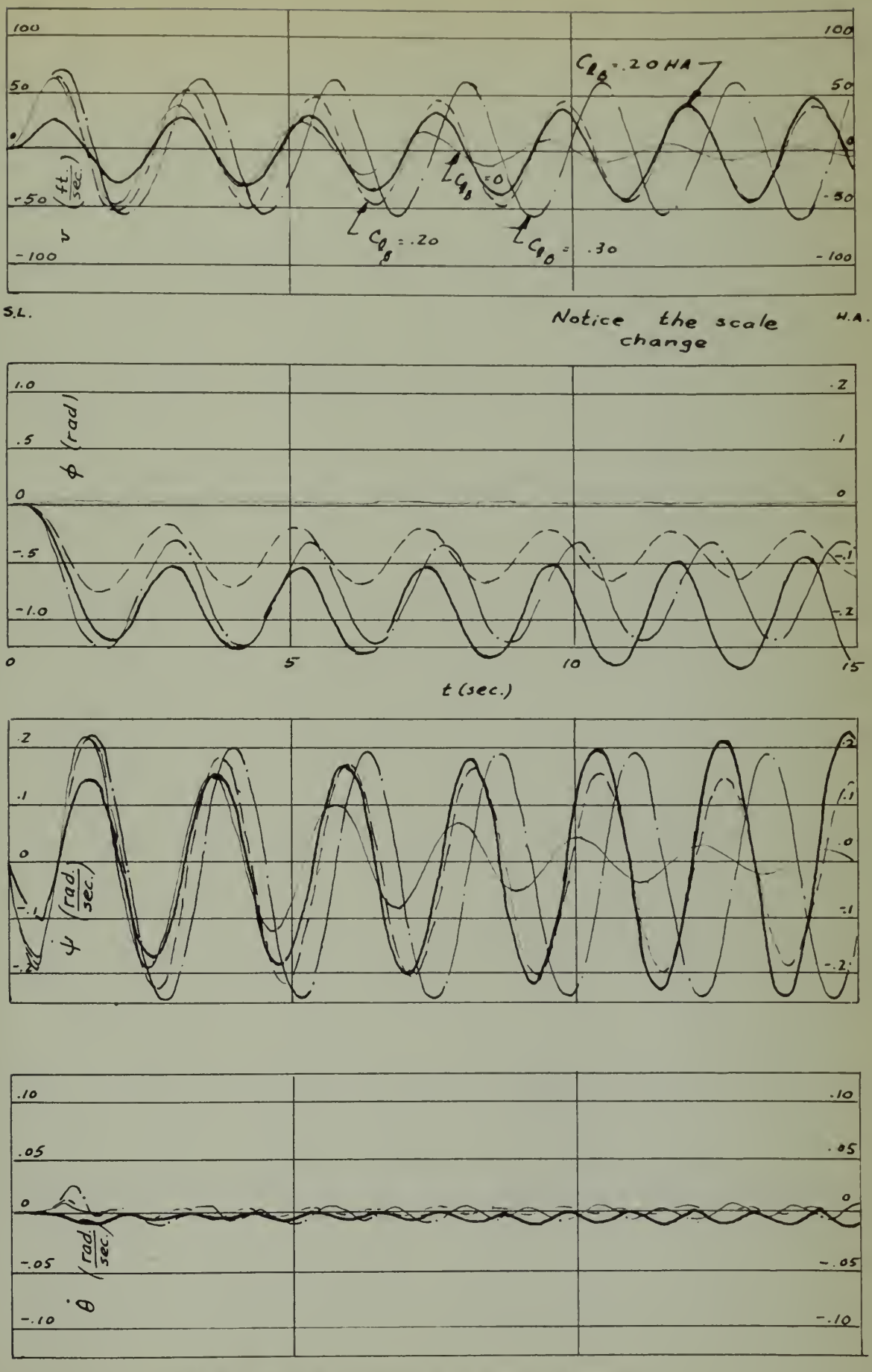
100
50
0
-50
-100
v (ft/sec)
C_{l_β} = .20 HA
C_{l_β} = 0
C_{l_β} = .20
C_{l_β} = .30
S.L.
Notice the scale change
H.A.
1.0
.5
0
-.5
-1.0
ϕ (rad)
.2
.1
-.1
-.2
0
5
10
15
t (sec.)
ψ (rad/sec.)
.10
.05
-.05
-.10
$\dot{\theta}$ (rad/sec)

C_{l_β}

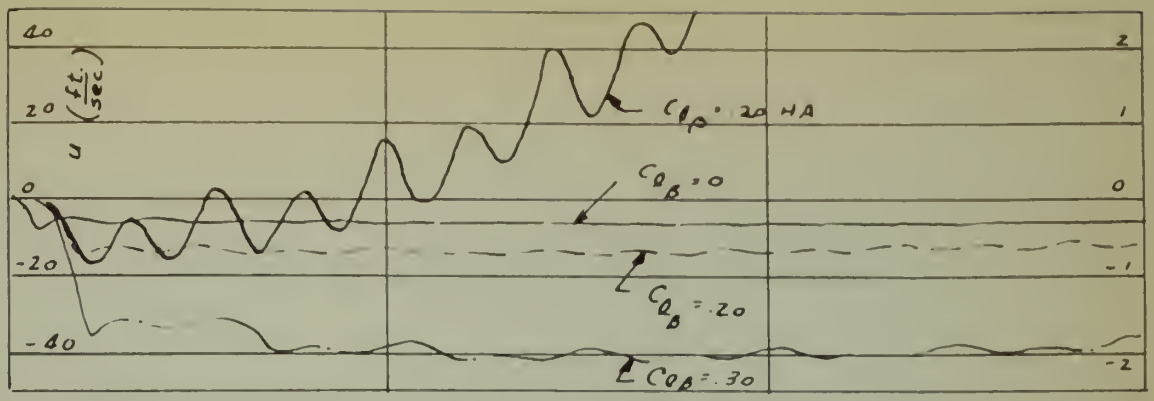

Notice the scale change

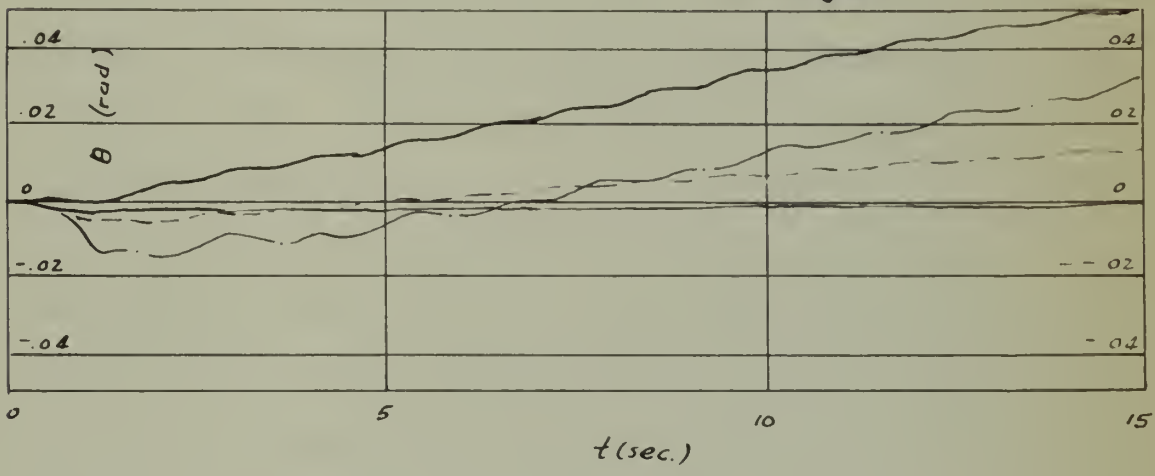

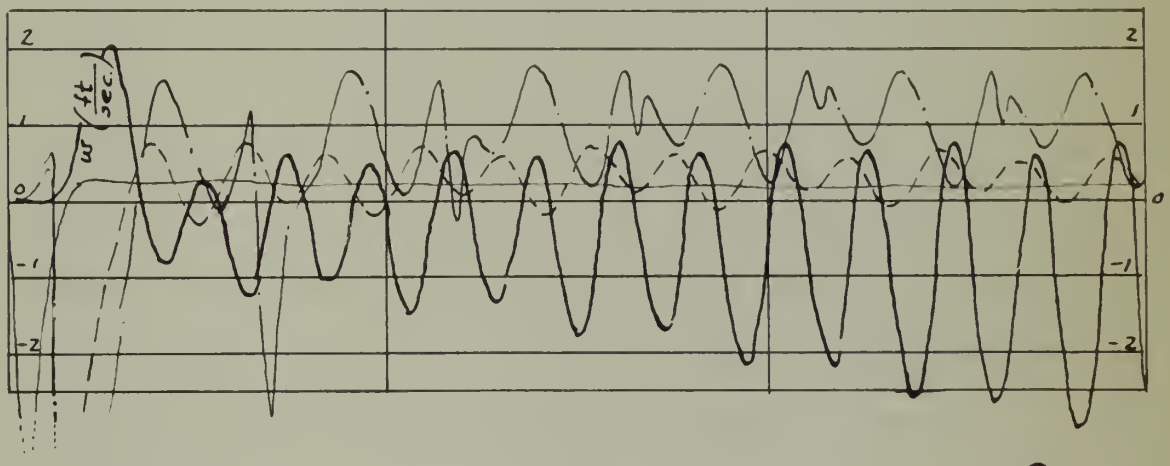

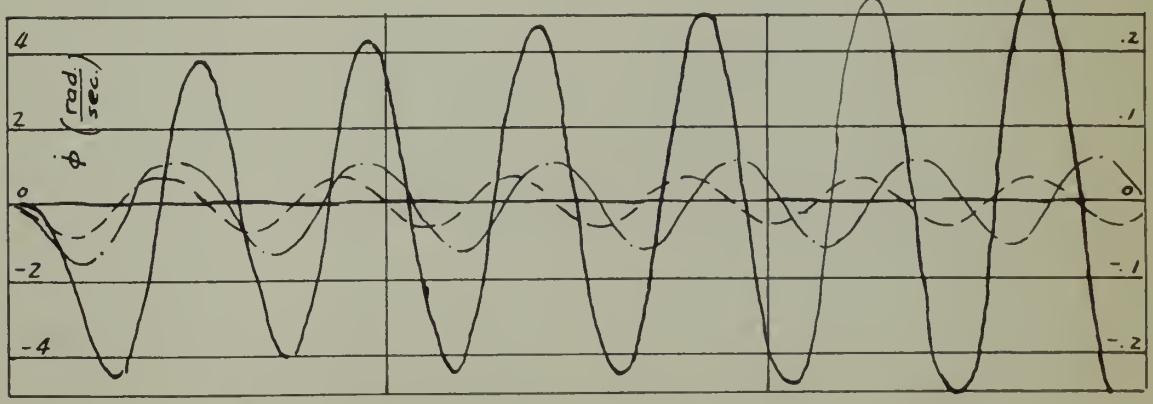

C_{l_β}

APPENDIX I

Development of the Equations of Motion

The equations of motion of the airframe are written by equating the forces and moments acting on the airframe to the plane's reactions in accordance with Newton's laws. The reference axes are considered fixed in space.

The aircraft is considered to be a rigid body; aeroelastic effects are not considered. The motion is referred to right-handed Cartesian axes. The axes used and the sign conventions observed are shown in Fig. 8 and Table I.

Newton's second law states that the rate of change of momentum of a body is proportional to the force applied to the body and the rate of change of the moment of momentum is proportional to the torque applied to the body. The mass of the airplane is considered constant for the duration of the dynamic maneuver considered.

$$(1) \qquad \Sigma F_x = \frac{d}{dt}(mU) = m\dot{U}$$

$$\Sigma F_y = \frac{d}{dt}(mV) = m\dot{V}$$

$$\Sigma F_z = \frac{d}{dt}(mW) = m\dot{W}$$

$$(2) \qquad \Sigma L = \frac{dh_x}{dt}$$

$$\Sigma M = \frac{dh_y}{dt}$$

$$\Sigma N = \frac{dh_z}{dt}$$

Investigating the dynamics of an infinitesimal element of mass dm of the airplane referred to the Cartesian coordinate system yields equation set (3).

$$(3)\quad \begin{aligned} dh_x &= (y^2+z^2)P\,dm - zx\,R\,dm - yx\,Q\,dm \\ dh_y &= (z^2+x^2)Q\,dm - xy\,P\,dm - yz\,R\,dm \\ dh_z &= (x^2+y^2)R\,dm - zx\,P\,dm - zy\,Q\,dm \end{aligned}$$

For a finite mass these become

$$(4)\quad \begin{aligned} h_x &= P\int(y^2+z^2)\,dm - Q\int xy\,dm - R\int xz\,dm \\ h_y &= Q\int(z^2+x^2)\,dm - R\int yz\,dm - P\int yx\,dm \\ h_z &= R\int(x^2+y^2)\,dm - P\int zx\,dm - Q\int zy\,dm \end{aligned}$$

The integral $\int(y^2+z^2)\,dm$ is recognized as the moment of inertia I_x of the whole airplane about the x-axis. Equation set (4) can be written

$$\begin{aligned} h_x &= P I_x - Q I_{xy} - R I_{xz} \\ h_y &= Q I_y - R I_{yz} - P I_{xy} \\ h_z &= R I_{zz} - P I_{xz} - Q I_{yz} \end{aligned}$$

The equations of motion relative to inertial axes becomes:

$$(5)\quad \begin{aligned} \Sigma F_x &= m\frac{dU}{dt} \\ \Sigma F_y &= m\frac{dV}{dt} \\ \Sigma F_z &= m\frac{dW}{dt} \end{aligned}$$

$$(6)\quad \begin{aligned} \Sigma L = \frac{dh_x}{dt} &= \dot{P} I_x + P\dot{I}_x - \dot{Q} I_{xy} - Q\dot{I}_{xy} - R I_{xz} - R\dot{I}_{xz} \\ \Sigma M = \frac{dh_y}{dt} &= \dot{Q} I_y + Q\dot{I}_y - \dot{R} I_{yz} - R\dot{I}_{yz} - \dot{P} I_{xy} - P\dot{I}_{xy} \\ \Sigma N = \frac{dh_z}{dt} &= \dot{R} I_z + R\dot{I}_z - \dot{P} I_{xz} - P\dot{I}_{xz} - \dot{Q} I_{zy} - Q\dot{I}_{zy} \end{aligned}$$

Equations (6) are written with respect to fixed inertial axes. It is expedient to use Eulerian axes with their origin at the c.g. which are fixed in the airplane and move with it. At any instant the airplane

in a maneuver has a motion referred to the Eulerian axes and the axes have a motion referred to fixed space. The earth and its atmosphere are regarded as fixed space. The absolute acceleration of the aircraft referred to the Eulerian axes can be written

(7) $$\vec{a}_{abs} = \frac{d\vec{V}_T}{dt} + \vec{\omega} \times \vec{V}_T$$

where $\vec{V}_T$ is the total velocity.

Similarly the absolute rate of change of the moment of momentum is written

(8) $$\frac{d\vec{h}_{abs}}{dt} = \frac{d\vec{h}}{dt} + \vec{\omega} \times \vec{h}$$

The first term arises from the change relative to the Eulerian axes fixed from instant to instant in the airplane and the second considers the change of the Eulerian axes relative to inertial axes fixed in space.

Moments and products of inertia measured relative to Eulerian axes are independent of time since the mass is assumed constant for the duration of a maneuver. Many of the terms in equation set (6) go to zero for this reason.

The term $\vec{\omega} \times \vec{V}_t$ of equation (7) can be written:

(8a) $$\vec{\omega} \times \vec{V}_t = \begin{vmatrix} \vec{i} & \vec{j} & \vec{k} \\ P & Q & R \\ U & V & W \end{vmatrix}.$$

Where $\vec{i}, \vec{j}, \vec{k}$ are unit vectors directed along the Eulerian X, Y, Z axes.

Expanding the cross product and combining with the components of the first term of (7) that equation can be written in component form as:

(9) $$\begin{aligned} a_x &= \dot{U} + QW - RV \\ a_y &= \dot{V} + RU - PW \\ a_z &= \dot{W} + PV - QU \end{aligned}$$

By parallel reasoning (8) can be written:

$$(10)\quad \left.\frac{dh_x}{dt}\right|_{abs} = \frac{dh_x}{dt} + h_z Q - h_y R = \dot{P} I_x - Q\dot{I}_{xy} - \dot{R} I_{xz} + QR(I_z - I_y) - PQ I_{xz} - Q^2 I_{zy} + R^2 I_{yz} + PR I_{xy}$$

$$\left.\frac{dh_y}{dt}\right|_{abs} = \frac{dh_y}{dt} + h_x R - h_z P = \dot{Q} I_y - \dot{R} I_{yz} - \dot{P} I_{xy} + PR(I_x - I_z) - QR I_{xy} - R^2 I_{xz} + P^2 I_{xz} + PQ I_{zy}$$

$$\left.\frac{dh_z}{dt}\right|_{abs} = \frac{dh_z}{dt} + h_y P - h_x Q = \dot{R} I_z - \dot{P} I_{xz} - \dot{Q} I_{zy} + PQ(I_y - I_x) - PR I_{yz} - P^2 I_{xy} + Q^2 I_{xy} + QR I_{xz}$$

With the Eulerian axes as chosen and shown in Fig. 8, the xz-plane is a plane of symmetry. There is both a positive and a negative value of y for each value of z; consequently $I_{yz} = \int yz\, dm = 0$ and $I_{xy} = \int xy\, dm = 0$.

The equations of motion of an aircraft referred to Eulerian axes can then be written:

$$(11)\quad \Sigma F_x = m[\dot{U} + QW - RV]$$

$$\Sigma F_y = m[\dot{V} + RU - PW]$$

$$\Sigma F_z = m[\dot{W} + PV - QU]$$

$$\Sigma L = \dot{P} I_x - \dot{R} I_{xz} + QR(I_z - I_y) - PQ I_{xz}$$

$$\Sigma M = \dot{Q} I_y + PR(I_x - I_z) - R^2 I_{xz} + P^2 I_{xz}$$

$$\Sigma N = \dot{R} I_z - \dot{P} I_{xz} + PQ(I_y - I_x) + QR I_{xz}$$

The left sides of the equations in set (11) are the summations of the external forces and moments applied to the airplane in flight. These external forces are gravity forces, aerodynamic forces, and thrust forces.

The gravity force may be considered to act at the center of gravity making no contribution to the summation of moments.

The resolution of the gravity force into components referred to disturbed Eulerian axes is shown in Fig. 1.

The force relations may be written

(12)
$$\sum F_x' = m[\dot{U} + QW - RV] - X_3$$
$$\sum F_y' = m[\dot{V} + RU - PW] - Y_3$$
$$\sum F_z' = m[\dot{W} + PV - QU] - Z_3$$

by transferring the gravity terms to the right-hand side of the equation. The gravity terms X_3, Y_3, and Z_3 are expanded in Fig. 1.

The left side of all the force and moment equations now include aerodynamic and thrust forces as well as moments due to control surface deflection.

The disturbed motion of an airplane at any instant can be considered the result of disturbing the airplane from some steady flight condition. This motion may be referred to as disturbed flight and the Eulerian axes as the disturbed axes. The forces acting on the airplane under these conditions may be regarded as the sum of the force required to produce steady flight plus an increment required for the disturbance. Accordingly, each of the total instantaneous velocity components can be written as the sum of a constant velocity component during steady flight and a change caused by the disturbance:

(13)
$$U = U_0 + u$$
$$V = V_0 + v$$
$$W = W_0 + w$$

$$P = P_o + p$$

$$Q = Q_o + q$$

$$R = R_o + r$$

Substituting in (12) considering that $\frac{dU_o}{dt} = \frac{dP_o}{dt} = 0$, etc., and using the expansion of the gravity terms from Fig. 1 after setting terms like $\sin\psi \sin\phi = 0$, $\sin\psi = \psi$ and $\cos\theta = 1$, the set of equations below can be written. The assumptions that the sine of an angle can be replaced by the angle, the cosine is equal to one and the product of sines can be replaced by zero produces results which, although approximate, are in good agreement with physical results according to Ref. 7. These assumptions, of course, apply to the disturbed angles.

(14) $$\Sigma F_x' = m[\dot{u} + Q_o W_o + W_o q + Q_o w - R_o V_o - R_o v - V_o r + wq - vr + g\sin\theta_o - (g\cos\theta_o \sin\phi_o)\psi + (g\cos\theta_o \cos\phi_o)\theta]$$

$$\Sigma F_z' = m[\dot{w} + P_o V_o + P_o v + V_o p - Q_o U_o - Q_o u - U_o q - qu + pv + (g\sin\theta_o)\theta + (g\cos\theta_o \sin\phi_o)\phi - (g\cos\theta_o \cos\phi_o)]$$

$$\Sigma F_y' = m[\dot{v} + U_o R_o + U_o r + R_o u - P_o W_o - P_o w - W_o p - wp + ru - (g\sin\theta_o)\psi - g\cos\theta_o \sin\phi_o - (g\cos\theta_o \cos\phi_o)\phi]$$

$$\Sigma L = \dot{p} I_x - \dot{r} I_{xz} + (Q_o R_o + Q_o r + R_o q + qr)(I_z - I_y) - (P_o Q_o + P_o q + Q_o p + pq) I_{xz}$$

$$\Sigma M = \dot{q} I_y + (P_o R_o + P_o r + R_o p + pr)(I_x - I_z) - (R_o^2 + 2R_o r + r^2) I_{xz} + (P_o^2 + 2P_o p + p^2) I_{xz}$$

$$\Sigma N = \dot{r} I_z - \dot{p} I_{xz} + (P_o Q_o + P_o q + Q_o p + pq)(I_y - I_x) + (Q_o R_o + Q_o r + R_o q + rq) I_{xz}$$

The aerodynamic forces and moments acting on an airplane, the left side of the above equations, are functions of the flight conditions and of the deflection of the control surfaces.

Each of the forces ($X, Y,$ and Z) and the moments ($L, M,$ and N) can be expressed for small oscillations by expanding by MacLaurin's theorem neglecting second order terms to obtain:

$$X = X_o + u\frac{\partial X}{\partial u} + q_1\frac{\partial X}{\partial q_1} + w\frac{\partial X}{\partial w} + \dot{w}\frac{\partial X}{\partial \dot{w}} \cdots$$

where $\frac{\partial X}{\partial u}$, $\frac{\partial X}{\partial q_1}$, etc. are partial derivatives of X with respect to u, q_1, etc. Exactly analogous expansions are made for $Y, Z, L, M,$ and N. These forces and moments can be expressed:

(15)
$$X = X_o + \frac{\partial X}{\partial u}u + \frac{\partial X}{\partial q_1}q_1 + \frac{\partial X}{\partial w}w + \frac{\partial X}{\partial \dot{w}}\dot{w} \cdots$$
$$Y = Y_o + \frac{\partial Y}{\partial r}r + \frac{\partial Y}{\partial v}v + \frac{\partial Y}{\partial p}p + \frac{\partial Y}{\partial \delta_a}\delta_a + \frac{\partial Y}{\partial \delta_r}\delta_r \cdots$$
$$Z = Z_o + \frac{\partial Z}{\partial u}u + \frac{\partial Z}{\partial q_1}q_1 + \frac{\partial Z}{\partial w}w + \frac{\partial Z}{\partial \delta_e}\delta_e \cdots$$
$$L = L_o + \frac{\partial L}{\partial r}r + \frac{\partial L}{\partial v}v + \frac{\partial L}{\partial p}p + \frac{\partial L}{\partial \delta_a}\delta_a + \frac{\partial L}{\partial \delta_r}\delta_r \cdots$$
$$M = M_o + \frac{\partial M}{\partial u}u + \frac{\partial M}{\partial q_1}q_1 + \frac{\partial M}{\partial w}w + \frac{\partial M}{\partial \delta_e}\delta_e \cdots$$
$$N = N_o + \frac{\partial N}{\partial v}v + \frac{\partial N}{\partial r}r + \frac{\partial N}{\partial p}p + \frac{\partial N}{\partial \delta_r}\delta_r + \frac{\partial N}{\partial \delta_a}\delta_a \cdots$$

Each of the terms in (15) has a physical significance. $X_o, Y_o,$ and Z_o, $L_o, M_o,$ and N_o are the forces and moments acting along and about the x, y, and z axes while the plane is in steady flight. The terms similar to $\frac{\partial X}{\partial u}u$ express the change in the given force or moment caused by the given disturbance quantity. The coefficients of the form $\frac{\partial L}{\partial p}$ are the basic dimensional stability derivatives. A complete discussion of stability derivatives may be found in Refs. (1), (2), (3), (7), (8), and (9).

Thrust effects are part of the left sides of equation set (14). The equations for steady flight condition become:

(16)
$$X_o = T_o \cos\xi$$
$$Z_o = -T_o \sin\xi$$
$$M_o = T_o z_j$$

Since the Eulerian axes remain fixed with reference to the airplane during a disturbance, the thrust components relative to disturbed axes become:

(17)
$$X = T_1 \cos\xi$$
$$Z = -T_1 \sin\xi$$
$$M = T_1 z_j$$

where T_1 the thrust during the disturbance, is $T_o + \Delta T$.

ΔT can be considered

(18)
$$\Delta T = \frac{\partial T}{\partial u} u + \frac{\partial T}{\partial \delta_{rpm}} \delta_{rpm}$$

and

(19)
$$X = T_o \cos\xi + (\cos\xi)\frac{\partial T}{\partial u} u + (\cos\xi)\frac{\partial T}{\partial \delta_{rpm}} \delta_{rpm}$$
$$Z = -T_o \sin\xi - (\sin\xi)\frac{\partial T}{\partial u} u - (\sin\xi)\frac{\partial T}{\partial \delta_{rpm}} \delta_{rpm}$$
$$M = T_o z_j + z_j \frac{\partial T}{\partial u} u + z_j \frac{\partial T}{\partial \delta_{rpm}} \delta_{rpm}$$

The equations for steady flight are found by substituting the expressions obtained above for the thrust and the aerodynamic forces (and moments) into the left sides of equation set (14) and setting the disturbed quantities equal to zero:

(20)
$$X_o - W\sin\theta_o + T_o \cos\xi = 0$$
$$Y_o + 0 + 0 = 0$$
$$Z_o + W\cos\theta_o - T_o \sin\xi = 0$$

$$L_o + 0 + 0 = 0$$

$$M_o + 0 + T_o z_j = 0$$

$$N_o + 0 + 0 = 0$$

If now the complete equations for the disturbed airplane are written with both steady flight and disturbed terms they will be of the form:

Aerodynamic forces + thrust forces = inertia force − gravity force

Equation set (20) can then be subtracted from the complete equations of motion for the disturbed airplane yielding:

(21) $$\frac{\partial X}{\partial u}u + \frac{\partial X}{\partial q}q + \frac{\partial X}{\partial w}w + \frac{\partial X}{\partial \dot{w}}\dot{w} + (\cos\xi)\frac{\partial T}{\partial u}u + (\cos\xi)\frac{\partial T}{\partial \delta_{rpm}}\delta_{rpm}$$
$$= m\left[\dot{u} + Q_o W_o + W_o q + Q_o w + wq - R_o Y_o - R_o v - V_o r - vr\right.$$
$$\left. -(g\cos\theta_o \sin\phi_o)\psi + (g\cos\theta_o\cos\phi_o)\theta\right]$$

$$\frac{\partial Y}{\partial r}r + \frac{\partial Y}{\partial v}v + \frac{\partial Y}{\partial p}p + \frac{\partial Y}{\partial \delta_a}\delta_a + \frac{\partial Y}{\partial \delta_r}\delta_r = m\left[\dot{v} + U_o R_o + U_o r + R_o u + ur\right.$$
$$\left. - P_o W_o - P_o w - W_o p - wp - (g\sin\theta_o)\psi - g\cos\theta_o \sin\phi_o - (g\cos\theta_o\cos\phi_o)\phi\right]$$

$$\frac{\partial Z}{\partial u}u + \frac{\partial Z}{\partial q}q + \frac{\partial Z}{\partial w}w + \frac{\partial Z}{\partial \delta_e}\delta_e - (\sin\xi)\frac{\partial T}{\partial u}u - (\sin\xi)\frac{\partial T}{\partial \delta_{rpm}}\delta_{rpm}$$
$$= m\left[\dot{w} + P_o V_o + P_o v + V_o p + pv - Q_o U_o - Q_o u - U_o q - qu\right.$$
$$\left. + (g\sin\theta_o)\theta + (g\cos\theta_o \sin\phi_o)\phi - (g\cos\theta_o\cos\phi_o)\right]$$

$$\frac{\partial L}{\partial r}r + \frac{\partial L}{\partial v}v + \frac{\partial L}{\partial p}p + \frac{\partial L}{\partial \delta_a}\delta_a + \frac{\partial L}{\partial \delta_r}\delta_r$$
$$= \dot{p}I_x - \dot{r}I_{xz} + (Q_o R_o + Q_o r + R_o q + qr)(I_z - I_y)$$
$$- (P_o Q_o + P_o q + Q_o p + pq)I_{xz}$$

$$\frac{\partial M}{\partial u}u + \frac{\partial M}{\partial q}q + \frac{\partial M}{\partial w}w + \frac{\partial M}{\partial \delta_e}\delta_e + z_j\frac{\partial T}{\partial u}u + z_j\frac{\partial T}{\partial \delta_{rpm}}\delta_{rpm}$$
$$= \dot{q}I_y + (P_o R_o + P_o r + R_o p + pr)(I_x - I_z)$$
$$- (R_o^2 + 2R_o r + r^2)I_{xz} + (P_o^2 + 2P_o p + p^2)I_{xz}$$

$$\frac{\partial N}{\partial v}v + \frac{\partial N}{\partial r}r + \frac{\partial N}{\partial p}p + \frac{\partial N}{\partial \delta_r}\delta_r + \frac{\partial N}{\partial \delta_a}\delta_a$$
$$= \dot{r}I_z - \dot{p}I_{xz} + (P_o Q_o + P_o q + Q_o p + pq)(I_y - I_x)$$
$$+ (Q_o R_o + Q_o r + R_o q + qr)I_{xz}$$

Dividing the force equations by m and the moment equations by the appropriate moment of inertia yields terms of the form:

$$\frac{1}{m}\frac{\partial X}{\partial u}u \quad \text{and} \quad \frac{1}{I_x}\frac{\partial L}{\partial r}r$$

Replacing $\frac{1}{m}\frac{\partial X}{\partial u}u$ by X_u and $\frac{1}{I_x}\frac{\partial L}{\partial r}r$ by L_r simplifies the notation. These quantities are called dimensional stability derivatives. A list of these stability derivatives in terms of the dimensionless forms appears as Tables III and IV. The flight path angle γ_o replaces θ_o. The equations in final form can be written:

(22) $X_u u + X_q q + X_w w + X_{\dot{w}}\dot{w} + \cos\xi\, T_u u + \cos\xi\, T_{\delta_{rpm}}\delta_{rpm}$
$= \dot{u} + W_o q + Q_o w + wq - R_o V_o - R_o v - V_o r - vr$
$- (g\cos\gamma_o \sin\phi_o)\psi$

$Y_r r + Y_v v + Y_p p + Y_{\delta_a}\delta_a + Y_{\delta_r}\delta_r = \dot{v} + U_o r - W_o p - wp + \bar{U}_o R_o + \bar{U}_o r$
$+ R_o u + ur - P_o w - (g\sin\gamma_o)\psi - g\sin\gamma_o \sin\phi_o - (g\cos\gamma_o\cos\phi_o)\phi$

$Z_u u + Z_q q + Z_w w + Z_{\delta_e}\delta_e - \sin\xi\, T_u u - T_{\delta_{rpm}}\delta_{rpm} =$
$\dot{w} + P_o V_o + P_o v + V_o p - Q_o U_o - Q_o u - V_o q - qu + pv$
$- (g\sin\theta_o)\theta + (g\cos\theta_o \sin\phi_o)\phi + (g\cos\theta_o\cos\phi_o) - g\cos\gamma_o$

$\dot{p} - \dot{r}\frac{I_{xz}}{I_x} + (Q_o R_o + Q_o r + R_o q + qr)\frac{(I_z - I_y)}{I_x} - (P_o Q_o + P_o q + Q_o p + pq)\frac{I_{xz}}{I_x}$
$= L_r r + L_v v + L_p p + L_{\delta_a}\delta_a + L_{\delta_r}\delta_r$

$\dot{q} + (P_o R_o + P_o r + R_o p + pr)\frac{(I_x - I_z)}{I_y} - (R_o^2 + 2R_o r + r^2)\frac{I_{xz}}{I_y}$
$+ (P_o^2 + 2P_o p + p^2)\frac{I_{xz}}{I_y} = M_u u + M_q q + M_w w + M_{\delta_e}\delta_e$

$\dot{r} - \dot{p}\frac{I_{xz}}{I_z} + (P_o Q_o + P_o q + Q_o p + pq)\frac{(I_y - I_x)}{I_z} + (Q_o R_o + Q_o r + R_o q + qr)\frac{I_{xz}}{I_z}$
$= N_v v + N_r r + N_p p + N_{\delta_r}\delta_r + N_{\delta_a}\delta_a$

APPENDIX II

Adaptation of the Equations of Motion to the Analogue Computer

The dynamic equations of motion of the airplane were developed in Appendix I. These are summarized below:

$$(II\text{-}1)\quad X_u u + X_q q + X_w w + X_{\dot{w}}\dot{w} + \cos\xi\, T_u u + \cos\xi\, T_{\delta_{rpm}}\delta_{rpm} = \dot{u} + W_0 q + Q_0 w + w q - R_0 V_0 - R_0 v - V_0 r - v r - (g\cos\gamma_0 \sin\phi_0)\psi$$

$$(II\text{-}2)\quad Y_r r + Y_v v + Y_p p + Y_{\delta_a}\delta_a + Y_{\delta_r}\delta_r = \dot{v} + U_0 r - W_0 p - w p + U_0 R_0 + U_0 r + R_0 u + u r - P_0 w - (g\sin\gamma_0)\psi - g\sin\gamma_0 \sin\phi_0 - (g\cos\gamma_0\cos\phi_0)\phi$$

$$(II\text{-}3)\quad Z_u u + Z_q q + Z_w w + Z_{\delta_e}\delta_e - \sin\xi\, T_u u - T_{\delta_{rpm}}\delta_{rpm} = \dot{w} + P_0 V_0 + P_0 v + V_0 p - Q_0 U_0 - Q_0 u - V_0 q - q u + p v - (g\sin\theta_0)\theta + (g\cos\theta_0 \sin\phi_0)\phi + (g\cos\theta_0\cos\phi_0) - g\cos\gamma_0$$

$$(II\text{-}4)\quad \dot{p} - \dot{r}\frac{I_{xz}}{I_x} + (Q_0 R_0 + Q_0 r - R_0 q + q r)\left(\frac{I_z - I_y}{I_x}\right) - (P_0 Q_0 + P_0 q + Q_0 p + p q)\frac{I_{xz}}{I_x} = L_r r + L_v v + L_p p + L_{\delta_a}\delta_a + L_{\delta_r}\delta_r$$

$$(II\text{-}5)\quad \dot{q} + (P_0 R_0 + P_0 r + R_0 p + p r)\left(\frac{I_x - I_z}{I_y}\right) - (R_0^2 + 2R_0 r + r^2)\frac{I_{xz}}{I_y} + (P_0^2 + 2P_0 p + p^2)\frac{I_{xz}}{I_y} = M_u u + M_q q + M_w w + M_{\delta_e}\delta_e$$

$$(II\text{-}6)\quad \dot{r} - \dot{p}\frac{I_{xz}}{I_z} + (P_0 Q_0 + P_0 q + Q_0 p + p q)\left(\frac{I_y - I_x}{I_z}\right) + Q_0 R_0 + Q_0 r + R_0 q + q r)\frac{I_{xz}}{I_z} = N_v v + N_r r + N_p p + N_{\delta_r}\delta_r + N_{\delta_a}\delta_a$$

These equations are general and allow initial velocities, angular or linear, with respect to any axis. Additional control terms, such as flap deflection may be included by adding the product of

the desired deflection and the appropriate stability derivative. Any attitude of the airplane is also permitted.

In order to fit the two analogue computers available certain assumptions were necessary. The plane was assumed to be in horizontal level flight with no initial velocities except U_o, forward velocity along the x-axis. Stability axes are chosen with the undisturbed x-axis alligned with the relative wind and the y-axis a principal axis. The product of inertia will be different from zero. The terms which describe power effects are permitted to go to zero by assuming gliding flight since these power terms are not essential to the dynamic effects which are studied. They merely add complexity.

Solving the resultant equations in terms of the highest derivative places them in the form required for analogue computer solution:

$$(II\text{-}7)\quad \dot{u} = X_u u + X_q q + X_w w + X_{\dot{w}} \dot{w} + vr - wq - g\theta$$

$$(II\text{-}8)\quad \dot{v} = Y_r r + Y_v v + Y_p p + Y_{\delta_a} \delta_a + Y_{\delta_r} \delta_r + wp - ru + g\theta$$

$$(II\text{-}9)\quad \dot{w} = Z_u u + Z_q q + Z_w w + Z_{\delta_e} \delta_e + qu - pv$$

$$(II\text{-}10)\quad \ddot{\psi} = \dot{r} = N_v v + N_r r + N_p p + N_{\delta_r} \delta_r + N_{\delta_a} \delta_a + \dot{p} \frac{I_{xz}}{I_z} - pq \left(\frac{I_y - I_x}{I_z}\right) - qr \frac{I_{xz}}{I_z}$$

$$(II\text{-}11)\quad \ddot{\phi} = \dot{p} = L_r r + L_v v + L_p p + L_{\delta_a} \delta_a + L_{\delta_r} \delta_r + \dot{r} \frac{I_{xz}}{I_x} - qr \frac{(I_z - I_y)}{I_x} + pq \frac{I_{xz}}{I_x}$$

$$(II\text{-}12)\quad \ddot{\theta} = \dot{q} = M_u u + M_q q + M_w w + M_{\delta_e} \delta_e + M_{\dot{w}} \dot{w} - pr \frac{(I_x - I_z)}{I_y} + r^2 \frac{I_{xz}}{I_y} - p^2 \frac{I_{xz}}{I_y}$$

The assumptions made simplify the equations sufficiently to permit use of the analogue computers. The inertial coupling terms remain. These products are handled by the servo-multipliers and permit the airframe studied to move with six degrees of freedom.

The dimensional stability derivatives are obtained from Table V, substituting these values in the equations above yields the analogue computer equations for the basic airframe:

Longitudinal Equations

$$(II-13)\quad \dot{u} = -.0151u + .0269w + vr - wq - 32.2\theta$$

$$(II-14)\quad \dot{w} = -.130u + 11.55q - 2.70w + 61.3\delta_e + 670q + qu - pv$$

$$(II-15)\quad \dot{q} = -.000282u - 16.86q - .034w + 76.8\delta_e - .00184\dot{w} + .888pr + .05r^2 - .05p^2$$

Lateral Equations

$$(II-16)\quad \dot{v} = +1.81r - .173v - .302p + 22.4\delta_r - 670r + wp - ru + 32.2\phi$$

$$(II-17)\quad \dot{p} = +.1785r - .054v - 6.53p + 62.5\delta_a + 2.34\delta_r + .0755\dot{r} - .83qr + .0755pq$$

$$(II-18)\quad \dot{r} = +.0125v - .190r + .0508p - 5.46\delta_r + 1.21\delta_a + .0323\dot{p} - .218pq - .0323qr$$

These equations of motion are entered directly in the analogue computers. The dimensional form of the stability derivatives permits the use of real time, that is, one second of machine time is equal to one second of real time. The coefficients, which are the dimensional stability derivatives, are entered as

potentiometer settings either directly or, if they are greater than one, as a fraction which is subsequently amplified to full value. The potentiometer settings along with the parameters they represent are presented in Tables VI and VII.

The stability derivatives which represent the change in a variable due to a control movement are based on a one radian control displacement. The product of the control movement and the corresponding stability derivative represents the forcing function which disturbs the airframe from its level flight equilibrium. Since the equations are entered directly with no machine scaling there is a one to one correspondence between machine units of 100 volts and unit movement, or in the case of angular control movement, unit radian throw. For a 10^{o} control movement a ratio is set up which establishes the potentiometer setting for a 10^{o} throw. A lesser or greater movement would, of course, be represented by a proportionately greater or lesser potentiometer setting. An example is calculated below to obtain the potentiometer setting representing M_{δ_e} for a 10^{o} control movement.

$M_{\delta_e} = 76.8$, REPRESENTS THE EFFECT CAUSED BY A δ_e OF 1 RADIAN.

1 MACHINE UNIT = 100 volts

$\therefore$ THE M_{δ_e} POTENTIOMETER SETTING IS

$\frac{76.8}{100}$ VOLTS OR .768

That is to say that when one machine unit, or 100 volts, is placed across the M_{δ_e} potentiometer set at .768, the analogue of the change to the pitching moment caused by an elevator throw of one radian will enter the equations of motion as a forcing function. Ten degrees would be this value multiplied by the fraction $\frac{10^\circ}{57.3^\circ}$ or .134. The other potentiometer settings representing the change caused by control movements are similarly computed. For the basic airplane these values appear in Tables VI and VII.

The computer diagram for the simultaneous solution of these six non-linear equations of motion is presented as Fig. 9. The inertial coupling terms, which are the product or moment of inertia factors and velocity terms such as $qr\,\frac{(I_z - I_y)}{I_x}$, are handled by the servo-multiplier units as indicated in Fig. 9.

A check was made on the analogue computer solutions obtained for the basic airplane (Case I) at sea level using equations (III-28) of Ref. 1 for the longitudinal motion and equations (III-97) for the lateral motion.

III-28, Ref. 1

$$\omega_{n_{sp}} = \sqrt{M_q Z_w - U_o M_w}$$

$$\zeta_{sp} = \frac{-1}{2\omega_{n_{sp}}} \sqrt{g(M_w Z_u - M_u Z_w}$$

$$\zeta_p = -\frac{X_u}{2\omega_{n_p}} - \frac{\zeta_{sp}\omega_{n_p}}{\omega_{n_{sp}}} - \frac{M_u(U_o X_w - g) - X_w Z_u M_q}{2\omega_{n_p}\omega_{n_{sp}}^2}$$

Calculation:

$$\omega_{M_{SP}} = \sqrt{(-16.86)(-2.70) - (+670)(-.034}$$

$$= 8.27 \text{ rad/sec}$$

$$\zeta_{SP} = -\frac{1}{2\times 8.27}\left[670\times 0 + (-2.70) + (-16.86)\right]$$

$$= 1.184, \text{ MORE THAN CRITICALLY DAMPED}$$

$$\omega_{M_P} = \frac{1}{8.27}\sqrt{32.2\left[(-.034)(-.130) - 0\right]}$$

$$\omega_{M_P} = .0456 \text{ Rad/sec.}$$

$$\zeta_P = -\frac{(-.015)}{2(.0456)} - \frac{(+1.184)(.0456)}{+8.27} - \frac{0-(+.0269)(-.130)(-16.86)}{2(.0456)(8.27)^2}$$

$\zeta_P = +.1691$; $\zeta_P = .17$ MEASURED USING FIG. III-28, REF. 1]

$$\omega_P = \sqrt{1-\zeta_P^2} = \sqrt{1-.0286} = .045 \text{ Rad/sec.}$$

$T_P = 139.6$ sec. ; T_P (MEASURED) = 139.5 sec.

III-97, Ref 1)

$$\frac{1}{T_S} = \frac{g/U_0\left(N_\beta L_r - L_\beta N_r\right)}{Y_v L_p N_r + L_p N_\beta + \left(\frac{g}{U_0}\right)L_\beta}$$

$$\frac{1}{T_r} = \frac{Y_v L_p N_r + L_p N_\beta + \left(\frac{g}{U_0}\right)L_\beta}{-N_\beta}$$

$$\omega_{M_D} = \sqrt{N_\beta}$$

$$\zeta_D = -\frac{-Y_v - L_p - N_r - \frac{1}{T_R} - \frac{1}{T_S}}{2\sqrt{N_\beta}}$$

$$\omega_D = \omega_{M_D}\sqrt{1-\zeta_D^2}$$

Calculations:

$$\frac{1}{T_S} = \frac{\frac{32.2}{670}\left[(+.0125)(+.1785) - (-.054)(-.190)\right]}{(-.173)(-6.53)(-.190) + (-6.53)(+.0125)(670) + \frac{32.2}{670}(-.054)(670)}$$

$$\frac{1}{T_S} = +.00457 \ \frac{1}{\text{sec}}$$

$$\frac{1}{T_R} = \frac{-56.655}{-(+.0125)(670)}$$

$$\frac{1}{T_R} = +6.77 \frac{1}{sec}$$

$$\omega_{M_D} = \sqrt{(670)(+.0125)}$$

$$= 2.89 \text{ rad/sec.}$$

$$\zeta_D = \frac{-(-.173) - (-.653) - (-.190) - (6.77) - (.00457)}{2 \times 2.89}$$

$$= +.0208 \; ; \; \zeta_{D(\text{MEASURED})} = .037$$

$$\omega_D = \omega_{M_D}\sqrt{1 - \zeta_D^2}$$

$$= 2.88 \text{ rad/sec.}$$

$$\frac{\omega_D}{2\pi} = N_D \; ; \quad \frac{1}{N_D} = T_D$$

$$T_D = \frac{2\pi}{2.88} = 2.18 \text{ sec.} \; ; \; T_D = 2.23 \text{ sec measured.}$$

SINCE THE CALCULATED VALUES CHECK THE RESULTS OBTAINED FROM THE REAC SOLUTIONS, THE REAC SET UP WAS ASSUMED TO BE CORRECT AND THE INVESTIGATION PROCEDED.

Thesis
E43
33157
Emanski
An investigation into some of the effects of cross coupling between the longitudinal and lateral equations of motion of a fightger type aircraft at subsonic speed.